

PhD thesis

Cosmological Aspects of Universal Extra Dimensions

by

Torsten Bringmann



Stockholm University
Department of Physics

August 2005

Thesis for the degree of doctor of philosophy in theoretical physics
Department of Physics
Stockholm University
Sweden

© Torsten Bringmann 2005
ISBN 91-7155-117-4 (pp i-vi, 1-111)
Printed by Universitetservice US-AB, Stockholm, 2005

Cosmological Aspects of Universal Extra Dimensions

Torsten Bringmann

*Department of Physics, Stockholm University,
AlbaNova, SE-10691 Stockholm, Sweden*

(August 2005)

Abstract

It is an intriguing possibility that our world may consist of more than three spatial dimensions, compactified on such a small scale that they so far have escaped detection. In this thesis, a particular realization of this idea – the scenario of so-called ‘universal extra dimensions’ (UED) – is studied in some detail, with a focus on cosmological consequences and applications.

The first part investigates whether the size of homogeneous extra dimensions can be stabilized on cosmological time scales. This is necessary in order not to violate the stringent observational bounds on a possible variation of the fundamental constants of nature.

An important aspect of the UED model is that it can provide a natural explanation for the mysterious dark matter, which contributes nearly thirty times as much as luminous matter like stars, galaxies etc. to the total energy content of the universe. In the second part of this thesis, the observational prospects for such a dark matter candidate are examined. In particular, it is shown how dark matter annihilations taking place in the Milky Way could give rise to exotic contributions to the cosmic ray spectrum in photons and antiprotons, leading to distinct experimental signatures to look for. This includes a comparison with similar effects from other dark matter candidates, most notably the neutralino, which appears in supersymmetric extensions of the standard model of particle physics.

Acknowledgements

I would like to thank my supervisor Lars Bergström for his support through the years. I have learned a lot and appreciated our fruitful collaborations, especially during the second half of my time as a PhD student.

My warmest thanks goes to my fellow PhD students Martin Eriksson and Michael Gustafsson, who made it such a great and rewarding experience to work in a team, both scientifically and on a personal level. They contributed significantly to my feeling home in Sweden.

It was a pleasure to have the roommates I had, especially Stefan Hofmann and Malcolm Fairbairn, with whom I had lots of interesting discussions about all kinds of physics-related and -unrelated things one could imagine. I have always appreciated the open atmosphere in this group; a very special thanks in this respect goes to Fawad Hassan and Joakim Edsjö for sharing their expertise at almost any time and in any situation. I am grateful to all present and past FoP and CoPS group members who made this corridor the pleasant place it is, not only during our notorious wednesday cake times.

Finally, but certainly not to the least, I would like to thank all those who have been an important part of my way through the last three years and who made life so enjoyable.

Notation and conventions

For the metric, a timelike signature (+ − − ...) is used, except for the discussion on the stabilization of extra dimensions in Chapter 4, where the conventions of Misner, Thorne and Wheeler [93] are adopted, which includes in particular a spacelike signature.

The number of spacetime dimensions is denoted by d . Higher-dimensional spacetime coordinates are indicated by a capital X with capital latin indices $M, N, \dots \in \{0, 1, \dots, d - 1\}$. Four-dimensional (4D) coordinates are given by a small x with greek indices μ, ν, \dots (or small latin letters i, j, \dots for spacelike indices), as in

$$\begin{aligned} x^\mu &\equiv X^\mu \quad (\mu = 0, 1, 2, 3), \\ x^i &\equiv X^i \quad (i = 1, 2, 3). \end{aligned}$$

Extra-dimensional coordinates are denoted by

$$y^p \equiv X^{3+p} \quad (p = 1, 2, \dots, d - 4).$$

The sum convention is always implicitly understood, i.e. one has to take the sum over any two repeated indices.

Following common practice, in the case of only one extra dimension, the above notation will be changed slightly by denoting extra-dimensional components with a sub- or superscript 5. Spacetime indices thus take values $\{0, 1, 2, 3, 5\}$ and the coordinate for the extra dimension will be $y \equiv y^1 \equiv X^5$.

Conventions for gamma matrices, Feynman diagrams etc. follow those of Peskin and Schroeder [103]. Higher-dimensional quantities like coupling constants and Lagrangians will be denoted with a 'hat' (as in $\hat{\kappa}^2, \hat{\mathcal{L}}_{\text{Higgs}}$) to distinguish them from their 4D analogs ($\kappa^2, \mathcal{L}_{\text{Higgs}}$). Finally, all expressions in this thesis are presented in natural units, where $c = \hbar = 1$. Useful conversion factors for energy and length scales are then given by:

$$\begin{aligned} 1 \text{ GeV} &= 1.78 \cdot 10^{-24} \text{ g} = 1.60 \cdot 10^{-3} \text{ erg} = 1.16 \cdot 10^{13} \text{ K}, \\ (1 \text{ GeV})^{-1} &= 1.97 \cdot 10^{-14} \text{ cm} = 6.38 \cdot 10^{-36} \text{ kpc} = 5.91 \cdot 10^{-4} \text{ s}. \end{aligned}$$

Acronyms often used in this thesis

ACT	Air Cherenkov telescope
BBN	Big Bang nucleosynthesis
CMB	Cosmic microwave background radiation
CMS	Center of mass system
ED	Extra (spatial) dimension
FRW	Friedmann-Robertson-Walker
KK	Kaluza-Klein
LKP	Lightest Kaluza-Klein particle
MSSM	Minimal supersymmetric standard model
NFW	Navarro-Frenk-White
SM	Standard model (of particle physics)
SN	Supernova
UED	Universal extra dimension(s)
WIMP	Weakly interacting massive particle
4D	Four dimensions, four-dimensional

Table of Contents

1	Introduction	1
2	The Cosmological Concordance Model	3
2.1	The Big Bang in a nutshell	4
2.2	Inflation as a paradigm	7
2.3	A universe in darkness	9
3	Extra Spatial Dimensions	15
3.1	General features of Kaluza-Klein theories	15
3.2	Modern extra-dimensional scenarios	18
3.3	Universal Extra Dimensions	20
3.3.1	Gauge fields	22
3.3.2	The Higgs sector	24
3.3.3	Ghosts	27
3.3.4	Fermions	28
3.3.5	Radiative corrections	32
4	Stabilization of Homogeneous Extra Dimensions	35
4.1	Constraints on time-varying extra dimensions	36
4.2	The higher-dimensional Friedmann equations	38
4.3	Dimensional reduction	39
4.4	Cosmological evolution of scale factors	40
4.4.1	Case study: Universal extra dimensions	41
4.5	Recovery of standard cosmology	43
5	Kaluza Klein Dark Matter	45
5.1	A new dark matter candidate	46
5.2	The galactic mass distribution	49
5.2.1	Smooth halo profiles	49
5.2.2	Substructure and clumps	50

5.3	Gamma rays from $B^{(1)}$ annihilations	53
5.3.1	The continuous signal	54
5.3.2	The two photon annihilation line signal	57
5.3.3	Discrimination against other dark matter candidates .	61
5.4	High-energetic antiprotons	68
6	Summary and Outlook	75
A	Feynman rules for the UED model	77
B	Generalizing to more than one UED	95
	References	98
	Accompanying papers	111

Chapter 1

Introduction

Since long back in time, people have kept wondering about the universe as a whole and put considerable effort into understanding its origin, its appearance today and the place we take in it – both in a physical and in a metaphysical sense, as these aspects usually were closely intertwined. Along the way, some cultures developed impressive astronomical knowledge – in ancient Babylon, for example, one could already predict the movement of the moon and the planets to an astonishing precision – but it was not long before the beginning of the last century that cosmology as a scientific discipline took its origin. Since then there has been an enormous gain in understanding, not the least due to the advance of ever more powerful observational techniques, and by now there has emerged a consensus on the basic picture of how the universe began and what it looks like on large scales. However, grand questions still remain unanswered, most notably those concerning the nature of the mysterious dark matter and dark energy, which make up 95 percent of the total energy and matter content of the universe – while visible objects like stars, galaxies and nebulae only account for less than about 1 percent, the rest being in ordinary, but non-luminous matter.

Seemingly completely unrelated, it was realized in the 1920s that in contrast to our everyday experience there might actually exist more than only three spatial dimensions. While this idea originally was regarded as a mere mathematical 'trick' allowing the unified description of Einstein's general relativity and Maxwell's electrodynamics, it took some time to realize its potential physical significance. After a temporary period of less activity in that field, interest in extra-dimensional theories exploded with the advent of string theory – a candidate for a unified description of all physics, which (at least in its usual formulation) turned out to be inconsistent unless one

allowed for the presence of extra dimensions.

In the following, the focus will be on a particular model, that of so-called *universal extra dimensions* (UED), where all standard model (SM) particles feel the presence of the extra dimensions and can propagate freely through the internal space. While containing the main general aspects of higher-dimensional theories, an appealing aspect of this idea is certainly its simplicity. Furthermore, from a particle physics' point of view, there are several attractive features connected to the UED scenario – such as providing a mechanism for electroweak symmetry breaking, or possible explanations for the observed number of fermion generations and the stability of the proton. The main reason why the UED model has received so much interest in recent years, however, seems to be its cosmological impact, namely the fact that it rather naturally gives rise to a viable dark matter candidate. As will be motivated in detail, this so-called Kaluza-Klein (KK) dark matter particle is a massive vector boson, providing an interesting phenomenological alternative to the supersymmetric neutralino, which is the most well studied dark matter candidate.

The outline of this thesis is as follows. Chapter 2 gives a brief review of the concordance model of cosmology, which summarizes the current knowledge about both the evolution and the overall composition of the universe. An introduction to some general aspects of higher-dimensional theories is then presented in Chapter 3, followed by a detailed description of the UED model. In order not to contradict observations, it is absolutely essential that extra dimensions are stable on cosmological timescales; this will be further elaborated on in Chapter 4, where also the stabilization prospects of the simple case of homogeneous extra dimensions are studied in more detail. In Chapter 5, the lightest KK particle appearing in the UED model will then be motivated as a both interesting and viable dark matter candidate; a short summary will be given of the phenomenology that has been worked out earlier, before presenting in detail the prospects for indirect detection of this type of dark matter particles in both the cosmic gamma-ray and antiproton spectrum. Chapter 6, finally, concludes with a short summary and outlook. The Feynman rules for the case of one UED, as well as some comments on a generalization to more than one UED, are collected in two appendices A and B.

The articles [I-VI], listed on page 111 and enclosed thereafter as a supplement, make up an integral part of this thesis. The main results of [I, II] about the stabilization of homogeneous extra dimensions are found in Chapter 4, while those about the indirect detection of Kaluza-Klein dark matter [III, IV, V] (and neutralino dark matter [VI]) are summarized in Chapter 5.

Chapter 2

The Cosmological Concordance Model

The last few years have seen the rise of cosmology from a discipline bound to large uncertainties, seemingly based on vague assumptions and unable to make any firm statements about the universe as a whole, to a science that can address these most fundamental questions with an outstanding precision. Today, one has a rather good handle on the basic picture and understands fairly well the evolution of the universe from a very dense, hot and uniform initial state to the vast and complex place that we observe today. While the theoretical foundations already were laid much earlier, a milestone being the formulation of the theory of general relativity in 1915 [56], it was only due to very recent developments in observational techniques that this success was made possible. Just to mention the most prominent, this includes all-sky precision measurements of the cosmic microwave background [118], the compilation of great large-scale structure catalogues [100, 121] and the systematic observation of distant supernovae [111, 101]. In fact, by now there has emerged a *concordance model* of cosmology that can explain basically all available observations and describes both the evolution and the current state of the universe with only a handful of parameters.

Despite this great success, grand questions still remain to be answered. Most notably, virtually nothing is known about the nature of roughly 95 % of what the universe consists of today. These mysterious contributions to the total energy budget are called dark matter and dark energy, respectively, but these names rather paraphrase our ignorance than give any hints about the underlying physics. The only thing that seems to be clear is that no standard explanation, including ordinary types of matter or energy as we

observe them on earth, is available for these phenomena – so one or the other form of new physics has to be involved and it is not unlikely that its discovery would mean a scientific revolution similar to that of general relativity or quantum mechanics.

This chapter gives a short overview of the concordance model of modern cosmology, starting with a brief summary of Big Bang theory (Section 2.1) and how an inflationary phase of an accelerating expansion in the early universe can provide the necessary initial data for it (Section 2.2). The observational evidence for the dark components of the universe, together with possible detection strategies, is then reviewed in Section 2.3.

2.1 The Big Bang in a nutshell

Standard cosmology rests on three pillars – general relativity, the cosmological principle and a description of matter as a perfect fluid. The *cosmological principle* states that the universe is homogeneous and isotropic on large scales, i.e. it looks basically the same at all places and in all directions. From this principle, it follows that spacetime can be described by the Friedmann-Robertson-Walker (FRW) metric,

$$ds^2 = g_{\mu\nu} dx^\mu dx^\nu = dt^2 - a^2(t) \left[\frac{dr^2}{1 - kr^2} + r^2 d\Omega^2 \right], \quad (2.1)$$

with $k = 0, 1, -1$ for a flat, positively and negatively curved universe, respectively. For the approximately flat geometry that we observe, the scale factor $a(t)$ thus relates physical distances λ_{phys} to coordinate (or comoving) distances r via $\lambda_{\text{phys}} = ar$.

An *ideal fluid* is defined by an energy-momentum tensor that takes the following form in the rest frame of the fluid:

$$T^{\mu\nu} = \text{diag}(\rho, p, p, p). \quad (2.2)$$

To relate its energy density ρ and pressure p , one usually also specifies an equation of state,

$$p = w\rho. \quad (2.3)$$

Inserting (2.1) and (2.2) into the field equations of general relativity,

$$R_{\mu\nu} - \frac{1}{2}R g_{\mu\nu} + \Lambda g_{\mu\nu} = \kappa^2 T_{\mu\nu}, \quad (2.4)$$

one arrives at the Friedmann equations

$$\dot{a}^2 = \frac{\kappa^2}{3}\rho a^2 + \frac{\Lambda a^2}{3} - k, \quad (2.5a)$$

$$\ddot{a} = -\frac{\kappa^2}{6}(\rho + 3p)a + \frac{\Lambda a}{3}, \quad (2.5b)$$

which describe the time evolution of the scale factor a and are thus the basic cosmological equations of motion. The second Friedmann equation, (2.5b), is often also referred to as the Raychaudhuri equation. Note that the cosmological constant Λ in these equations appears in the form of a perfect fluid with constant energy density and pressure $\rho_\Lambda = -p_\Lambda = \Lambda/\kappa^2$. By expressing all energy densities in terms of a *critical density* $\rho_c \equiv 3\dot{a}^2/(\kappa^2 a^2)$, one can bring the first Friedmann equation into the form

$$\Omega + \Omega_\Lambda = 1 + k/\dot{a}^2, \quad (2.6)$$

where $\Omega \equiv \rho/\rho_c$ and $\Omega_\Lambda \equiv \rho_\Lambda/\rho_c$. This means that if the various contributions to the total energy density add up to the critical density, the universe is flat ($k = 0$).

The spectra of remote galaxies are observed to be more redshifted for larger distances to our galaxy, the usual interpretation being that we live in an expanding universe; in the FRW metric (2.1), the redshift z is readily obtained as

$$1 + z \equiv \frac{\nu_{\text{emit}}}{\nu_0} = \frac{a_0}{a_{\text{emit}}}, \quad (2.7)$$

where ν_{emit} is the signal frequency at the time of emission and ν_0 the frequency as it is observed today. The strong energy condition requires on the other hand that

$$\rho + 3p > 0. \quad (2.8)$$

From the second Friedmann equation it therefore follows that the growth of the scale factor a has always been decelerating (neglecting for the moment the possible existence of a cosmological constant). Since we observe $\dot{a} > 0$ today, this means that the universe started off with an initial singularity at which $a = 0$. This is the basis for the notion of a *Big Bang* as the beginning of both space and time. An important observation is the fact that in such a spacetime, there appears a horizon which characterizes the maximal length that any particle or piece of information can have propagated since the Big Bang:

$$d_H(t) = a(t) \int_0^{r(t)} \frac{dr'}{\sqrt{1 - kr'^2}} = a(t) \int_0^t \frac{dt'}{a(t')}. \quad (2.9)$$

This *particle horizon* d_H is usually well approximated by the *Hubble radius* $H^{-1} \equiv a/\dot{a}$.¹

From the two Friedmann equations, or directly from energy conservation, $T^\mu_{;\mu} = 0$, one obtains

$$(\rho a^3)^\cdot + p(a^3)^\cdot = 0. \quad (2.10)$$

Assuming $w = \text{const.}$ in the equation of state, this can be integrated to give

$$\rho \propto a^{-3(w+1)}. \quad (2.11)$$

Radiation (highly relativistic matter), for example, has an equation-of-state parameter $w = 1/3$ and thus scales as $\rho \propto a^{-4}$. Going back in time, it will therefore start to dominate the total energy budget over any contribution from (non-relativistic) matter with $w = 0$ and $\rho \propto a^{-3}$ – or, of course, a constant contribution ρ_Λ . The energy density for black body radiation is given by $\rho_r \propto g_{\text{eff}} T^4$, where g_{eff} is the effective number of degrees of freedom. The temperature in the early universe increases therefore as

$$T \propto g_{\text{eff}}^{-1/4} a^{-1} \quad (2.12)$$

with a decreasing scale factor a , which motivates the picture of a *hot* Big Bang.

Starting from a reasonably dense and hot initial state – beyond which one would have to take into account effects from unknown physics at very high energies – one can now reconstruct the thermal history of the universe as it is sketched in Table 2.1. This picture shows a remarkable agreement with basically all cosmological data, of which the abundances of light elements as formed during Big Bang nucleosynthesis (BBN) and the existence of the cosmic microwave background (CMB), providing a snapshot of the universe at an age of about 300 000 years, are the most prominent. The isotropy of the latter, as well as that of the distribution of galaxies on very large scales, gives a further justification to the underlying assumptions of the cosmological principle.

¹ Whenever $a \propto t^n$, with $n < 1$, as is the case for both a radiation- and a matter-dominated universe, one has $d_H = t/(1 - n)$ and $H^{-1} = t/n$. During an inflationary phase (see next section) with $H \approx \text{const.}$, however, d_H grows exponentially with time.

t	T	event
10^{-42} s	10^{19} GeV	Planck-epoch (quantum gravity)
$\sim 10^{-35}$ s	~ 0	inflation
10^{-10} s	100 GeV	electroweak phase transition
10^{-4} s	100 MeV	formation of protons and neutrons
10^{-2} s	10 MeV	$\gamma, \nu, e^-, e^+, n, p$ in thermal equilibrium
1 s	1 MeV	ν decoupling, e^-e^+ annihilation
100 s	0.1 MeV	nucleosynthesis of light elements (BBN)
10^4 y	1 eV	matter starts to dominate
10^5 y	0.1 eV	formation of atoms, CMB
10^9 y	10^{-4} eV	protogalaxies and first stars begin to form
10^{10} y	2.728 K	today

Table 2.1: A very rough guide through the thermal history of the universe.

2.2 Inflation as a paradigm

Given a set of initial data, standard Big Bang theory is enormously successful in explaining almost any cosmological observation. A more thorough analysis, however, shows that these initial data describing the very early universe have to be fine-tuned in an extreme way in order to match all the measurements that are made today. The two most well-known examples of this are the *flatness* and the *horizon problems*. As to the first one, if the universe does not start out exactly flat, an analysis of the Friedmann equations shows that it tends to become more and more curved as it evolves; it is therefore hard to understand the close to flat geometry that we observe today. The horizon problem, on the other hand, points out that for example the CMB shows a large degree of homogeneity – even though the sky actually consists of about 10^5 patches that did not have any causal contact between the Big Bang and the emission of the CMB photons.

Another shortcoming of classical cosmology is that it cannot account for the rich structure the universe exhibits today, since the FRW metric describes a completely homogeneous and isotropic universe. Of course, it is relatively straight-forward to use a perturbed version of this metric instead, start with some statistical distribution of density fluctuations and evolve them in time. The primordial power spectrum that describes these initial

density fluctuations, however, must again be treated as an input to the theory and has no independent justification. In particular, all observations of large-scale structures, from the CMB to the distribution of galaxy clusters, suggest that the primordial power spectrum is scale-invariant, which means that the spectrum does not depend on any length scale, if taken at the moment of horizon-entry of that particular scale. Within the framework of Big Bang theory alone, there is no way to understand why this should be the case.

In the beginning of the 1980s it was proposed that the very early universe might have undergone a period of accelerating expansion [72]. Such an era of *inflation*, it was claimed, would provide the necessary initial conditions for Big Bang cosmology and thus a solution to all the problems and shortcomings mentioned above. (See footnote 1 for a direct explanation of how the horizon problem is solved).

From the Raychaudhuri equation (2.5b) it follows that the strong energy condition (2.8) must be violated during inflation. The easiest way to accomplish this – besides by a pure cosmological constant – is via a scalar field Φ in a potential $V(\Phi)$; for a FRW metric, its energy density and pressure are given by

$$\rho_{\Phi} = \frac{1}{2}\dot{\Phi}^2 + V(\Phi) + \frac{(\nabla\Phi)^2}{2a^2}, \quad (2.13)$$

$$p_{\Phi} = \frac{1}{2}\dot{\Phi}^2 - V(\Phi) - \frac{(\nabla\Phi)^2}{6a^2}. \quad (2.14)$$

For an approximately homogeneous universe with a slowly rolling scalar field, i.e. $\frac{1}{2}\dot{\Phi}^2 \ll V(\Phi)$, one finds an equation of state with nearly constant $\rho_{\Phi} \approx V(\Phi) \approx -p_{\Phi}$. From (2.10), this results in an exponentially growing

$$a(t) \sim e^{(\kappa/\sqrt{3})V(\Phi)t}. \quad (2.15)$$

The evolution of the field Φ itself is given by its equation of motion in the background FRW metric,

$$\ddot{\Phi} + 3H\dot{\Phi} + V'(\Phi) = 0. \quad (2.16)$$

In the beginning, it moves only very slowly down the potential due to the presence of the Hubble damping term, but eventually it will roll faster and faster and then start to oscillate rapidly around the minimum of $V(\Phi)$. At this moment, inflation stops and the scalar field decays into SM particles; after such a phase of *reheating*, the universe evolves as in ordinary Big Bang cosmology.

Quantum fluctuations of the scalar field during inflation become effectively classical in the expanding background [105] and these perturbations in the scalar field density are later inherited by ordinary matter, thus giving rise to a primordial power spectrum for density fluctuations. As it turns out, this spectrum is generically scale-invariant up to small corrections, with the details depending on the exact shape of the potential $V(\Phi)$. Inflation does thus not only provide the desired form of the spectrum but also in principle testable tiny deviations from it.

Currently, there is no really convincing candidate for a scalar field that could drive inflation and at the same time is well motivated from particle physics. Rather than being a concrete model, inflation should therefore more be viewed as a general mechanism, or paradigm, that is capable of providing satisfying initial conditions for Big Bang cosmology. In such general terms, the scalar field is often referred to as the *inflaton*. A particularly simplistic version is that of *chaotic inflation* [87], where the inflaton is initially displaced from its real vacuum by, e.g., quantum fluctuations; any region, however tiny in size but with a large enough displacement of the inflaton, would blow up as described above and, after only a relatively short phase of inflation, fill a volume corresponding to the whole observable universe today.

2.3 A universe in darkness

The observation of distant type Ia supernovae shows that they appear fainter than one would expect, taking into account their redshift, i.e. distance, and the fact that one has a fairly good handle on the intrinsic brightness of these objects [111, 101]. This situation is usually interpreted as an indication that the universe is currently undergoing an *accelerated* expansion, just as during inflation. One can explain, or rather parametrize, such a behaviour by introducing a *dark energy* component to the total energy budget of the universe. This name already indicates its mysterious nature, about which virtually nothing is known; the only fact that can be deduced from observations is that it dominates the universe today and that it has an equation of state parameter w close to -1 . The observation of the anisotropies in the CMB [118] gives independent evidence for a dark energy component and, together with the SN Ia data, allows for a quite accurate determination of its energy density.²

²The evidence coming from CMB observations actually depends on a prior that excludes very low values of the Hubble constant today – which, however, is strongly suggested by the results of large structure surveys [100, 121].

The explanation for the observed dark energy might in principle just be a cosmological constant Λ as it appears in Einstein's equations. However, in order to get the value that is observed today, i.e. an energy density of about 120 orders of magnitudes less than the at first sight more natural Planck scale, one has to invoke extreme fine-tuning. Connected to this is the often quoted 'why now?' or *coincidence* problem: on cosmological time scales, the Λ domination began only rather recently and within a very short period of time it would lead to an exponentially expanding de Sitter universe, where all galaxies are redshifted beyond observability – so why do we live during that very short transition from matter- to Λ -domination that actually allows us to observe a universe that resembles ours? To remedy these problems, one has tried to explain the dark energy by the introduction of a scalar field, which would have a similar effect today as the inflaton during inflation. The initial hope connected to such a *quintessence* field [131] was that one could avoid any fine-tuning problems thanks to the existence of tracker solutions that naturally explained why such a field would start to dominate only relatively shortly after the beginning of matter domination. As it turned out, however, the problem of fine-tuning was just reformulated and now re-appeared in adjustable parameters of the model. Follow-up models like *k-essence* [14] currently do not give satisfactory explanations for the nature of the dark energy either. Finally, due to the Lorentz invariance of the vacuum, all matter fields should contribute to the total energy-momentum tensor with vacuum quantum fluctuations that have the same form as a cosmological constant. A naive calculation of these contributions, however, gives a vacuum energy density that is many orders of magnitude above the observed one, even if large cancellations that would follow from the existence of supersymmetry are taken into account [127]. To answer these unresolved questions, often summarized under the name of the *cosmological constant problem(s)*, and to provide an explanation for the nature of dark energy, is one of the most outstanding challenges in modern physics.

Dark energy is not the only mysterious component of the universe. On the contrary, observations on a wide range of distance scales indicate that there must be a large amount of non-relativistic, pressureless matter that greatly outnumbers all known objects emitting visible light, or electromagnetic radiation at any other frequency. This *dark matter* can thus not be seen directly, not even with the most powerful telescopes, but betrays its existence only indirectly through its gravitational influence on other objects. Such indirect evidence comes from various independent sources, ranging from galaxy rotation curves [102] and the mass-to-light ratio of galaxy clusters [16], to the comparison of N-body simulations with the results from

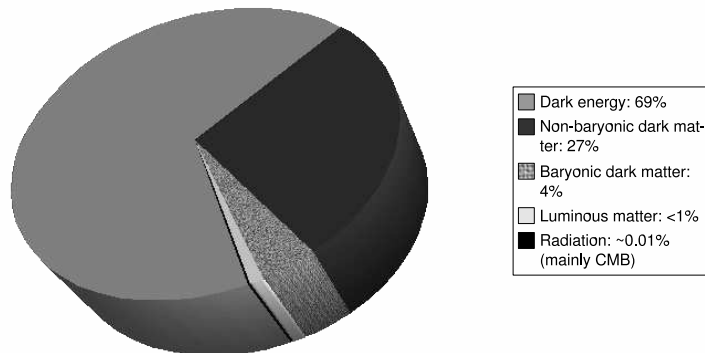


Figure 2.1: The composition of the universe as inferred from CMB observations and large scale structure surveys [121]. Less than 1% of the total energy content is due to visible matter in stars, galaxies etc., and only about 5% comes in the form of baryons. The nature of 95% is thus completely unknown.

large-scale structure surveys [100, 121]. What is more, in order not to spoil the successful predictions of BBN [98] and to account for the observed CMB spectrum [118], ordinary matter in the form of baryons can only contribute about 12% to the dark matter, so the rest must be attributed to some new, yet unknown physics. Fig. 2.1 shows the resulting picture that the cosmological concordance model provides for the overall composition of the universe today, taking into account all the observational evidence that has been mentioned so far.

Contrary to the case of dark energy, however, there do exist reasonable candidates to explain the dark matter content of the universe. A popular assumption is that dark matter is made up of a yet unknown species of particles that were produced in the early universe; these particles would obviously have to be stable on cosmological time scales, electrically neutral and colourless. One of the most attractive examples are *weakly interacting massive particles* (WIMPs) that arise in all kinds of extensions of the standard model of particle physics. In the early universe, they would decouple from the thermal bath of SM particles once their interaction rate falls behind the expansion rate of the universe. More accurately, as for any other particle, the evolution of the WIMP number density n is described by the *Boltzmann equation*,

$$\frac{dn}{dt} + 3Hn = -\langle\sigma v\rangle (n^2 - n^{\text{eq}2}) , \quad (2.17)$$

where $\langle\sigma v\rangle$ is the thermally averaged annihilation cross section times the relative velocity and n^{eq} is the numer density at thermal equilibrium; the latter gets exponentially suppressed, $n^{\text{eq}} \sim e^{-m_{\text{WIMP}}/T}$, once the temperature T of the universe has dropped to a point where the WIMP becomes non-relativistic. While the complete dynamics can be complicated and only be obtained by solving the full Boltzmann equation, it is usually a good estimate that the resulting relic density of these particles today is given by

$$\Omega_{\text{WIMP}} h^2 \sim \frac{3 \cdot 10^{-27} \text{ cm}^3 \text{ s}^{-1}}{\langle\sigma v\rangle}, \quad (2.18)$$

where h is the Hubble constant in units of $100 \text{ km s}^{-1} \text{ Mpc}^{-1}$ [81]. For masses and coupling strengths roughly at the electroweak scale, Ω_{WIMP} automatically comes out to be of the right order of magnitude to account for the observed dark matter density. The most important case when a more rigorous analysis of the Boltzmann equation has to be performed, leading to potentially large corrections to the naive expression (2.18), is that of *co-annihilations* [70]. These appear if the lightest WIMP, that would later constitute the dark matter, is accompanied by other new particles that are almost degenerate in mass and thus thermally accessible during the freeze-out process of the former. A prototype WIMP is the neutralino, the lightest supersymmetric particle. In this thesis, the focus will be on another WIMP candidate that is motivated by an extra-dimensional extension of the SM; it will be discussed in detail in Chapter 5.

Since a large part of this thesis is devoted to a particular dark matter candidate, it seems appropriate to discuss in the remainder of this chapter the various detection strategies that have been developed to identify the (particle) nature of dark matter in general. These can be grouped into two different approaches. In *direct detection* experiments one tries to trace the dark matter particles themselves: when, e.g., a WIMP scatters elastically off an atom in a large detector, the transferred recoil energy can in principle be used as a signature to look for. The experimental challenge lies in the very small WIMP cross sections on the one hand and a relatively high background due to radioactive contamination and activation on the other hand. Consequently, this type of experiments is usually placed underground to shield the cosmic radiation, such as the Edelweiss experiment in the Frejus Underground Laboratory [113] or CDMS II in the Soudan mine [7]. The DAMA [30] direct detection experiment is the only one so far that actually has claimed the detection of dark matter particles, the signature being an annual modulation of the signal as expected due to the earth's movement

around the sun and thus through the galactic halo of dark matter; this detection, however, is highly debated and has not been confirmed by similar, more sensitive experiments.

The purpose of *indirect detection* experiments, on the other hand, is to look for possible products of dark matter annihilations. The stability of dark matter particles over cosmological time scales is usually guaranteed by a symmetry which forbids the decay into SM particles. For the neutralino and the particular dark matter candidate that later will be discussed in this thesis, however, this symmetry takes the form of a parity operation, so pair-annihilation *is* possible. The largest annihilation rates are then expected from regions with high dark matter densities such as the center of the Milky Way or other (nearby) galaxies. Even the innermost region of very massive celestial bodies like the earth or the sun are of interest, where dark matter particles can become gravitationally trapped and accumulate until their density eventually saturates due to self-annihilation. The only annihilation products that can escape the interior of the sun or the earth are neutrinos, and in order to detect them, there are great neutrino telescopes planned or already in operation – like AMANDA [5] and ICECUBE [6] that use the antarctic ice as detector material.

Potentially promising signals from the galactic center can be searched for in all kinds of cosmic rays. Photons and neutrinos have the advantage that they do not interact with the interstellar medium, so the uncertainty in their respective fluxes results mainly from the shape of the dark matter distribution – which, however, is only rather poorly known (see Section 5.2). Gamma rays are among the most studied signatures of WIMP dark matter; they are observable both from space-based missions like EGRET [91] and GLAST [65], which is to be launched in 2007, and from ground-based atmospheric Cherenkov telescopes (ACTs) such as VERITAS [86], CANGAROO [122], HESS [3] and MAGIC [61]. These two types of experiments are complementary in energy range; while the (space-based) direct detectors of gamma rays have an upper bound above which they can no longer resolve the energy of the incident photons (300 GeV for GLAST), ACTs are bounded from below in that gamma rays with energies less than about 30 GeV do not produce electromagnetic showers in the atmosphere, so they cannot be detected by these types of telescopes.

Antiparticles like positrons or antiprotons are also very interesting signals to look for since their background flux is much lower than that of their corresponding partners. Due to their charge, however, their interaction with the interstellar medium can no longer be neglected. Instead, one has to treat their propagation as a diffusion process, with only rather poorly determined

parameters and – in contrast to the case of photons and neutrinos – little chance to make a clear connection between their origin and the direction from where they are detected. An experimental issue here is to correctly discriminate between different particle species – which becomes more difficult for higher energies since then the deflection in external magnetic fields goes down. Upcoming experiments like PAMELA [40] and AMS-02 [19] will be able to probe the spectrum of antiparticles to an unprecedented accuracy and to much higher energies than what has been achieved before.

A general difficulty for these types of indirect dark matter detection is to correctly account for the various astrophysical processes that may occur in the galactic center or halo; it is therefore important to provide unambiguous signatures like, e.g., the gamma ray line signal from direct dark matter annihilation (see Section 5.3.2).

Chapter 3

Extra Spatial Dimensions

It seems to be a trivial empirical fact that our world consists of four space-time dimensions. However, at the beginning of the 20th century Nordström, and in particular Kaluza and Klein (KK) realized, that there actually may exist additional spatial dimensions – as long as they are compactified on such a small scale that we have not yet been able to resolve them [97, 82, 84]. An analogy often used as a demonstration of this idea is that of an ant living on a hose: To us, i.e. from a distance, the hose looks one-dimensional, while the ant living on its surface experiences a two-dimensional world.

The basic idea of this proposal will be illustrated in Section 3.1 with the introduction of some new concepts and general consequences arising from the presence of extra spatial dimensions (EDs). Section 3.2 then presents a very short historical review of some of the various existing extra-dimensional scenarios, before a particular model, that of so-called *universal extra dimensions* (UED), is introduced and discussed in full detail in Section 3.3. It is this scenario that has particularly interesting cosmological implications and that will be the main focus for the rest of this thesis.

3.1 General features of Kaluza-Klein theories

An important conceptual issue that is connected to the existence of tiny, curled-up EDs is a larger spectrum of states from the point of view of a four-dimensional observer, i.e. one generically expects new particles to appear in such theories. Qualitatively, this can be understood in the following way: Imagine some particle propagating in one of the extra-dimensional directions – we cannot directly ‘see’ its movement, but still the particle has some additional (kinetic) energy compared to the same particle at rest and

this energy appears as a higher mass to a four-dimensional observer. More quantitatively, consider the case of a scalar field Φ with mass m in five dimensions. Assuming spacetime to be flat, it is described by the Klein-Gordon equation:

$$\left(\square^{(5)} + m^2\right) \Phi(x^\mu, y) = (\partial_t^2 - \nabla^2 - \partial_y^2 + m^2) \Phi(x^\mu, y) = 0. \quad (3.1)$$

If the fifth dimension is compactified on some scale R ,

$$y \sim y + 2\pi R, \quad (3.2)$$

this means that any function of y can be expanded into a Fourier series. In particular, Φ may be decomposed as $\Phi(x^\mu, y) = \sum_n \Phi^{(n)}(x^\mu) e^{-i\frac{2\pi n y}{R}}$ and the Fourier components $\Phi^{(n)}$ are then found to fulfill the Klein-Gordon equation in four dimensions:

$$(\square + m_n^2) \Phi^{(n)}(x^\mu) = (\partial_t^2 - \nabla^2 + m_n^2) \Phi^{(n)}(x^\mu) = 0, \quad (3.3)$$

with

$$m_n^2 = m^2 + \left(\frac{n}{R}\right)^2. \quad (3.4)$$

In the four-dimensional description of the theory there appears thus an (infinite) *tower of massive KK states* $\Phi^{(n)}$.¹ The mass of the first KK-excitation is inversely proportional to the radius of the ED, i.e. one needs a small radius in order to explain why such a particle has not (yet) been seen. This corresponds to the naive expectation that the low-energy (or large distance) limit of four-dimensional physics should not be affected by the existence of very small EDs. However, the exact structure of the KK-tower depends on the geometry of the internal dimensions and, of course, on the type of the fields that are allowed to propagate there.

Another important aspect shared by all theories involving EDs is that one expects at least some coupling constants to vary with the size of the internal space. To understand this, consider for example the gravitational action in $4 + n$ dimensions,

$$S = \frac{1}{2\hat{\kappa}^2} \int d^{4+n} X \sqrt{|g|} \mathbb{R}, \quad (3.5)$$

where \mathbb{R} is the higher-dimensional curvature scalar. Assume now that spacetime is separable and that the metric can be written in the form

¹Note that if the ED had a timelike signature, all these states were tachyons. Another reason why extra *temporal* dimensions are undesirable is the existence of closed timelike loops, leading to possible violations of causality [18].

$g_{AB} dX^A dX^B = g_{\mu\nu}(x^\rho) dx^\mu dx^\nu + \tilde{g}_{pq}(x^\rho, y^s) dy^p dy^q$. Integrating over the internal dimensions then results in

$$S = \frac{1}{2\kappa^2} \int d^n y \sqrt{|\tilde{g}|} \int d^4 x \sqrt{|g|} R + \dots, \quad (3.6)$$

where R now is the 4D curvature scalar constructed from $g^{\mu\nu}$. This action describes four-dimensional gravity with an effective coupling 'constant' that is related to the (fundamental) higher-dimensional one by

$$\kappa^2 = V^{-1} \kappa^2, \quad (3.7)$$

where $V = \int d^n y \sqrt{\tilde{g}} \sim R^n$ is the volume of the internal space. The missing terms '...' appearing in (3.6) come from the expansion of the higher-dimensional curvature scalar, $R[g^{MN}] = \bar{R}[g^{\mu\nu}] + \dots$, and in Section 4.3 it is shown that they correspond to scalar fields appearing in the effective, four-dimensional theory (see also [34, 71]). A similar argumentation to the one presented here for the gravitational field can be put forward for other fields that contribute to the higher-dimensional action [85, 124, 64]. For all such fields one thus expects their coupling constants to vary with the size of the EDs. As one might expect, there are tight observational constraints on such a variation, so one must essentially demand stable EDs for the whole idea presented here to make sense. This issue will be taken up in Chapter 4.

There is yet another aspect that is common to all extra-dimensional theories: for small distances between two test masses, one expects a deviation from Newton's law, $V(r) \propto r^{-1}$, for the gravitational potential between them. This can be understood from the fact that the Laplace operator (in flat space) locally takes the form

$$\nabla^2 = \left(\frac{\partial}{\partial X^1} \right)^2 + \dots + \left(\frac{\partial}{\partial X^{d-1}} \right)^2, \quad (3.8)$$

so for very small distances, the solution to the Laplace equation $\nabla^2 V = 0$ is given by

$$V(r) \propto r^{-(d-3)}. \quad (3.9)$$

Taking the full (globally defined) Laplace operator for the case of a compactified internal space, one therefore expects a potential that interpolates between the expression (3.9) for small and Newton's law for large distances. As it begins to feel the presence of EDs, gravity thus gets stronger – which is just the same observation as already expressed in the relation (3.7) between 4D and fundamental coupling constants. Again, the same will be

true not only for gravity, but for all interactions living in higher dimensions. Conventionally, deviations from Newton's law are parameterized as

$$V(r) \propto \frac{1}{r} \left(1 + \alpha e^{-r/\lambda} \right). \quad (3.10)$$

The leading order corrections due to the presence of EDs can always be written in this form, also for the case of curved EDs [83]. Direct measurements of Newton's law with torsion pendulae have started to probe the gravitational potential in the sub-mm regime; see [79] for a recent review on the resulting constraints on the (α, λ) parameter plane.

3.2 Modern extra-dimensional scenarios

The original proposal of Nordström [97], Kaluza [82] and Klein [84] was to study 5D general relativity in an attempt to unify gravity and electromagnetism. Klein, in particular, imposed a 'cylinder condition' for the higher-dimensional metric g_{MN} , i.e. compactified the ED on a small circle and demanded that the derivatives in the EDs can be neglected (which corresponds to saying that the KK masses, introduced in the previous section, are large enough not to influence the known low-energy physics). An additional (rather ad hoc) assumption was that g_{55} , i.e. the radius of the ED, is constant in both space and time. Identifying part of the higher-dimensional metric as a vector potential,

$$g_{5\mu} \equiv \kappa A_\mu, \quad (3.11)$$

it is then relatively straight-forward to show, that the Einstein-Hilbert action (3.5) in 5D reduces to gravity plus electromagnetism in 4D,

$$S = \int d^4x \sqrt{|g|} \left(\frac{R}{2\kappa^2} - \frac{1}{4} F_{\mu\nu} F^{\mu\nu} \right), \quad (3.12)$$

where $F_{\mu\nu} = \partial_\mu A_\nu - \partial_\nu A_\mu$ as usual.

This unification of two seemingly very different interactions came rather as a surprise. Furthermore, taking into account that one had started out with a 5D theory in *vacuum*, it was considered remarkable that not only the gravitational but even the electromagnetic field could now be thought of as purely geometrical in origin. Of course, this sparked an immense interest in whether also the weak and strong forces could fit into this scheme, leading to a unification of all interactions of nature. In fact, it was found in

the 1960s that allowing for more compactified EDs could lead even to non-Abelian vector fields in the 4D theory [48]: That the identification (3.11) was possible can be traced back to the fact that an infinitesimal coordinate transformation in y just takes the form of a gauge transformation of an Abelian vector field; in a similar way, non-Abelian transformations are generated by infinitesimal isometries of a more complex internal manifold. The smallest number of dimensions that can give rise to a group containing $SU(3) \times SU(2) \times U(1)$ is 11 [129]. Towards the end of the 1970s, finally, supergravity Kaluza-Klein models became popular. There, one finds particles with spin higher than 2 in the spectrum of the 4D theory as soon as one considers more than 7 EDs. Since such particles are usually thought of as not being quantizable consistently, it therefore became natural to restrict oneself to 11 spacetime dimensions. However, there are also several problems connected to 11D supergravity – for example, there seems to be no natural way to get chiral fermions [129], and there is no hope of renormalizability to all orders in perturbation theory. For a nice review on Kaluza-Klein theories see [18].

After the first excitement had faded away, the idea of EDs was considered less and less attractive – until the rise of superstring theory which revived these old ideas when it was realized that a consistent quantization only seemed possible in 10 spacetime dimensions. The basic idea of string theory is to replace point particles by strings, which describe a two-dimensional world sheet (in contrast to the one-dimensional world line of a particle) as they move through spacetime. Quantization then leads to a spectrum of different oscillations (of the same ‘type’ of string) which correspond to the different particles that we observe. An attractive aspect of using strings instead of particles is that the ultra-violet divergences of quantum field theory (associated to correlation functions for very small distances) can be cured as they are smeared out over the length of the string, which thus appears as a natural effective cutoff in the theory. It is hoped, though far from being proven yet, that string theory – or its generalization to M theory [130] – can provide a consistent, unified description for matter, gauge bosons and gravity.

In string theory, there appear non-perturbative, lower-dimensional objects, called *branes*, to which the endpoints of open strings are attached [106]. Closed strings, on the other hand, can propagate freely through the entire higher-dimensional spacetime, often referred to as the *bulk*. The spectrum of closed strings always contains a massless spin-2 field, which is identified as the graviton, and that of open strings contains various massless vector fields, which can be thought of as the observed gauge fields. This led to the

idea that we, and all the matter and gauge fields, might live on a (3+1)-dimensional brane, while gravity is not confined to it and therefore fully feels the presence of the EDs. As proposed by Arkani-Hamed, Dimopoulos and Dvali (ADD) [13], this observation might be used as a motivation for a phenomenological attempt to explain the *hierarchy problem*, i.e. the feableness of gravity as compared to other interactions: By allowing for the presence of relatively large EDs, one can see from (3.7) that the fundamental scale of gravity can be much higher than what it appears to be in 4D. For two EDs, one would for example need a compactification scale of approximately a mm to explain a fundamental scale of gravity at the electroweak scale.

It was realized by Randall and Sundrum (RS1) that it is possible to solve the hierarchy problem even for a scenario where the EDs are quite small [109]. They proposed that spacetime is not separable but has a warped geometry of the form

$$ds^2 = e^{-2kr_c|\phi|} \eta_{\mu\nu} dx^\mu dx^\nu + r_c^2 dr^2, \quad (3.13)$$

where k is a mass scale of the order of the Planck mass and r_c the size of the ED. In this model, we and all SM particles are confined to a brane at $\phi = \pi$; gravity appears weak on that brane due to the exponential suppression factor in front of the (3 + 1)-dimensional Minkowski metric.

Later, the same authors realized in [110] that one may actually consider the limit of an infinitely large ED, $r_c \rightarrow \infty$, and still recover Newton's law of gravity for an observer on the brane if the curvature scale of the bulk anti-deSitter space is less than about a mm. The possibility of a *non-compact* ED came certainly as a surprise and can be traced back to the special form that the spectrum of continuous KK modes takes in the case of a warped geometry. This second model (RS2), however, does no longer provide a solution to the hierarchy problem.

3.3 Universal Extra Dimensions

The model of *universal extra dimensions* (UEDs) was introduced some years ago by Appelquist, Cheng and Dobrescu [10] and is basically the higher-dimensional version of the standard model of particle physics. As a consequence, *all* SM fields are accompanied by a whole tower of increasingly more massive states; following the same line of arguments as in the first part of this chapter, the KK masses for these states are then given by

$$M^{(n)} \equiv \sqrt{m_{\text{EW}}^2 + \left(\frac{n}{R}\right)^2} \quad (3.14)$$

for SM particles with electroweak masses m_{EW} .

From now on, it will be assumed for simplicity that there is only one UED.² Current collider bounds then set an upper limit of $R^{-1} \gtrsim 300$ GeV on the compactification scale [10, 2], while the LHC will probe scales down to about 1.5 TeV [46]. For comparison: Direct measurements of deviations from Newtons law give much less stringent bounds on the allowed size of one ED, $R^{-1} \geq (160 \mu\text{m})^{-1} \sim 0.1$ eV [79].

A naive higher-dimensional version of the SM, compactified on a circle, would actually not only give new massive fields in the form of KK towers, but also additional massless, scalar degrees of freedom; this is because the fifth component of a 5D vector field transforms as a scalar under 4D Lorentz transformations. Light scalar fields, however, are not observed and their existence is heavily constrained by solar system observations and fifth force experiments [128]. A possible solution to this problem lies in a compactification on an *orbifold* S^1/\mathbb{Z}_2 rather than on a circle. In addition to the usual identification $y \sim y + 2\pi R$, there is then a mirror symmetry between points that are mapped onto each other under the orbifold projection $y \rightarrow -y$. With

$$y \sim 2\pi R - y, \quad (3.15)$$

compactification thus effectively takes place on a line segment $[0, \pi R]$. Under such an orbifold projection $P_{\mathbb{Z}_2}$ any field ϕ transforms even, $P_{\mathbb{Z}_2}\phi(x^\mu, y) = \phi(x^\mu, -y)$, or odd, $P_{\mathbb{Z}_2}\phi(x^\mu, y) = -\phi(x^\mu, -y)$. Obviously, odd fields do not have zero modes,

$$\phi_{\text{even}}(x^\mu, y) = \frac{1}{\sqrt{2\pi R}}\phi_{\text{even}}^{(0)}(x^\mu) + \frac{1}{\sqrt{\pi R}}\sum_{n=1}^{\infty}\phi_{\text{even}}^{(n)}(x^\mu)\cos\frac{ny}{R}, \quad (3.16a)$$

$$\phi_{\text{odd}}(x^\mu, y) = \frac{1}{\sqrt{\pi R}}\sum_{n=1}^{\infty}\phi_{\text{odd}}^{(n)}(x^\mu)\sin\frac{ny}{R}, \quad (3.16b)$$

and in that way the above mentioned problem can be avoided by assigning suitable transformation properties under $P_{\mathbb{Z}_2}$ (the factors in front have been extracted for later convenience). As it turns out, the same idea also allows for chiral fermions in the effective 4D theory – even though chiral fermions do not exist in five dimensions (see Section 3.3.4). The idea of a compactification on an orbifold is inspired by string theory, where one uses this approach as an approximate way of describing the compactification on Calabi-Yau spaces, which have a much more complex structure but

²See Appendix B for some comments on a generalization of this. The discussion on the stability of EDs in Chapter 4 is also not restricted to the case of only one ED.

give the same low-energy spectrum of states and provide basically the same mechanism of producing chiral fermions [50, 51].

Since the SM in higher dimensions exhibits dimensionful couplings, it is not renormalizable (see, e.g., [103]). The UED model should therefore be viewed as an *effective* theory in four dimensions that is valid up to some cutoff scale Λ . From the demand that the loop-expansion parameters should be smaller than unity, i.e. that perturbation theory is still valid, one can estimate that new physics should not appear before a cutoff of $\Lambda \sim 20R^{-1}$ [10]. Theoretical motivations to consider the UED scenario as introduced above include a way to achieve electroweak symmetry breaking without the explicit need of a Higgs field [12], as well as providing possible explanations for the observed number of fermion generations [52] or the very long life-time of the proton [11]. It furthermore provides in a natural way a viable dark matter candidate (see Section 5.1), which is the main motivation to study it in this thesis.

In the remainder of this chapter, the field content and interactions of the effective four-dimensional theory of the UED model will be discussed in full detail (see Appendix A for a list of the resulting Feynman rules).

3.3.1 Gauge fields

As already mentioned, the fifth component of a gauge field A_M transforms as a scalar under 4D Lorentz transformations, so it should be odd under orbifold projections in order to avoid light scalar fields in the 4D theory. Demanding that the first four components A_μ transform even, so that their zero modes can reproduce the ordinary 4D fields, this actually follows directly from gauge invariance: Since

$$A_\nu^r(x^\mu, y) = A_\nu^r(x^\mu, -y) \sim A_\nu^r(x^\mu, y) + D_\nu \theta^r(x^\mu, y), \quad (3.17)$$

one knows that the gauge functions $\theta^r(x^\mu, y)$ of an arbitrary gauge group have to transform even. Therefore, $\partial_y \theta^r$ transforms odd and

$$A_5^r(x^\mu, y) = -A_5^r(x^\mu, -y) \quad (3.18)$$

has to show the same behaviour.

Let us now consider the standard model in 5D. Neglecting $SU(3)$, the gauge field Lagrangian reads

$$\hat{\mathcal{L}}_{\text{gauge}} = -\frac{1}{4} F_{MN} F^{MN} - \frac{1}{4} F_{MN}^r F^{rMN}, \quad (3.19)$$

with the $U(1)$ field strength

$$F_{MN} = \partial_M B_N - \partial_N B_M \quad (3.20)$$

and the $SU(2)$ field strength

$$F_{MN}^r = \partial_M A_N^r - \partial_N A_M^r + \hat{g} \epsilon^{rst} A_M^s A_N^t. \quad (3.21)$$

The four-dimensional theory is now obtained by inserting the appropriate expansions (3.16a, 3.16b) of the higher-dimensional fields and integrating over the internal dimension. In particular, since the fifth components of the gauge fields have no zero modes, the familiar SM Lagrangian will be recovered in the low-energy limit.

A more detailed look at the contributions from the $U(1)$ gauge group gives

$$\begin{aligned} \mathcal{L}_{\text{gauge}}^{(\text{kin})} &= \int_0^{2\pi R} dy - \frac{1}{4} (\partial_M B_N - \partial_N B_M) (\partial^M B^N - \partial^N B^M) \\ &= -\frac{1}{4} \left(\partial_\mu B_\nu^{(0)} - \partial_\nu B_\mu^{(0)} \right) \left(\partial^\mu B^{(0)\nu} - \partial^\nu B^{(0)\mu} \right) \\ &\quad - \frac{1}{4} \sum_{n=1}^{\infty} \left(\partial_\mu B_\nu^{(n)} - \partial_\nu B_\mu^{(n)} \right) \left(\partial^\mu B^{(1)\nu} - \partial^\nu B^{(1)\mu} \right) \\ &\quad + \frac{1}{2} \sum_{n=1}^{\infty} \left(\partial_\mu B_5^{(n)} + \frac{n}{R} B_\mu^{(n)} \right) \left(\partial^\mu B_5^{(n)} + \frac{n}{R} B^{(n)\mu} \right), \quad (3.22) \end{aligned}$$

with the same expressions valid for the kinetic parts of the other gauge fields as well. At each KK level, there thus appears a massive vector field $B^{(n)}$. The scalar fields $B_5^{(n)}$, however, do not constitute physical degrees of freedom, since one can make them disappear by a gauge transformation (3.17) with $\theta = -(R/n) B_5^{(n)}$. This is reasonable already from a naive counting of degrees of freedom: massless 5D and massive 4D vector fields both have three degrees of freedom, so there is simply no room left for an additional scalar degree of freedom.

The scalar fields thus play the role of Goldstone bosons that give the KK vector modes their mass. This picture is slightly complicated by the fact that there are additional Goldstone bosons associated to each vector boson, which are connected to the usual Higgs mechanism of electroweak symmetry breaking. As discussed in detail in the next section, the mass eigenstates of the theory are then linear combinations of these contributions, resulting in a spectrum of Goldstone as well as physical scalar modes.

The cubic and quartic terms appearing in (3.19) give rise to interaction terms in the 4D Lagrangian. At zero KK level one recovers the SM result, with

$$g \equiv \frac{1}{\sqrt{2\pi R}} \hat{g} \quad (3.23)$$

being the ordinary 4D $SU(2)$ coupling constant. (This relation holds for *all* 5D coupling constants and their 4D counterparts.) At higher KK levels, one finds couplings between both vectors and scalars; the resulting Feynman rules are listed in Appendix A.

3.3.2 The Higgs sector

The Higgs field is a complex $SU(2)$ doublet,

$$\phi \equiv \frac{1}{\sqrt{2}} \begin{pmatrix} \chi^2 + i\chi^1 \\ H - i\chi^3 \end{pmatrix}, \quad \chi^\pm \equiv \frac{1}{\sqrt{2}}(\chi^1 \mp i\chi^2), \quad (3.24)$$

with a 5D Lagrangian that reads

$$\hat{\mathcal{L}}_{\text{Higgs}} = (D_\alpha \phi)^\dagger (D^\alpha \phi) - V(\phi). \quad (3.25)$$

Setting the hypercharge to 1/2, the covariant derivative appearing above is given by

$$D_\alpha = \partial_\alpha - i\hat{g} A_\alpha^r \frac{\sigma^r}{2} - \frac{i}{2} \hat{g}_Y B_\alpha, \quad (3.26)$$

where σ^r are the Pauli matrices,

$$\sigma^1 = \begin{pmatrix} 0 & 1 \\ 1 & 0 \end{pmatrix}, \quad \sigma^2 = \begin{pmatrix} 0 & -i \\ i & 0 \end{pmatrix}, \quad \sigma^3 = \begin{pmatrix} 1 & 0 \\ 0 & -1 \end{pmatrix}, \quad (3.27)$$

and \hat{g}_Y the higher-dimensional $U(1)$ coupling.

The potential $V(\Phi)$ is chosen in such a way that spontaneous symmetry breaking occurs, a prototype being the 'mexican hat' potential³

$$V(\phi) = -\mu^2 \phi^\dagger \phi + \lambda (\phi^\dagger \phi)^2 \quad (3.28)$$

with

$$\lambda = \frac{\mu^2}{\hat{v}^2} = \frac{m_H^2}{2\hat{v}^2}. \quad (3.29)$$

With such a potential, the Higgs field acquires a non-zero vacuum expectation value \hat{v} that can be chosen to lie in the H direction. To reformulate the

³In 4D, the most general renormalizable Lagrangian is actually of the form (3.25), with a potential like (3.28).

theory as an expansion about the true vacuum, one therefore has to replace $H \rightarrow H + \hat{v}$ in the Higgs Lagrangian (3.25).

It is now useful to introduce the standard combinations of vector fields as they appear in the Glashow-Weinberg-Salam electroweak theory:

$$W_M^\pm \equiv \frac{1}{\sqrt{2}}(A_M^1 \mp iA_M^2), \quad (3.30a)$$

$$A_M \equiv s_w A_M^3 + c_w B_M, \quad (3.30b)$$

$$Z_M \equiv c_w A_M^3 - s_w B_M, \quad (3.30c)$$

with

$$s_w \equiv \sin \theta_w = \frac{\hat{g}_Y}{\sqrt{\hat{g}^2 + \hat{g}_Y^2}}, \quad c_w \equiv \cos \theta_w = \frac{\hat{g}}{\sqrt{\hat{g}^2 + \hat{g}_Y^2}}, \quad (3.31)$$

so that $e = s_w g = c_w g_Y$. Suppressing Lorentz indices, the quadratic part of the Higgs kinetic term in (3.25) is then given by

$$\hat{\mathcal{L}}_{\text{Higgs,kin}}^{(2)} = \frac{1}{2}(\partial H)^2 + \frac{1}{2}(\partial\chi^3 - m_Z Z)^2 + |\partial\chi^+ - m_W W^+|^2, \quad (3.32)$$

where

$$m_W \equiv \frac{\hat{g}\hat{v}}{2} = \frac{gv}{2}, \quad m_Z \equiv \frac{m_W}{c_w} \quad (3.33)$$

are the usual SM masses for the vector bosons.

Both in (3.22) and in (3.32) there appear unwanted cross-terms that mix scalar and vector degrees of freedom. They can easily be eliminated by adding suitable gauge-fixing terms to the Lagrangian:

$$\hat{\mathcal{L}}_{\text{gaugefix}} = -\frac{1}{2} \sum_i (\mathcal{G}^i)^2 - \frac{1}{2} (\mathcal{G}^Y)^2, \quad (3.34)$$

$$\mathcal{G}^i = \frac{1}{\sqrt{\xi}} [\partial^\mu A_\mu^i - \xi (-m_W \chi^i + \partial_5 A_5^i)], \quad (3.35a)$$

$$\mathcal{G}^Y = \frac{1}{\sqrt{\xi}} [\partial^\mu B_\mu - \xi (s_w m_Z \chi^3 + \partial_5 B_5^i)]. \quad (3.35b)$$

This is a non-covariant generalization of the R_ξ gauge. From the effective 4D theory's point of view, however, one is anyway restricted to 4D Lorentz transformations and under these, the above expressions remain invariant.

With these lengthy but necessary preparations, one can now introduce those linear combinations of the scalar degrees of freedom that will turn out to be the mass eigenstates of the 4D theory:

$$a_0^{(n)} \equiv \frac{M^{(n)}}{M_Z^{(n)}} \chi^{3(n)} + \frac{m_Z}{M_Z^{(n)}} Z_5^{(n)}, \quad (3.36a)$$

$$G_0^{(n)} \equiv \frac{m_Z}{M_Z^{(n)}} \chi^{3(n)} - \frac{M^{(n)}}{M_Z^{(n)}} Z_5^{(n)}, \quad (3.36b)$$

$$a_{\pm}^{(n)} \equiv \frac{M^{(n)}}{M_W^{(n)}} \chi^{\pm(n)} + \frac{m_W}{M_W^{(n)}} W_5^{\pm(n)}, \quad (3.36c)$$

$$G_{\pm}^{(n)} \equiv \frac{m_W}{M_W^{(n)}} \chi^{\pm(n)} - \frac{M^{(n)}}{M_W^{(n)}} W_5^{\pm(n)}, \quad (3.36d)$$

where $M^{(n)} \equiv n/R$. To finally find the total scalar spectrum of the 4D theory, one has to add up the quadratic scalar contributions from (3.19), (3.28), (3.32) and (3.34) and then integrate over the internal dimension (the Higgs doublet Φ should be present at zero KK level, so it has to transform even under orbifold projections). The result is:

$$\begin{aligned} \mathcal{L}_{\text{scalar}}^{(\text{kin})} = & \sum_{n=0}^{\infty} \left\{ \frac{1}{2} \left(\partial_{\mu} H^{(n)} \partial^{\mu} H^{(n)} - M_H^{(n)2} H^{(n)2} \right) \right. \\ & + \frac{1}{2} \left(\partial_{\mu} G_0^{(n)} \partial^{\mu} G_0^{(n)} - \xi M_Z^{(n)2} G_0^{(n)2} \right) \\ & + \left. \left(\partial_{\mu} G_+^{(n)} \partial^{\mu} G_-^{(n)} - \xi M_W^{(n)2} G_+^{(n)} G_-^{(n)} \right) \right\} + \\ & \sum_{n=1}^{\infty} \left\{ \frac{1}{2} \left(\partial_{\mu} a_0^{(n)} \partial^{\mu} a_0^{(n)} - M_Z^{(n)2} a_0^{(n)2} \right) \right. \\ & + \left(\partial_{\mu} a_+^{(n)} \partial^{\mu} a_-^{(n)} - M_W^{(n)2} a_+^{(n)} a_-^{(n)} \right) \\ & + \left. \frac{1}{2} \left(\partial_{\mu} A_5^{(n)} \partial^{\mu} A_5^{(n)} - \xi M^{(n)2} A_5^{(n)2} \right) \right\}. \quad (3.37) \end{aligned}$$

At zero level, one recovers the SM case with one physical Higgs field $H^{(0)}$ and three Goldstone bosons $G_0^{(0)} = \chi^{3(0)}$, $G_{\pm}^{(0)} = \chi^{\pm(0)}$. For higher KK levels, however, one has four physical scalar fields $H^{(n)}$, $a_0^{(n)}$ and $a_{\pm}^{(n)}$. In

addition, there are four Goldstone bosons $A_5^{(n)}$, $G_0^{(n)}$ and $G_\pm^{(n)}$ that generate the masses for the KK vector modes $A_\mu^{(n)}$, $Z_\mu^{(n)}$ and $W_\mu^\pm^{(n)}$, respectively.

The zero mode contributions of the cubic and quartic terms in (3.25) reproduce of course just the interactions of the SM model Lagrangian. The corresponding Feynman rules, together with those for higher KK modes are collected in Appendix A.

3.3.3 Ghosts

Ghosts are needed in order to cancel the unphysical contributions from time-like and longitudinal polarization states of non-Abelian vector fields (as well as Abelian vector fields in the case of spontaneous symmetry breaking). Following the Faddeev-Popov quantization method, the ghost Lagrangian is determined by how the gauge fixing terms that were introduced in (3.35) vary under infinitesimal gauge transformations

$$\delta A_M^i = \frac{1}{\hat{g}} \partial_M \theta^i + \epsilon^{ijk} A_M^j \theta^k, \quad (3.38a)$$

$$\delta B_M^i = \frac{1}{\hat{g}_Y} \partial_M \theta^Y. \quad (3.38b)$$

It is given by

$$\hat{\mathcal{L}}_{\text{ghost}} = -\bar{c}^a \frac{\delta \mathcal{G}^a}{\delta \theta^b} c^b, \quad (3.39)$$

where $a, b \in \{i, Y\}$ and the ghost fields c^a are anti-commuting, complex scalars that transform even under orbifold projections.

Under the gauge transformations (3.38), the Higgs transforms as

$$\delta \Phi = \left[i \frac{\theta^i \sigma^i}{2} + i \frac{\theta^Y}{2} \right] \Phi \equiv \frac{1}{\sqrt{2}} \begin{pmatrix} \delta \chi^2 + i \delta \chi^1 \\ \delta H - i \delta \chi^3 \end{pmatrix}, \quad (3.40)$$

with

$$\delta \chi^1 = \frac{1}{2} \left[\theta^1 H - \theta^2 \chi^3 + \theta^3 \chi^2 + \theta^Y \chi^2 \right], \quad (3.41a)$$

$$\delta \chi^2 = \frac{1}{2} \left[\theta^1 \chi^3 + \theta^2 H - \theta^3 \chi^1 - \theta^Y \chi^1 \right], \quad (3.41b)$$

$$\delta \chi^3 = \frac{1}{2} \left[-\theta^1 \chi^2 + \theta^2 \chi^1 + \theta^3 H - \theta^Y H \right]. \quad (3.41c)$$

After a rescaling $c^a \rightarrow (\hat{g}_{(Y)} \sqrt{\xi})^{1/2} c^a$, the kinetic part of the 4D ghost Lagrangian then becomes

$$\mathcal{L}_{\text{ghost}}^{(\text{kin})} = \sum_{n=0}^{\infty} \bar{c}^{a(n)} \left\{ -\partial^2 \delta^{ab} - \xi M^{ab(n)} \right\} c^{b(n)}, \quad (3.42)$$

where the mass matrix $M^{ab(n)}$ is given by

$$M^{(n)} = \begin{pmatrix} M_W^{(n)2} & 0 & 0 & 0 \\ 0 & M_W^{(n)2} & 0 & 0 \\ 0 & 0 & M_W^{(n)2} & -\frac{1}{4}v^2 gg_Y \\ 0 & 0 & -\frac{1}{4}v^2 gg_Y & \frac{1}{4}v^2 g_Y^2 + M^{(n)2} \end{pmatrix}. \quad (3.43)$$

Performing the electroweak rotation (3.30), the ghosts will thus end up with masses $\sqrt{\xi}M_W^{(n)}$ and $\sqrt{\xi}M_Z^{(n)}$. The fact that these masses are gauge-dependent, just as those of the Goldstone modes, indicates the unphysical nature of these fields.

Finally, the interaction terms of the ghosts with gauge fields and scalars can be derived in a straight-forward way from the cubic part of the higher-dimensional ghost Lagrangian (see Appendix A).

3.3.4 Fermions

Before discussing the fermionic content of the 5D UED model, let us start this section with a short general introduction to spinors in d dimensions. The operators acting on them are Dirac matrices Γ^M that represent the Clifford algebra:

$$\{\Gamma^M, \Gamma^N\} = 2\eta^{MN}. \quad (3.44)$$

For even $d = 2k + 2$, these are $2^{k+1} \times 2^{k+1}$ -matrices that can explicitly be constructed in an iterative way starting from the Pauli matrices [107]. For odd $d = 2k + 3$, one takes the matrices for the case of one space-time dimension less and adds

$$i\Gamma \equiv i^{1+k}\Gamma^0\Gamma^1\dots\Gamma^{2k+1} \quad (3.45)$$

(or $-i\Gamma$) to give the missing matrix Γ^{2k+2} . From the gamma-matrices one can then construct a set of matrices

$$\Sigma^{MN} \equiv \frac{i}{4} [\Gamma^M, \Gamma^N] \quad (3.46)$$

that satisfy the Lorentz algebra, i.e.

$$[\Sigma^{MN}, \Sigma^{OP}] = i(\eta^{NO}\Sigma^{MP} - \eta^{MO}\Sigma^{NP} + \eta^{MP}\Sigma^{NO} - \eta^{NP}\Sigma^{MO}). \quad (3.47)$$

The so-called *Dirac* representation of both algebras is spanned by spinors $\mathbf{s} = (s_0, \dots, s_k)$, where $s_a = \pm\frac{1}{2}$ are the eigenvalues of the operators

$$S_a \equiv \Gamma^{a+}\Gamma^{a-} - \frac{1}{2}. \quad (3.48)$$

The raising and lowering operators appearing here are defined as

$$\Gamma^{0\pm} \equiv \frac{i}{2}(\pm\Gamma^0 + \Gamma^1), \quad (3.49a)$$

$$\Gamma^{a\pm} \equiv \frac{i}{2}(\Gamma^{2a} \pm i\Gamma^{2a+1}) \quad (\text{for } a = 1, \dots, k) \quad (3.49b)$$

and anticommute with each other:

$$\{\Gamma^{a+}, \Gamma^{b-}\} = \delta^{ab} \quad (3.50a)$$

$$\{\Gamma^{a+}, \Gamma^{b+}\} = \{\Gamma^{a-}, \Gamma^{b-}\} = 0. \quad (3.50b)$$

In odd dimensions, this (2^{k+1} -dim.) Dirac representation is irreducible as a representation of the Lorentz algebra. In *even* dimensions it can be reduced to two inequivalent (2^k -dim.) *Weyl* representations that only act on the subspaces with $\Gamma \mathbf{s} = \pm \mathbf{s}$:

$$\mathbf{2}^{k+1}_{\text{Dirac}} = \mathbf{2}^k_{\text{Weyl}} + \mathbf{2}^{k'}_{\text{Weyl}}. \quad (3.51)$$

(This is because $\{\Gamma, \Gamma^M\} = 0$ and therefore $[\Gamma, \Sigma^{MN}] = 0$; in odd dimensions, however, Γ is itself an element of the Clifford algebra and does thus no longer (anti-)commute with Γ^M or Σ^{MN}).

The eigenvalue of Γ is called *chirality*; it takes the value $+1$ if there is an even number of $s_a = +\frac{1}{2}$ and -1 for an odd number. This property can be used to construct projection operators

$$P_{R,L} \equiv \frac{1}{2}(1 \pm \Gamma), \quad P_{R,L}^2 = P_{R,L}, \quad P_L P_R = P_R P_L = 0, \quad (3.52)$$

that project out the chiral parts of any spinor

$$\psi = P_R \psi + P_L \psi \equiv \psi_R + \psi_L. \quad (3.53)$$

As a side-remark, chiral states in 4D are states of definite *helicity*, which is defined as the projection of the particle's spin onto the direction of its motion; states of positive (negative) chirality have also positive (negative) helicity and are therefore called right-handed (left-handed). Finally, with the help of the projection operators introduced above, one can easily see that chiral fermions have to be massless, since any mass term in the Lagrangian would mix states of different chiralities:

$$\hat{\mathcal{L}}_f = \bar{\psi}(i\mathcal{D} - m)\psi = i\bar{\psi}_R \mathcal{D} \psi_R + i\bar{\psi}_L \mathcal{D} \psi_L - m(\bar{\psi}_R \psi_L + \bar{\psi}_L \psi_R). \quad (3.54)$$

To conclude this detour, chiral fermions only exist in an even number of dimensions.

Let us now return to the UED model. According to what has been said above, one can use

$$\Gamma = i\gamma^0\gamma^1\gamma^2\gamma^3 \equiv \gamma^5 \quad (3.55)$$

both in four and in five dimensions to split up any spinor in its chiral parts as in (3.53). Under 5D Lorentz transformations, ψ_R and ψ_L would then obviously mix. Restricting oneself to 4D Lorentz transformations, however, they do *not* mix. Therefore, one may assign different orbifold transformation properties to these states and thereby recover the SM situation at the zero mode level, where one has singlets ψ_s and doublets ψ_d of definite chirality:

$$\psi_d = \frac{1}{\sqrt{2\pi R}}\psi_{dL}^{(0)} + \frac{1}{\sqrt{\pi R}}\sum_{n=1}^{\infty}\left(\psi_{dL}^{(n)}\cos\frac{ny}{R} + \psi_{dR}^{(n)}\sin\frac{ny}{R}\right), \quad (3.56a)$$

$$\psi_s = \frac{1}{\sqrt{2\pi R}}\psi_{sR}^{(0)} + \frac{1}{\sqrt{\pi R}}\sum_{n=1}^{\infty}\left(\psi_{sR}^{(n)}\cos\frac{ny}{R} + \psi_{sL}^{(n)}\sin\frac{ny}{R}\right). \quad (3.56b)$$

Note that in the above expressions, for every SM fermion

$$\psi^{(0)} = \psi_{dL}^{(0)} + \psi_{sR}^{(0)} = \psi_d^{(0)} + \psi_s^{(0)} \quad (3.57)$$

there appear *two* fermions at each KK level:

$$\psi_s^{(n)} \equiv \psi_{sL}^{(n)} + \psi_{sR}^{(n)} \quad (3.58a)$$

$$\psi_d^{(n)} \equiv \psi_{dL}^{(n)} + \psi_{dR}^{(n)}. \quad (3.58b)$$

To make this more evident, let us consider the kinetic part of the fermion Lagrangian, with the anticipation of a fermion mass m_{EW} from electroweak symmetry breaking,

$$\hat{\mathcal{L}}_{\text{fermion}}^{(\text{kin})} = i\bar{\psi}_d\Gamma^M\partial_M\psi_d + i\bar{\psi}_s\Gamma^M\partial_M\psi_s - m_{\text{EW}}(\bar{\psi}_s\psi_d + \bar{\psi}_d\psi_s). \quad (3.59)$$

Next, introduce those KK fermions that will turn out to be the mass eigenstates of the 4D theory:

$$\xi_d^{(n)} \equiv \cos\alpha^{(n)}\psi_d^{(n)} + \sin\alpha^{(n)}\psi_s^{(n)}, \quad (3.60a)$$

$$\xi_s^{(n)} \equiv \sin\alpha^{(n)}\gamma^5\psi_d^{(n)} - \cos\alpha^{(n)}\gamma^5\psi_s^{(n)}, \quad (3.60b)$$

where the mixing angle

$$\tan 2\alpha^{(n)} = \frac{m_{\text{EW}}}{n/R} \quad (3.61)$$

is effectively driven to zero except for the top quark. With the expansions (3.56) and $\Gamma^\mu = \gamma^\mu$, $\Gamma^5 = i\gamma^5$, one then finds

$$\begin{aligned}\mathcal{L}_{\text{fermion}}^{(\text{kin})} &= \int_0^{2\pi R} dy \hat{\mathcal{L}}_{\text{fermion}}^{(\text{kin})} \\ &= \bar{\psi}^{(0)} (i\partial\!\!\!/ - m_{\text{EW}}) \psi^{(0)} \\ &\quad + \sum_{n=1}^{\infty} \bar{\xi}_s^{(n)} \left(i\partial\!\!\!/ - M^{(n)} \right) \xi_s^{(n)} \\ &\quad + \sum_{n=1}^{\infty} \bar{\xi}_d^{(n)} \left(i\partial\!\!\!/ - M^{(n)} \right) \xi_d^{(n)},\end{aligned}\tag{3.62}$$

where the fermion KK masses $M^{(n)}$ are given by the usual relation (3.14).

Fermions couple to gauge bosons through the covariant derivative that appears in the kinetic part of the Lagrangian:

$$\begin{aligned}\hat{\mathcal{L}}_{\text{fermion}}^{(\text{vector})} &= i(\bar{\psi}'_{d,U}, \bar{\psi}'_{d,D}) \Gamma^M \left(-i\hat{g} A_M^r \frac{\sigma^r}{2} - iY_d \hat{g}_Y B_M \right) \begin{pmatrix} \psi'_{d,U} \\ \psi'_{d,D} \end{pmatrix} \\ &\quad + i\bar{\psi}'_{s,U} \Gamma^M (-iY_{s,U} \hat{g}_Y B_M) \psi'_{s,U} \\ &\quad + i\bar{\psi}'_{s,D} \Gamma^M (-iY_{s,D} \hat{g}_Y B_M) \psi'_{s,D},\end{aligned}\tag{3.63}$$

where U and D denote up-type ($T^3 = +1/2$) and down-type ($T^3 = -1/2$) fermions, respectively, and $Y_{s,U}$, $Y_{s,D}$, Y_d are the hypercharges of the corresponding $SU(2)$ representations. Note that the ψ' in the above expression are $SU(2) \times U(1)$ eigenstates, *not* the 5D mass eigenstates ψ that appear in (3.59). For leptons, the states $\psi_{s,U}$ (i.e. right-handed neutrinos) do not exist and therefore one can replace $\psi' \rightarrow \psi$ [103]. For quarks, one still can choose $\psi'_s = \psi_s$, but the doublet eigenstates are related by unitary matrices $U_{U,D}$:

$$\psi'_{d,U}{}^i = U_U^{ij} \psi_{d,U}^j, \quad \psi_{d,D}{}^i = U_D^{ij} \psi_{d,D}^j,\tag{3.64}$$

where i, j run over all (three) families. The matrix $V = U_U^\dagger U_D$ is known as *Cabbibo-Kobayashi-Maskawa* mixing matrix.

Finally, there is the Yukawa coupling of fermions to the Higgs field:

$$\hat{\mathcal{L}}_{\text{fermion}}^{(\text{Yukawa})} = -\hat{\lambda}_D [(\bar{\psi}_{d,U}, \bar{\psi}_{d,D}) \cdot \tilde{\Phi}] \psi_{s,D} - \hat{\lambda}_U [(\bar{\psi}_{d,U}, \bar{\psi}_{d,D}) \cdot \tilde{\Phi}] \psi_{s,U} + \text{h.c.},\tag{3.65}$$

where the conjugated Higgs field is defined by $\tilde{\Phi}_a \equiv \epsilon_{ab} \Phi_b^\dagger$. Taking into account all three families of fermions, the coupling strengths $\hat{\lambda}_d$ and $\hat{\lambda}_u$ are actually given by 3×3 matrices – but in the basis of fermion mass

eigenstates that is chosen here, they are diagonal in flavour. Performing the shift $H \rightarrow H + \hat{v}$ from electroweak symmetry breaking corresponds to replacing

$$\hat{\mathcal{L}}_{\text{fermion}}^{(\text{Yukawa})} \rightarrow \hat{\mathcal{L}}_{\text{fermion}}^{(\text{Yukawa})} - \left(\frac{\hat{\lambda}_D \hat{v}}{\sqrt{2}} \bar{\psi}_{d,D} \psi_{s,D} - \frac{\hat{\lambda}_U \hat{v}}{\sqrt{2}} \bar{\psi}_{d,U} \psi_{s,U} + \text{h.c.} \right), \quad (3.66)$$

which gives a mass $m_{\text{EW}} = (\hat{\lambda}_{D,U} \hat{v})/\sqrt{2}$ to the fermions.

Finally, from (3.63) and (3.65), one can derive the 4D Feynman rules for interactions between fermions and gauge bosons or scalar fields (see Appendix A).

3.3.5 Radiative corrections

So far, only electroweak mass contributions to the various states of the 4D theory have been discussed. For KK modes, however, radiative corrections can generically be expected to be much more important: assuming a compactification scale of about 1 TeV, the relative contribution of the former to the first KK level mass is given by $(m_{\text{EW}} R)^2$ and ranges from 10^{-12} for electrons to 10^{-2} for the top quark, while the latter should give corrections of the order $\mathcal{O}(\alpha)$ from the relevant gauge couplings, which is at the percent level.

Radiative mass corrections arise from vacuum polarization diagrams, i.e. higher-order contributions to the two-point correlation functions. In order to calculate the net effect of the presence of EDs, one has to subtract the corresponding diagram in four dimensions from its higher-dimensional analogue; with this prescription, all ultra-violet divergences that are present already in the 4D theory are cancelled and the result is a mass shift δm^2 that is purely due to radiative corrections deriving from the presence of EDs [46].

One can isolate two types of contributions to these mass shifts. The first one is attributed to the compactification on a circle \mathbb{S}^1 , which does not break 5D Lorentz invariance locally, but globally. As a non-local effect, loops can wind around the compact dimension as shown in Fig. 3.1; since there is no analogue of such loops in the 4D theory, their contribution will survive the subtraction scheme described above. The second type is a local effect that derives from the fact that 5D translational invariance is broken at the boundaries of $\mathbb{S}^1/\mathbb{Z}_2$. By expressing all fields in terms of auxiliary fields that do not obey the orbifold symmetry, one can effectively describe the $\mathbb{S}^1/\mathbb{Z}_2$ compactification by introducing modified 5D propagators in the same theory

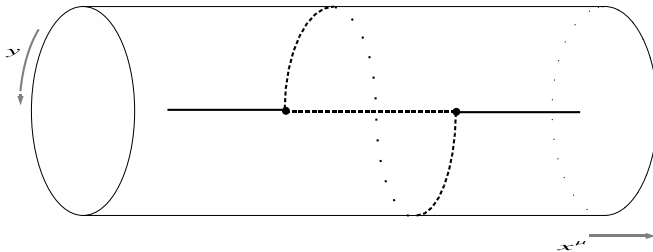


Figure 3.1: Example of a loop winding around the EDs, giving rise to a 5D Lorentz invariance breaking contribution to the two-point correlation function.

compactified on \mathbb{S}^1 [66]. In contrast to the first type of contributions to the mass-shift, this one is no longer finite by itself but has to be renormalized by introducing counterterms localized at the orbifold fixpoints. In order to keep the model-dependence on unknown physics at the cutoff scale Λ under control, one usually follows the self-consistent assumption that these boundary terms are small at that scale. In that case there is no mixing among different KK modes and each mode receives, in addition to the first effect, a contribution to its mass that is logarithmically proportional to Λ .

The resulting spectrum of the first KK level has been calculated in [46] and is shown in Fig. 3.2. As can be seen, the degeneracy of KK masses at tree level is lifted at the one-loop level and the *lightest KK particle* (LKP) can be identified as the first KK excitation of the photon. Having a closer look at the mass matrix for the A^3 and B gauge bosons,

$$\begin{pmatrix} \left(\frac{n}{R}\right)^2 + \delta m_{A^3}^{(n)2} + \frac{1}{4}v^2g^2 & -\frac{1}{4}v^2gg_Y \\ -\frac{1}{4}v^2gg_Y & \left(\frac{n}{R}\right)^2 + \delta m_B^{(n)2} + \frac{1}{4}v^2g^2 \end{pmatrix}, \quad (3.67)$$

one finds that the n th KK level Weinberg angle is given by

$$\tan 2\theta^{(n)} = \frac{v^2gg_Y}{2[\delta m_{A^3}^{(n)2} - \delta m_B^{(n)2} + \frac{v^2}{4}(g^2 - g_Y^2)]}. \quad (3.68)$$

Generically, one has $\delta m_{A^3}^{(n)2} - \delta m_B^{(n)2} \gg v^2gg_Y$ (see also Fig. 3.2), which means that the Weinberg angle is effectively driven to zero at any KK level. Therefore, the LKP is well approximated by $B^{(1)}$, the first KK excitation of the weak hypercharge boson and in the following, these two expressions will be used interchangeably.

Instead of taking the exact expressions as determined in [46], one might also consider to follow a more phenomenological approach and treat the

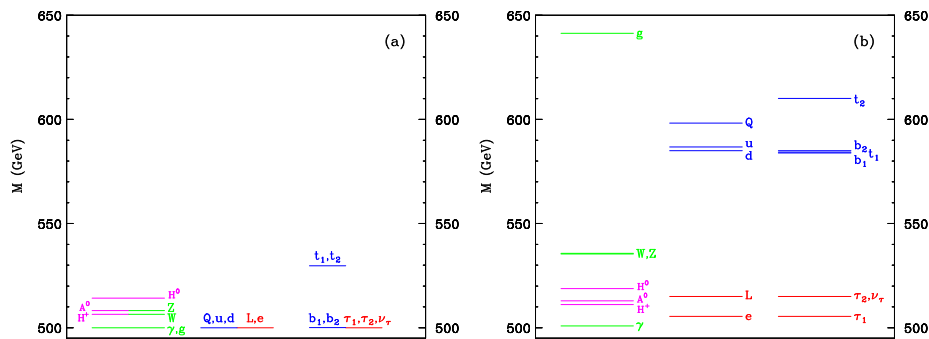


Figure 3.2: (Taken from [46]). The full spectrum of the UED model at the first KK level, a) at tree level and b) including one loop radiative corrections, for $R^{-1} = 500$ GeV and $\Lambda R = 20$. The first column shows the gauge and Higgs bosons, where $\{H^0, H^\pm, A^0\}$ correspond to $\{H, a_\pm, a_0\}$ in the notation introduced in Section 3.3.2. In the second column, the quark doublet (Q) and singlets (u, d) as well as lepton doublet (L) and singlet (e) are shown for the first two families; In the last column, finally, this is repeated for the third family to illustrate the large electroweak mass shift of the top quark.

radiative corrections to the KK masses as an independent input to the theory (see, e.g., [114]). For simplicity, it is then often assumed that all KK modes except for the LKP are degenerate in mass; this approach should in general not have a great influence on the phenomenology of the model, except for some special situations like co-annihilations (see the discussion in Chapter 5.1).

Chapter 4

Stabilization of Homogeneous Extra Dimensions

As outlined in the last chapter, a generic property of theories involving EDs is that the observed four-dimensional couplings can no longer be regarded as fundamental constants of nature but rather emerge as effective quantities in the low-energy limit of the theory. This means that all interactions with fields fundamentally living in more than four dimensions exhibit couplings that vary with the volume – and sometimes even shape – of the internal space.

Possible variations of the observed coupling constants, on the other hand, are heavily constrained (see Section 4.1). Since most of these constraints come from cosmological considerations, this means that the EDs have to be effectively stabilized on cosmological timescales. One of the main tasks in KK cosmology is therefore to provide a dynamical explanation for this stabilization and, in order not to spoil the successes of standard cosmology, to find late-time solutions to the higher-dimensional equations of motion that describe $(4 + n)$ -dimensional spacetimes of the form $F^4 \times K$, with F^4 being the ordinary Friedmann solution and K a compact, (nearly) static n -dimensional manifold. The case of non-compact EDs (see Section 3.2) is of course also of importance, but will not be considered here.

The general setup and the resulting Friedmann equations to study the evolution of a homogeneous, higher-dimensional universe are presented in Section 4.2. An alternative way to arrive at the equations of motion, this time from the point of view of the effective lower-dimensional theory, is then

described in Section 4.3. In both cases, as shown in Section 4.4, one is lead to the conclusion that homogeneous EDs can easily be stabilized during both radiation and vacuum energy dominated epochs of the cosmological evolution; during matter domination, however, one encounters generic problems. Section 4.5 discusses the possibility of explicitly adding stabilization mechanisms to the original theory; it turns out that even in this case one cannot get exactly static solutions as soon as the amount of non-relativistic matter in the universe is no longer negligible – though it seems that the existing bounds on time-varying EDs can nevertheless be satisfied rather easily.

The material presented in this chapter is based to a large degree on the accompanying papers [I] (Sections 4.2 and 4.4) and [II] (Section 4.3 and part of Section 4.5).¹ Note that in this chapter the sign-conventions of [93] are used, meaning in particular that the signature of the metric is space- rather than timelike as in the rest of this thesis.

4.1 Constraints on the allowed time variation of extra dimensions

Since gravity cannot be disentangled from spacetime itself, Newtons constant (i.e. the 4D gravitational coupling constant) $G = \kappa^2/8\pi$ will inevitably vary with the volume of the internal space for *any* extra-dimensional scenario. As it has become obvious from the discussion in Section 3.3, the UED model exhibits furthermore the interesting feature that *all* interactions pick up the same volume factor (3.7), relating higher dimensional (i.e. fundamental and thus truly constant) and 4D (i.e. observed) coupling 'constants'. In the following, the most important bounds on a possible time variation of any of these constants will therefore be presented in the form of a short overview. For a more detailed review, see [124].

The variation of the gravitational constant today is best constrained by radar measurements of the orbital separation of Earth, Venus and Mercury, which gives $\dot{G}/G \lesssim 10^{-12} \text{ yr}^{-1}$ [9]. On cosmological time scales, one may use the fact that a variation in G would change the expansion rate of the universe during BBN; this translates into the demand that $\Delta G/G \lesssim 0.2$ between BBN and today [124]. While a time-varying G certainly also would have impacts on the CMB, it is hard to draw any definite conclusions about the allowed amount of variation in a model-independent way; this is because not only the value of G at photon decoupling, but (due to the integrated

¹The contribution to the proceedings of 'Phi in the Sky. Workshop on the cosmological role of scalar fields.' [41] can be read as a comprehensive summary of the work in [I, II].

Sachs-Wolfe effect) its entire evolution history since then will influence the spectrum of the CMB anisotropies.

Limits on a possible variation of the electromagnetic coupling constant α_{em} are much tighter and derive from various different eras of the cosmological evolution. In fact, there has even been the claim that one can see a variation $\Delta\alpha_{\text{em}}/\alpha_{\text{em}} \sim 10^{-5}$ at $z \sim 1$ from the absorption lines of distant quasars [125, 126] – which, however, has been contested by Bahcall *et al.* [17]; the newest upper bound from this kind of observations lies nearly two orders of magnitude below the originally claimed effect [119]. A change in the electromagnetic coupling would also clearly have an impact on the synthesis of light elements during BBN; this places an upper bound of $\Delta\alpha_{\text{em}}/\alpha_{\text{em}} \lesssim 10^{-2}$ at $z_{\text{BBN}} \sim 10^{10}$ [25]. CMB observations can in principle be used to infer $\Delta\alpha_{\text{em}}/\alpha_{\text{em}} \lesssim 10^{-2}$ at $z \sim 10^3$ [75], but there is a strong degeneracy with other cosmological parameters and this method therefore only works if one has a good handle on them, i.e. if they can be determined by independent observations. Finally, one may even use the ^{149}Sm abundances as found in the natural reactor at Oklo, West Gabon, to get a constraint of $\Delta\alpha_{\text{em}}/\alpha_{\text{em}} \lesssim 10^{-8}$ at $z \sim 0.14$ [63]. However, this last constraint should be taken with a grain of salt when considering the allowed variation of α_{em} in a cosmological context; this is because it is taken from a region of particularly high matter density – i.e. the earth – and depending on how the radion (the scalar field that corresponds to the volume of the internal space, see Section 4.3) couples to the matter part of the 4D Lagrangian, one may actually be able to evade his constraint.

A change in the coupling strength of the weak interaction shows an effect in similar areas as discussed above for the case of α_{em} . For example, the value of the Fermi constant G_F has of course an impact on nucleosynthesis; in order not get a wrong prediction for the observed helium abundance, in particular, one arrives at almost the same constraints as before, i.e. $\Delta G_F/G_F \lesssim 10^{-2}$ at z_{BBN} [43]. However, these kinds of analyses are generally hampered by the fact that some of the effects may be mimicked by, e.g., an independent variation of the Yukawa couplings; it seems therefore difficult to draw any definite conclusions that are independent of how electroweak symmetry breaking takes place or how the Fermion masses are generated [124].

To summarize, the cosmologically maybe most important conclusion is that the volume of the internal space must not have changed by more than about one percent since BBN. One should, however, remember that this and other constraints usually only derive from ‘snapshots’ of the cosmological history and little is known about what could have happened in between.

4.2 The higher-dimensional Friedmann equations

By varying the action

$$S = \frac{1}{2\hat{\kappa}^2} \int d^{4+n} X \sqrt{-g} \left(R - 2\Lambda + 2\hat{\kappa}^2 \hat{\mathcal{L}}_{\text{matter}} \right) \quad (4.1)$$

one arrives at Einstein's field equations in $d = 4 + n$ dimensions:

$$R_{AB} - \frac{1}{2} R g_{AB} + \Lambda g_{AB} = \hat{\kappa}^2 T_{AB}. \quad (4.2)$$

For a separable spacetime like $F^4 \times K$, the internal space has to be an Einstein space as a consequence of these field equations [117]. A natural, though obviously rather simplified cosmological ansatz for (4.2) is thus a higher-dimensional metric of the form

$$g_{AB} dX^A dX^B = g_{\mu\nu} dx^\mu dx^\nu + b^2(x^\mu) \tilde{g}_{pq} dy^p dy^q, \quad (4.3)$$

where \tilde{g}_{pq} depends on the internal coordinates y^p only. Taking $g_{\mu\nu}$ to be of FRW form (2.1) and assuming $b = b(t)$, one now has *two* scale factors $a(t)$ and $b(t)$ that describe the cosmological evolution of the ordinary, large dimensions and the internal space, respectively. Such a choice of the metric determines the energy-momentum tensor to be of the form²

$$T_{00} = -\hat{\mathcal{L}}_{\text{matter}} = \hat{\rho}, \quad T_{ij} = \hat{p}_a g_{ij}, \quad T_{3+p3+q} = \hat{p}_b b^2 \tilde{g}_{pq}, \quad (4.4)$$

which is that of a homogeneous but in general anisotropic perfect fluid in its rest frame.

From the field equations (4.2), one now finds the higher-dimensional version of the ordinary Friedmann equations:

²Note that there is a typo in the corresponding expressions in [II, 41]. Furthermore, some of the sign conventions there do not really follow standard practice. While neither of this changes any of the results of [II, 41], it might still be quite confusing; when in doubt, please refer to this thesis for the (hopefully) correct version. Note furthermore that $\bar{g}^{\mu\nu}$ and 'hatted' quantities are introduced in a way that is different from [I, II, 41], but consistent with the conventions of the rest of this thesis.

$$3 \left[\left(\frac{\dot{a}}{a} \right)^2 + \frac{k_a}{a^2} \right] + 3n \frac{\dot{a}\dot{b}}{ab} + \frac{n(n-1)}{2} \left[\left(\frac{\dot{b}}{b} \right)^2 + \frac{k_b}{b^2} \right] = \Lambda + \hat{\kappa}^2 \hat{\rho} \quad (4.5a)$$

$$2 \frac{\ddot{a}}{a} + \left(\frac{\dot{a}}{a} \right)^2 + \frac{k_a}{a^2} + 2n \frac{\dot{a}\dot{b}}{ab} + n \frac{\ddot{b}}{b} + \frac{n(n-1)}{2} \left[\left(\frac{\dot{b}}{b} \right)^2 + \frac{k_b}{b^2} \right] = \Lambda - \hat{\kappa}^2 \hat{\rho}_a \quad (4.5b)$$

$$\frac{\ddot{b}}{b} + 3 \frac{\dot{a}\dot{b}}{ab} + (n-1) \left[\left(\frac{\dot{b}}{b} \right)^2 + \frac{k_b}{b^2} \right] = \frac{2\Lambda}{n+2} + \frac{\hat{\kappa}^2}{n+2} (\hat{\rho} - 3\hat{\rho}_a + 2\hat{\rho}_b) \quad (4.5c)$$

where a dot denotes differentiation with respect to t .

One can immediately see that for exactly static extra dimensions, and after an appropriate rescaling of Λ , the first two equations are nothing but the ordinary Friedmann equations (2.5). The question then is, how (4.5c) can be satisfied simultaneously.

4.3 Dimensional reduction

Before returning to this question, let us first take a different perspective and consider the dimensionally reduced theory rather than the field equations (4.2) that were obtained by varying the higher-dimensional action. After integrating (4.1) over the internal dimensions, with the ansatz (4.3) for the metric, one arrives at the following four-dimensional action:

$$S = \frac{1}{2\bar{\kappa}^2} \int d^4x \sqrt{-g} b^n \left(R + b^{-2} \tilde{R} + n(n-1)b^{-2} \partial_\mu b \partial^\mu b - 2\Lambda + 2\hat{\kappa}^2 \hat{\mathcal{L}}_{\text{matter}} \right), \quad (4.6)$$

where $\bar{\kappa}^2 \equiv \hat{\kappa}^2 / \int d^n y \sqrt{\tilde{g}}$ and R (\tilde{R}) is the curvature scalar constructed from $g_{\mu\nu}$ (\tilde{g}_{pq}). By a conformal transformation to a new metric $\bar{g}_{\mu\nu} = b^n g_{\mu\nu}$, this action can be rewritten in the so-called *Einstein frame*, where the 4D curvature scalar appears without any conformal prefactors:

$$S = \int d^4x \sqrt{-\bar{g}} \left(\frac{1}{2\bar{\kappa}^2} \bar{R} - \frac{1}{2} \partial_\mu \Phi \partial^\mu \Phi - V_{\text{eff}}(\Phi) \right). \quad (4.7)$$

This describes four-dimensional gravity minimally coupled to a scalar field $\Phi \equiv \sqrt{\frac{n(n+2)}{2\bar{\kappa}^2}} \ln b$ (sometimes referred to as *radion*), with a potential

$$V_{\text{eff}}(\Phi) = -\frac{\tilde{R}}{2\bar{\kappa}^2} e^{-\sqrt{\frac{2(n+2)\bar{\kappa}^2}{n}}\Phi} + \frac{1}{\bar{\kappa}^2} \left(\Lambda - \hat{\kappa}^2 \hat{\mathcal{L}}_{\text{matter}} \right) e^{-\sqrt{\frac{2n\bar{\kappa}^2}{n+2}}\Phi}. \quad (4.8)$$

The equations of motion derived from (4.7) are as expected equivalent to the higher-dimensional field equations (4.5) that were obtained with the approach of the last section. Equation (4.5c), in particular, gets a rather intuitive interpretation – it is the equation of motion for the radion,

$$\bar{\nabla}_\mu \bar{\nabla}^\mu \Phi = V'_{\text{eff}}(\Phi). \quad (4.9)$$

The quest for static solutions has thus been reformulated into the question whether the effective potential $V_{\text{eff}}(\Phi)$ exhibits minima or not.

As a by-product, the alternative approach of this section allows one to address a subtle issue related to higher-dimensional theories of gravity, that has received attention only rather recently and has been completely neglected in the first days of Kaluza-Klein cosmology: Since there are in principle infinitely many, mathematically equivalent frames that are related to each other by a conformal transformation, caution must be taken as to which of the conformally related metrics one identifies as the physical one. The requirement that the conformally transformed system in four dimensions has positive definite energy actually singles out a unique conformal factor [117, 47, 59], which is just the one that transforms to the Einstein frame (4.7). This suggests that $\bar{g}_{\mu\nu}$ – rather than the naive first guess $g_{\mu\nu}$ – should be regarded as the physical metric, with $d\bar{t} \equiv b^{\frac{n}{2}} dt$ being the measured cosmological time and $\bar{a} \equiv b^{\frac{n}{2}} a$ the ordinary 4D scale factor.

This issue does not seem to be completely settled yet, though. In particular, the choice of the Einstein frame results in a non-minimal coupling of the scalar field to the rest of the matter part via the form of the effective potential in (4.8). This has sometimes been used as an argument why one instead should regard the *Jordan frame* as the physical one, see e.g. the discussion given in [47, 59]. Even the explicit view that all conformally related frames are not only mathematically but also physically equivalent finds sometimes still support [60].

Given the tight bounds on the allowed time-variation of b , however, the difference between a and \bar{a} (or t and \bar{t}) should of course be negligible for all practical purposes.

4.4 Cosmological evolution of scale factors

From equation (4.5c) it is obvious that static solutions can only exist if

$$\hat{\rho} - 3\hat{p}_a + 2\hat{p}_b = \text{const.} \quad (4.10)$$

(and Λ and k_b are tuned in a suitable way). Only in that case, to use the language of Section 4.3, the minimum of the effective potential $V_{\text{eff}}(\Phi)$

becomes time-independent. If furthermore $\Lambda = k_b = \hat{\rho} - 3\hat{p}_a + 2\hat{p}_b = 0$, the effective potential is flat, i.e. independent of Φ .

So when can one expect (4.10) to hold? Obviously, one possibility is given by $\hat{\rho}$, \hat{p}_a and \hat{p}_b being constant separately – as is the case for a cosmological constant. Also during radiation domination (with $\hat{p}_a = \frac{1}{3}\hat{\rho}$) one can have static solutions if the pressure in the extra dimensions is constant or negligible. However, for periods of the cosmological evolution with other equations of state one cannot expect to find static solutions unless one allows for rather contrived equation-of-state parameters. In particular, during matter domination (with $\hat{p}_a \ll \hat{\rho}$) one would need $\hat{p}_b = -\frac{1}{2}\hat{\rho}$, which is very hard to motivate.

With exactly static solutions being no longer an alternative, one has to study in detail the evolution of the scale factor $b(t)$ and make sure that it does not violate the existing bounds that were reviewed in Section 4.1. To do this, the details of the model must be specified, particularly the equation-of-state parameters during various eras of the cosmological evolution. In the following, this is done for the special case of Kalua-Klein dark matter appearing in the UED model (see Section 3.3 and 5.1). The runaway-behaviour for b that is found, however, does not seem to be very specific for UEDs but rather a general feature of homogeneous extra-dimensional models. In fact, problems with the stabilization of EDs even arise in certain braneworld models once one allows for non-relativistic contributions to the matter content [15].

4.4.1 Case study: Universal extra dimensions

Let us assume that the LKP constitutes most of the dark matter. The momentum of the LKP in the direction of the internal space is basically given by the compactification scale, which is about 1 TeV. This is much larger than the particle's rest mass, even if the LKP was not the $B^{(1)}$ but the first KK excitation of any other SM particle, so from a higher-dimensional perspective our universe has always been dominated by relativistic matter (neglecting for the moment the rather recent vacuum energy domination). This means that one has an equation of state

$$\hat{p}_a = \frac{1}{3}\hat{\rho}, \quad \hat{p}_b = 0 \quad (4.11)$$

during what looks like radiation domination and

$$\hat{p}_a = 0, \quad \hat{p}_b = \frac{1}{n}\hat{\rho} \quad (4.12)$$

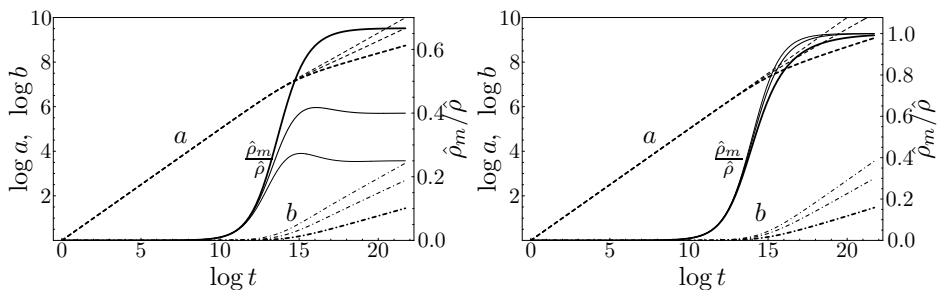


Figure 4.1: The evolution of the scale factors a and b , as well as the fractional energy density in non-relativistic matter $\hat{\rho}_m/\hat{\rho}$ for $n = 1$ (thin), 2 (medium) and 7 (thick) with $(\hat{\rho}_m/\hat{\rho})_i = 10^{-7}$ and $\Lambda = k_b = 0$. The figure on the left (from [I]) shows the case of KK dark matter, where the matter-dominated period is described by an equation of state $\hat{p}_a = 0$, $\hat{p}_b = 1/n\hat{\rho}$. The right figure (from [41]) shows the case where the LKP-contribution to the dark matter is negligible and one instead has $\hat{p}_a = \hat{p}_b = 0$ during matter-domination.

during what looks like matter domination from a four-dimensional point of view.³

Starting with a tiny amount of LKPs in the radiation-dominated regime, Fig. 4.1 shows the evolution of the scale factors for such a set-up. For comparison, the case of $\hat{p}_a = \hat{p}_b = 0$ during matter-domination (i.e. negligible LKP contribution to the dark matter) is also included. In both cases, the scale factor b starts to grow much faster than allowed by the constraints given in Section 4.1 once the energy density in matter reaches about 10% of the total energy density. In fact, also the evolution of the scale factor a (as well as that of \bar{a}) deviates significantly from that of standard cosmology. In conclusion, such a behaviour is definitely ruled out.

³For more details see [I]. It should be noted that the interpretation of $p_a = \hat{p}_a \hat{\kappa}^2/\kappa^2$ as the ordinary pressure in 4D implicitly relies on the (incorrect) assumption that $g_{\mu\nu}$ is the physical metric. As remarked before, for approximate static solutions this is a subtlety without great practical relevance.

4.5 Stabilization and the recovery of standard cosmology

In order to find a dynamical explanation for the stabilization (and compactification) of extra dimensions one usually introduces additional background fields. Since their role is to separate ordinary from the internal space, they typically contribute an effective action of the form

$$S^{\text{bg}} = - \int d^{4+n} X \sqrt{-g} W(b) \quad (4.13)$$

to the theory. This means that one has to replace $\hat{\mathcal{L}}_{\text{matter}} \rightarrow -(\hat{\rho} + W)$ in (4.8), where $\hat{\rho}$ now denotes the energy density of everything but the background fields. As a result of this, the effective potential V_{eff} would no longer be flat during radiation or vacuum energy domination, but have a minimum at which the scalar field can be stabilized. However, during matter domination, or for virtually any other equation of state, this minimum is still time-dependent through its dependence on $\hat{\rho}$ [II]. Exactly static solutions during matter domination are therefore not possible to achieve in this framework either, even though the ansatz (4.13) is very general.

On the other hand, if the potential well at the minimum of $W(\Phi) = W(b(\Phi))$ is steep enough, the time-dependent term $\hat{\rho}$ in V_{eff} should only shift the minimum slightly. In that way, the runaway-behaviour of the scale factor b that was found in Section 4.4.1 could be avoided; this would allow an *effective* stabilization of the EDs and thus a recovery of standard cosmology.

To quantify this last remark, assume that $\Lambda = k_b = 0$. Starting off very near the minimum Φ_0 due to the contribution of $W(\Phi)$, the effective potential (4.8) can be written as

$$\begin{aligned} V_{\text{eff}}(\Phi) &\simeq \frac{m^2}{2}(\Phi - \Phi_0)^2 + \frac{\kappa^2}{\bar{\kappa}^2} \rho e^{-\sqrt{\frac{2n\bar{\kappa}^2}{n+2}}\Phi} \\ &\equiv \frac{m^2}{2}(\Phi - \Phi_0)^2 + \rho e^{-(1-3w_a+2w_b)\sqrt{\frac{n\bar{\kappa}^2}{2(n+2)}}(\Phi-\Phi_0)}, \end{aligned} \quad (4.14)$$

where in the last step the 4D energy density ρ as it appears in the Einstein frame was identified by using

$$\hat{\rho} \propto a^{-3(1+w_a)} b^{-n(1+w_b)} = \bar{a}^{-3(1+w_a)} \bar{b}^{-n/2(-1-3w_a+2w_b)}, \quad (4.15)$$

with $w_{a,b} \equiv \hat{p}_{a,b}/\hat{\rho}$; it is that part of the effective potential that does not depend on the scalar field Φ for small deviations about its minimum. With

this, the actual minimum of the effective potential is given by

$$\Phi_{\min} = \Phi_0 + \frac{1 - 3w_a + 2w_b}{m^2} \sqrt{\frac{n\bar{\kappa}^2}{2(n+2)}} \rho e^{-(1-3w_a+2w_b)\sqrt{\frac{n\bar{\kappa}^2}{2(n+2)}}(\Phi_{\min}-\Phi_0)}. \quad (4.16)$$

Let us now estimate the effect of such a shift in the minimum since BBN, where the density in non-relativistic matter was $\rho \sim \rho_0 z_{BBN}^3 \sim 10^{19} \text{ eV}^4$. Setting $w_a = w_b = 0$ for simplicity, one finds that the resulting change in the scale factor b is only about 0.006 % for a mass as tiny as $m = 10^{-16} \text{ eV}$ (this is almost independent of n). For $m = 5 \cdot 10^{-19} \text{ eV}$, however, b already grows by a factor of roughly 10 between BBN and today if it evolves adiabatically and remains in the minimum of the effective potential.

Equation (4.16) thus nicely summarizes the main aspects of this chapter: If condition (4.10) is not satisfied, homogeneous extra dimensions cannot be stabilized since the minimum of the effective potential is time-dependent; the change in the scale factor $b/b_0 = \exp\left[\sqrt{\frac{2\bar{\kappa}^2}{n(n+2)}}(\Phi_{\min}-\Phi_0)\right]$, however, remains relatively small once one allows for an explicit stabilization mechanism. In fact, this does not come as a surprise but can be traced back to the fact that the coupling of Φ to $\hat{\mathcal{L}}_{\text{matter}}$ – and thus to ρ – is suppressed by the (4D) Planck-scale. Still, it is important to realize that an explicit stabilization mechanism actually *is* needed if one allows for extra spatial dimensions and that there exist constraints on the associated effective potential regarding the steepness around its minimum.

Let us conclude this chapter by mentioning two possibilities for how such a stabilizing potential might arise. A first idea might certainly be just to include a cosmological constant Λ and the curvature scalar \tilde{R} for the internal space. From (4.8), these contributions result in a mass term

$$m_\Lambda^2 = -\Lambda \frac{8(n+1)}{n(n+2)} \left(\frac{2\Lambda}{\tilde{R}}\right)^{\frac{n}{2}} \quad (4.17)$$

in the effective potential. This stabilization mechanism can thus only work for a (rather large) *negative* cosmological constant and a hyperbolic internal space. (Λ and \tilde{R} must have the same sign for the effective potential to have an extremum at all).

A more realistic proposal is therefore the one that was recently investigated by Bucci *et al.* [42]. In a toy model reminiscent of the full UED scenario, they calculated the effective potential due to quantum corrections and find a radion mass of about $m \sim 10^{-6} \text{ eV}$. Given the analysis above, this would clearly suffice to effectively stabilize the extra dimensions.

Chapter 5

Kaluza Klein Dark Matter

As motivated in the introductory chapters, WIMPs are particularly attractive dark matter candidates. In Section 3.3, the model of universal extra dimensions was presented in some detail. Here, it will be shown that the lightest Kaluza-Klein particle (LKP) appearing in this model is an interesting realization of such a WIMP, and for extra dimensions at the TeV scale it will automatically come out with the right relic density today. In contrast to the perhaps most studied example of a WIMP, the supersymmetric neutralino, it is not a Majorana fermion. Instead, it is well approximated by the massive vector particle $B^{(1)}$, the first KK excitation of the weak hypercharge gauge boson. Consequently, there is a rich and new phenomenology to explore.

In the first part of this chapter, it will be motivated that the LKP indeed is a viable dark matter candidate that is stable over cosmological time scales; this part also contains a short review on its direct and indirect detection properties that have been studied in recent years. The remainder of the chapter is then devoted to other, previously neglected signatures in the cosmic ray spectrum that would result from $B^{(1)}$ annihilations in the Milky Way. Since the annihilation rate depends crucially on the dark matter distribution, Section 5.2 describes briefly various possible halo profiles, including the case of substructures, or dark matter 'clumps'. Section 5.3 then presents the expected gamma-ray spectrum from $B^{(1)}$ annihilations in the galactic center, including both the continuous part of the spectrum and the line signal from direct annihilation. Internal bremsstrahlung is found to be a very important component to the former; for comparison, this effect is therefore analysed also for other scenarios, where the dark matter is composed of scalar particles or neutralinos. In Section 5.4, finally, possible

distortions in the antiproton spectrum from $B^{(1)}$ annihilations throughout the diffusive halo are discussed.

This chapter contains a summary of the main results from the accompanying paper [III] on the continuous gamma-ray signal (Section 5.3.1), paper [IV] on the line signal (Section 5.3.2) and paper [VI] that discusses the importance of internal bremsstrahlung for heavy neutralinos (Section 5.3.3). The antiproton spectrum (Section 5.4) has been investigated in detail in paper [V].

5.1 A new dark matter candidate

In the presence of one UED, one has to compactify the extra dimension on an orbifold $\mathbb{S}^1/\mathbb{Z}_2$ in order to get the right amount of degrees of freedom in the low energy limit of the 4D theory. This has been discussed in detail in Section 3.3. The boundaries of the orbifold, however, break translational invariance and therefore extra-dimensional momentum – corresponding to KK number in the 4D theory – is no longer a conserved quantity. Such KK number violating couplings appear as higher-order quantum corrections to the KK number conserving couplings at tree level that are collected in Appendix A. They are located at the orbifold fixpoints and can be calculated using the same procedure that was described in Section 3.3.5 for the determination of radiative corrections to the KK masses [46].

If the counterterms at the orbifold fixpoints are identical, however, there is a remnant of the original full translational invariance left, namely translations by πR that take one fixpoint to the other. The corresponding conserved quantity, to all orders in perturbation theory, is *KK parity* and given by $(-1)^n$, where n is the sum of the KK numbers of all particles that appear in the interaction under consideration. This can easily be seen by recalling that any higher-dimensional field can be expanded in Fourier series (3.16), and for each term in such a series one has

$$\cos \frac{n(y + \pi R)}{R} = (-1)^n \cos \frac{ny}{R}, \quad (5.1a)$$

$$\sin \frac{n(y + \pi R)}{R} = (-1)^n \sin \frac{ny}{R}. \quad (5.1b)$$

Due to KK parity, the LKP is therefore stable and can not decay into SM particles. This is reminiscent of the case of supersymmetry, where R -parity ensures the stability of the lightest supersymmetric particle [81].

The fact that the LKP, well approximated by the $B^{(1)}$, is both stable, electrically neutral and colourless, makes it *prima facie* an interesting dark

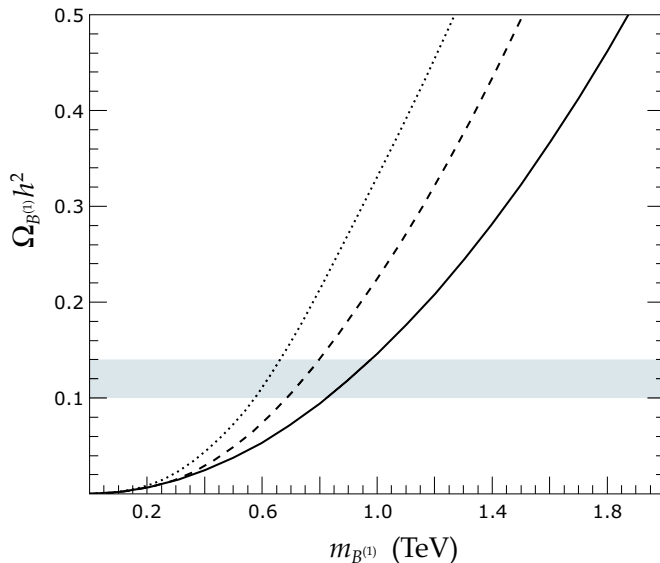


Figure 5.1: (From [58], as based on [114]) The $B^{(1)}$ relic density without coannihilations (solid line), and including coannihilations with three $SU(2)$ singlet leptons with a mass shift of 5% (dashed line) and 1% (dotted line). The grey band indicates the WMAP bound of $\Omega_{CDM} h^2 = 0.12 \pm 0.02$.

matter candidate. The next step then is to calculate its relic density today in order to see whether it matches the observational needs. For that purpose, one has to solve the Boltzmann equation for all KK modes, or at least for those that have a mass close to that of the $B^{(1)}$, and determine their number density after freeze-out; eventually, all heavier KK modes will then decay into the $B^{(1)}$ and SM particles. This has been done in [114] and the result is shown in Fig. 5.1: for a compactification scale of $0.5 \text{ TeV} \lesssim m_{B^{(1)}} \lesssim 1 \text{ TeV}$, which is just outside the range of present colliders, one finds a $B^{(1)}$ relic density in accordance with the WMAP [118] data of $\Omega_{CDM} h^2 = 0.12 \pm 0.02$. One should, however, bear in mind that in this calculation the effect of co-annihilations has been taken into account only in a rather simplistic and approximative way; doing a full numerical analysis of the Boltzmann equation, and taking into account the whole spectrum of states with their respective radiative mass shifts as discussed in Section 3.3.5, could therefore substantially alter the predictions for the $B^{(1)}$ relic density.

The detection properties of KK dark matter have already been studied in some detail in previous analyses and look quite promising for next genera-

tion's detectors. As far as direct detection is concerned, the spin-dependent cross-section between $B^{(1)}$ particles and target nuclei can be three to four magnitudes larger than the spin-independent cross-section. On the other hand, there is a rather strong dependence on the mass number which compensates for this difference; an analysis of these two effects shows that detectors with heavy target nuclei like germanium and xenon are best suited for $B^{(1)}$ direct detection. The best present limit of $m_{B^{(1)}} \gtrsim 0.4 \text{ TeV}$ from such experiments comes from the Edelweiss [113] experiment and is thus roughly comparable to the limit from accelerator data. The planned ton-scale detectors GENIUSII and XENON will be able to probe the whole mass range that gives cosmologically interesting relic densities [45, 115].

The study of indirect detection of KK dark matter has mainly been focussed on neutrinos from $B^{(1)}$ particles trapped in the sun and the earth [45, 76], as well as positrons [77, 78] and gamma rays [45, 33] from $B^{(1)}$ annihilations in the galactic halo and center, respectively. The number density of LKPs in the sun, but not yet in the earth, is likely to have reached an equilibrium between capture and annihilation rate. The branching ratio for annihilation into neutrinos is about 1%, which translates into the need of a kilometer scale neutrino telescope in order to detect such a monochromatic, high-energetic neutrino signal from the sun. Such a signal could potentially even be used to discriminate between the $B^{(1)}$ and a neutralino since the latter would most likely not yet have reached its equilibrium concentration in the sun. Another interesting channel is the annihilation into electron-positron pairs, $B^{(1)}B^{(1)} \rightarrow e^+e^-$: with a branching ratio of about 20%, one would expect this to give a distinguished peak signal in the positron spectrum, at an energy equal to the $B^{(1)}$ mass. Due to propagation effects, however, the peak is washed out and only for relatively low masses one would actually be able to see such a striking signature above the positron background - unless one allows for high boost factors due to clumpy halo distributions, see Section 5.2.2. Finally, the photon spectrum that has been studied previously does not show any characteristics that would make it particularly promising for indirect LKP detection. As discussed in Section 5.3, this situation changes drastically when taking into account internal bremsstrahlung of lepton final pairs as well as the line signal from direct $B^{(1)}$ annihilation.

5.2 The galactic mass distribution

The number of LKP (or any other dark matter particle of mass $m_{B(1)}$) pair annihilations per unit time and volume element is given by

$$\frac{dn}{dt} = \frac{1}{2} \langle \sigma v \rangle \frac{\rho^2(\mathbf{r})}{m_{B(1)}^2}, \quad (5.2)$$

where v is the relative velocity of the two particles, σ the cross section for the annihilation channel in question and $\rho(\mathbf{r})$ the LKP (mass) density at the position \mathbf{r} where the annihilation takes place. The rate of the particles produced in the final state thus depends quadratically on ρ , making it most promising to look for regions of high dark matter concentrations when investigating possible observational consequences. On the other hand, this also means that any attempt to accurately predict cosmic ray fluxes as a means of indirect dark matter detection is greatly hampered by the fact that the exact distribution of dark matter in our galaxy is still unknown to a large extent. It therefore seems appropriate at this stage to discuss possible halo profiles in some detail, including in particular the existence of substructures, before presenting various indirect detection channels for (mostly) LKP dark matter in the remainder of this chapter.

5.2.1 Smooth halo profiles

Direct observations can only poorly constrain the form of the halo profile in the Milky Way, especially in its central parts, so it is usually taken from N-body simulations of gravitational clustering. These simulations, however, currently reach resolutions of merely 0.1 kpc for galaxies with the size of the Milky Way. This means that the innermost slope of the density profile can only be inferred by an extrapolation and is therefore principally bound to have a considerable amount of uncertainty. Another thing to be aware of is the fact that these N-body simulations still cannot account for the presence of baryons (and their coupling to photons) and therefore only include interaction- and pressureless (dark) matter. An important aspect of baryons is that they can fall faster into the potential well of the halo than the dark matter particles themselves, because they are charged and thus can get rid of their angular momentum by the emission of photons. After the infall of baryons the potential well becomes steeper, which eventually should also lead to higher central dark matter concentrations; this mechanism is known as *baryonic compression*.

Having all that in mind, an often used parameterization of possible spherical halo profiles is given by

$$\rho(\mathbf{r}) = \rho_0 \left(\frac{R_0}{r} \right)^\gamma \left[\frac{1 + (R_0/a)^\alpha}{1 + (r/a)^\alpha} \right]^{\frac{\beta-\gamma}{\alpha}}, \quad (5.3)$$

where the parameters (α, β, γ) determine the halo model in question, $R_0 = 8.5$ kpc is the distance of the sun to the galactic center and $\rho_0 \sim 0.3 \text{ GeV cm}^{-3}$ the local halo density. The scale radius a determines where the transition for the radial dependence of ρ from large ($\rho \propto r^{-\beta}$) to small ($\rho \propto r^{-\gamma}$) galactocentric distances takes place. N-body simulations favour cuspy halo distributions like the NFW profile [95] with $(\alpha, \beta, \gamma) = (1, 3, 1)$, or the even more cuspy Moore profile [94] with $(1.5, 3, 1.5)$. Sometimes, one considers for comparison also the case of an isothermal sphere, $(2, 2, 0)$, which has a constant density core and results in rather conservative values for cosmic ray fluxes. There are indications that the scale radius a is not really an independent parameter but strongly correlated with the virial mass of the galaxy [57]; for the Milky Way and an isothermal sphere (NFW, Moore) profile, one finds $a = 4$ kpc (21.7 kpc, 34.5 kpc) [62]. Finally, the most recent simulations actually suggest a universal halo profile of the form

$$\rho(\mathbf{r}) \approx \rho_0 \exp \left[- (r/a)^{\frac{1}{n}} \right], \quad (5.4)$$

with $n \approx 5$ [96, 92]. However, taking into account the effects of baryons in a simple model of adiabatic contraction [36], this profile is effectively transformed to a Moore profile [54, 108, 67].

Apparently, cuspy profiles with $\gamma \geq 1$ exhibit divergent dark matter densities in the central part of the halo. Since this is obviously an unphysical result, one usually introduces by hand an inner cutoff radius r_c , below which the density stays constant. The most extreme (i.e. smallest possible) value for r_c is obtained by the observation that self-annihilation of dark matter particles forbids too high densities; it can be calculated by demanding that the innermost part of the halo is in an equilibrium state, where the self-annihilation rate $\langle \sigma_{\text{ann}} v \rangle \rho / m_{B(1)}$ equals the typical inverse time scale for the formation of the singularity, $(G\bar{\rho})^{\frac{1}{2}}$, with $\bar{\rho}$ being the average halo density at collapse [22].

5.2.2 Substructure and clumps

Following numerically the evolution of primordial density fluctuations, one finds that structure forms hierarchically, with the smallest structures forming first and only later merging to larger structures. It is therefore plausible

that there exist substructures (“clumps”) within the smooth halo distributions discussed in the last section. This is highly relevant for the indirect detection of dark matter, since the overall flux of a given cosmic ray species at earth is always obtained by an effective average over the corresponding local dark matter annihilation rates (5.2). Thus, as the difference $\langle \rho^2 \rangle - \langle \rho \rangle^2 > 0$ gets generically larger for more inhomogeneous dark matter distributions, the existence of clumps can potentially greatly enhance the expected annihilation signal.

Dark matter clumps have recently seen a revival of interest, triggered by the discovery that for every WIMP candidate there appears a natural cut-off M_c in the power spectrum, below which density perturbations are washed out by collisional damping and subsequent free streaming (see [69] for a review); above the cutoff, the power spectrum falls steeply with larger masses. As a consequence, a considerable part of the dark matter should have collapsed into substructures with a mass of about M_c , thereby forming the first gravitationally bound objects in the cosmological evolution. Numerical simulations seem to confirm these analytical predictions; with promising looking survival probabilities, there is furthermore a good chance that these microhalos can give a sizeable contribution to the total amount of dark matter in the solar neighbourhood today [49].

Let $\rho_{\text{cl}}(M_{\text{cl}}, \mathbf{r}_{\text{cl}})$ be the typical density profile inside a dark matter clump of mass M_{cl} , and $n_{\text{cl}}(M_{\text{cl}}, \mathbf{r})$ the number density of such clumps at a position \mathbf{r} in the halo. The effect of dark matter annihilations inside the clumps alone is then obtained by replacing

$$\rho^2(\mathbf{r}) \rightarrow \int dM_{\text{cl}} \int d^3\mathbf{r}_{\text{cl}} n_{\text{cl}}(M_{\text{cl}}, \mathbf{r} - \mathbf{r}_{\text{cl}}) (\rho_{\text{cl}}(M_{\text{cl}}, \mathbf{r}_{\text{cl}}))^2 \quad (5.5)$$

$$\simeq \rho_0 \int dM_{\text{cl}} M_{\text{cl}} \delta(M_{\text{cl}}) n_{\text{cl}}(M_{\text{cl}}, \mathbf{r}) \quad (5.6)$$

in the source function for the cosmic ray species under consideration. The dimensionless quantity

$$\delta \equiv \frac{1}{\rho_0} \frac{\int d^3\mathbf{r}_{\text{cl}} (\rho_{\text{cl}}(M_{\text{cl}}, \mathbf{r}_{\text{cl}}))^2}{\int d^3\mathbf{r}_{\text{cl}} \rho_{\text{cl}}(M_{\text{cl}}, \mathbf{r}_{\text{cl}})} \quad (5.7)$$

that appears here is a measure of the effective density contrast between an average dark matter clump and the local halo density. The last step in (5.6) is valid if n_{cl} does not change very much on scales of the order of the size of a clump, i.e. for the whole region of integration one has $n_{\text{cl}}(M_{\text{cl}}, \mathbf{r} - \mathbf{r}_{\text{cl}}) \approx n_{\text{cl}}(M_{\text{cl}}, \mathbf{r})$. This should be a good approximation for any realistic scenario,

in particular when the dominant part of substructures comes in very small clumps.

A natural assumption is that the microhalos trace the mass distribution except for regions very close to the galactic center, where strong tidal forces or interactions with stars are expected to have destroyed all substructure by now. Assuming for simplicity furthermore that the clumps mainly come in one particular size, their number density is given by

$$n_{\text{cl}} = \frac{f}{M_{\text{cl}}} \rho(\mathbf{r}) \Theta(r - R_d), \quad (5.8)$$

where R_d is the radius inside which all substructure has been completely disrupted and f the fraction of the dark matter outside R_d that comes in clumps. With this, the replacement (5.5) simplifies to

$$\rho^2(\mathbf{r}) \rightarrow f\delta\rho_0 \rho(\mathbf{r}) \Theta(r - R_d). \quad (5.9)$$

For the indirect dark matter detection by means of photons, the bulk annihilation signal is expected from a region very close to the galactic center (see next section) and the contribution from clumps is therefore most likely negligible.¹ Antiprotons, however, originate from all over the halo and in that case the contribution from clumps in the simplified model described here gives about $f\delta/2$ times the flux that is expected without clumps (see Section 5.4 and [V] for more details). The numerical simulations do not yet reach sufficient resolutions to calculate δ in a satisfying way, but values for $f\delta$ of up to several hundred or thousand do not seem unreasonable [49, V]. Clumps may thus significantly enhance the annihilation flux in antiprotons (as well as that in positrons or other charged particles).

¹This is true for the *average* effect of many small clumps. The situation can change drastically if one instead considers the effect of individual, possibly very nearby clumps. In fact, one may be tempted to interpret the recent serendipitous discovery of a gamma-ray point source without optical counterpart [4] along these lines.

5.3 Gamma rays from $B^{(1)}$ annihilations

As a means of indirect dark matter detection, gamma rays are interesting for two reasons. First, since they propagate through the interstellar (or intergalactic) medium almost without interacting, they can directly probe regions of high dark matter concentrations such as the galactic center, other galaxies or nearby dark matter clumps. Prospects for the detection of an exotic contribution to the gamma-ray spectrum become, secondly, more and more promising with the advent of new, giant telescopes with unprecedented sensitivity and energy resolution.

When looking towards a region of enhanced dark matter density, the expected integrated gamma-ray flux at earth is given by

$$\Phi_\gamma(\psi) = \frac{N_\gamma \langle \sigma v \rangle_\gamma}{8\pi m_{B^{(1)}}^2} \int_{\text{l.o.s.}} d\ell(\psi) \rho^2(\mathbf{r}), \quad (5.10)$$

where the integral is along the line of sight for a given angle ψ of observation, $\langle \sigma v \rangle_\gamma$ the annihilation rate into photons and N_γ the number of photons per $B^{(1)}$ pair annihilation. A real detector has only a finite angular resolution $\Delta\Omega$, so one has to average over the angular dependence of the line-of-sight integral that appears above. It is then convenient to introduce the dimensionless quantity

$$\langle J \rangle_{\Delta\Omega}(\psi) \equiv \frac{1}{8.5 \text{ kpc}} \left(\frac{1}{0.3 \text{ GeV cm}^{-3}} \right)^2 \frac{1}{\Delta\Omega} \int_{\Delta\Omega} d\Omega \int_{\text{l.o.s.}} d\ell(\psi) \rho^2(\mathbf{r}), \quad (5.11)$$

which contains all the astrophysical uncertainties connected to the expected gamma-ray flux (as opposed to the underlying particle physics that enters through $m_{B^{(1)}}$ and $\langle \sigma v \rangle_\gamma$) [28]. With this, the flux becomes

$$\Phi_\gamma(\psi) = 9.4 \cdot 10^{-13} \left(\frac{N_\gamma \langle \sigma v \rangle_\gamma}{10^{-26} \text{ cm}^3 \text{ s}^{-1}} \right) \left(\frac{1 \text{ TeV}}{m_{B^{(1)}}} \right)^2 \cdot \Delta\Omega \langle J \rangle_{\Delta\Omega}(\psi) \text{ cm}^{-2} \text{ s}^{-1} \text{ sr}^{-1}. \quad (5.12)$$

For example, when looking towards the galactic center with a detector like the H.E.S.S. telescope, i.e. with an opening angle of $\Delta\Omega = 10^{-5} \text{ sr}$, one obtains

$$\Delta\Omega \langle J \rangle_{\Delta\Omega}(0) = 0.13 b \text{ sr}. \quad (5.13)$$

In this expression, one has to set $b = 1$ if the dark matter density ρ follows a NFW profile [44]. On the other hand, starting with an initial NFW distribution, but taking into account the effect of baryonic compression due

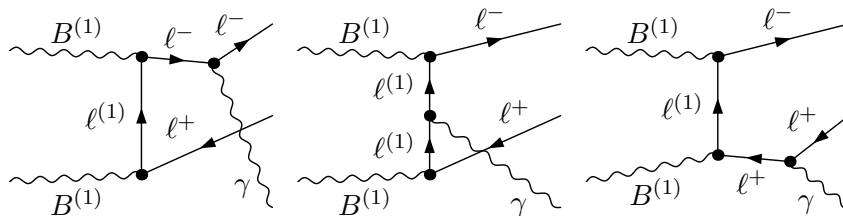


Figure 5.2: Contributions to $B^{(1)}B^{(1)} \rightarrow \ell^+\ell^-\gamma$. In principle, there also exist diagrams with an s -channel Higgs boson; due to the small Higgs mass $m_H^2 \ll s$, however, these are greatly suppressed as compared to the ones shown above.

to the dense stellar cluster that is observed to exist very near the galactic center, the boost factor b may be as high as 1000 [108, 32].

In this section, it will be shown that photons radiated away from charged particle final states give a large contribution to the high-energy part of the photon spectrum, providing a promising signature when it comes to discriminating a possible annihilation signal from the gamma-ray background (which most probably is dominated by astrophysical processes). This is a very generic result, so this spectral signature is not only discussed for the $B^{(1)}$, but for comparison also for the case of neutralino and scalar dark matter. Finally, the line signal from direct annihilations into photons, if detected, would of course provide independent “smoking gun” evidence for particle dark matter; in Section 5.3.2, the corresponding rates for the $B^{(1)}$ are therefore presented and contrasted with today’s and future’s detector performances.

5.3.1 The continuous signal

The main annihilation channel of $B^{(1)}$ pairs is into charged leptons, which is a good motivation to consider internal bremsstrahlung processes as depicted in Fig. 5.2, where an additional photon appears in the final state. The computation of the corresponding Feynman amplitudes is straight forward and, as found in [III], the resulting differential photon multiplicity is well approximated by

$$\frac{dN_\gamma^\ell}{dx} \equiv \frac{d(\sigma_{\ell^+\ell^-\gamma v})/dx}{\sigma_{\ell^+\ell^-v}} \simeq \frac{\alpha}{\pi} \frac{(x^2 - 2x + 2)}{x} \ln \left[\frac{m_{B^{(1)}}^2}{m_\ell^2} (1-x) \right], \quad (5.14)$$

where $x \equiv E_\gamma/m_{B^{(1)}}$. The factor of α/π in front is expected from the electromagnetic coupling and the phase space difference between two- and

three-body final states. In addition to that, there is a large logarithm due to a collinear divergence that is known from standard electrodynamics: highly relativistic leptons tend to lose their energy very rapidly by the emission of photons parallel to their direction of movement.

In addition to this primary source of photons, there are several secondary contributions to the photon spectrum. Synchrotron radiation from the final state leptons, for example, can be a significant source of photons at low energies; when compared to the observed radio flux from the galactic center, one may use this to derive bounds on the UED model that are comparable to those coming from electroweak precision measurements at colliders [33]. Inverse Compton scattering on CMB photons and starlight might contribute even at higher energies, but generally this is expected to be only a small correction [8]. Finally, the fragmentation of final state quarks and τ leptons contributes to the total photon spectrum even at the high energies that will be the focus here, mainly through the decay of neutral π^0 bosons. To account for this, parametrizations for the respective photon multiplicities $dN_\gamma^{q,\tau}/dx$ are adopted, as obtained in [62] by using the Monte Carlo code PYTHIA [116].

The total differential number of photons per $B^{(1)}$ pair annihilation is then obtained by

$$dN_\gamma^{\text{eff}}/dx \equiv \sum_i \kappa_i dN_\gamma^i/dx, \quad (5.15)$$

where the sum is over all contributing processes and κ_i are the corresponding branching ratios. Previous analyses of the photon flux correspond to the relatively soft and sharply falling spectrum from quark fragmentation alone that is shown as a dashed line in Fig. 5.3. For intermediate energies, τ fragmentation (dotted line) becomes much more important, while at energies close to the $B^{(1)}$ mass, internal bremsstrahlung dominates, giving rise to a very hard total gamma-ray spectrum with a sharp cutoff at the highest kinematically accessible energies. Following a conservative approach, internal bremsstrahlung from charged final states other than leptons has been neglected here due to the small annihilation branching ratio into vector bosons on the one hand and in order to avoid the complexity of a detailed study of quark fragmentation on the other hand. (Note, however, that PYTHIA's way of handling quark final states should in principle take into account internal bremsstrahlung, though certainly not to a fully satisfying extent, see also [35]). These other charged final states might thus in principle further enhance the photon yield at high energies, though this is not expected to be a large effect.

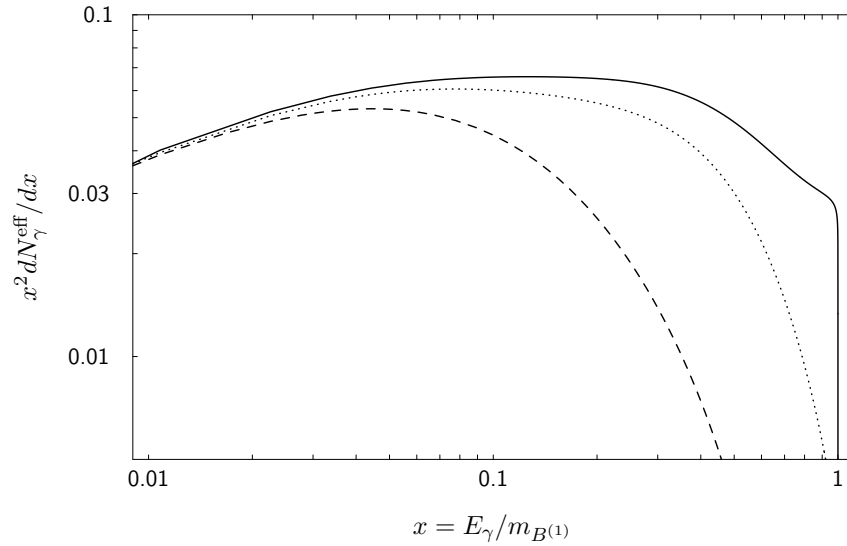


Figure 5.3: The total number of photons per $B^{(1)}B^{(1)}$ annihilation (solid line). Also shown is what quark fragmentation alone would give (dashed line), and adding to that τ lepton production and decay (dotted line). Here, a $B^{(1)}$ mass of $m_{B^{(1)}} = 0.8$ TeV and a 5% mass splitting at the first KK level was assumed, though the result is actually quite insensitive to these parameters.

The origin of the TeV gamma-ray signal from the direction of the galactic center, as observed by the H.E.S.S. collaboration [3], is still unexplained. In Fig. 5.4, the corresponding data points are shown together with the expected spectrum from annihilating Kaluza-Klein dark matter with $m_{B^{(1)}} = 0.8$ TeV, smeared over the detector resolution of 15 %. While annihilating LKPs certainly cannot explain the whole range of data, it is interesting to note that the expected flux comes out to be of the right order of magnitude for rather reasonable assumptions about the boost factor b . Once one understands the underlying physics of the background signal better, one may thus well be able to extract such an exotic contribution from the total spectrum, especially since one has quite a remarkable signature to look for. Another point to notice is that even if one expects a sharp cutoff around 1 TeV for KK dark matter, the shape of the spectrum for lower energies comes remarkably close to what is observed for the whole range of energies. To illustrate this, the hypothetical case of an LKP with $m_{B^{(1)}} = 9$ TeV is also included in Fig. 5.4; while a $B^{(1)}$ with such a high mass is excluded because it would overclose the universe, one might speculate that there exist other reasonable extensions of

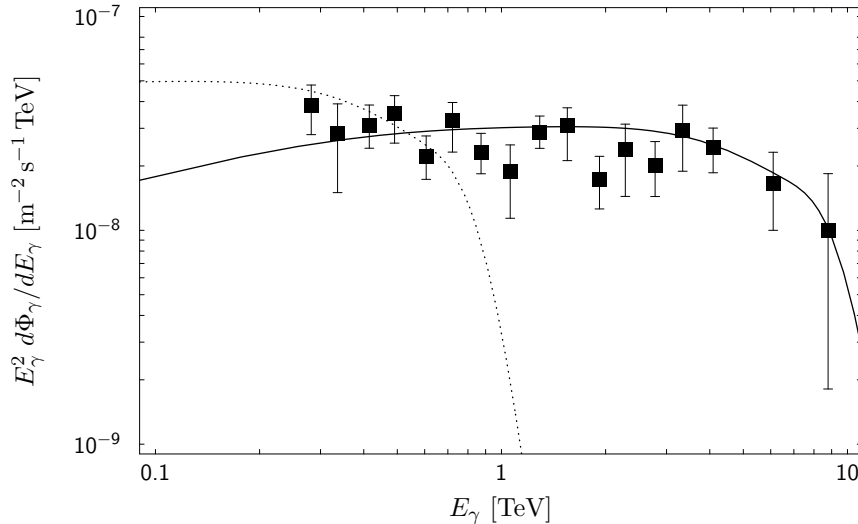


Figure 5.4: The H.E.S.S. data [3] compared to the gamma ray flux expected from a region of 10^{-5} sr encompassing the galactic center, for a $B^{(1)}$ mass of 0.8 TeV, a 5% mass splitting at the first KK level, and a boost factor b around 200 (dotted line). The solid line corresponds to a hypothetical 9 TeV WIMP with similar couplings, a total annihilation rate given by the WMAP relic density bound, and a boost factor of around 1000. Both signals have been smeared to simulate an energy resolution of $\sigma = 15\%$, appropriate for the H.E.S.S. telescope.

the SM that would allow such high masses. In fact, for a hypothetical dark matter particle with similar – but about three times stronger – couplings to SM particles as the $B^{(1)}$, one would automatically both get the right relic density for a 10 TeV particle and be able to reproduce the flat TeV spectrum as observed by the H.E.S.S. collaboration.

5.3.2 The two photon annihilation line signal

The direct annihilation of $B^{(1)}$ particles into photons, $B^{(1)}B^{(1)} \rightarrow \gamma\gamma$, is loop-suppressed so the resulting photon flux from, e.g., the galactic center cannot be expected to be very large. On the other hand, the detection of such a monochromatic line signal would definitely be a “smoking gun” signature for the existence of particle dark matter, so it is of great interest to carefully study this process, just as it has been done previously for the case of neutralino annihilation [27, 29].

By an analysis of the Lorentz structure of the Feynman amplitude, one

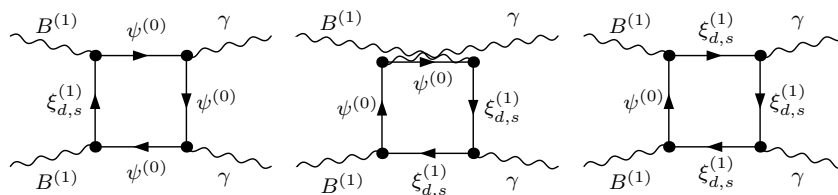


Figure 5.5: Fermion box contributions to $B^{(1)}B^{(1)} \rightarrow \gamma\gamma$, including only the first level of KK excitations. Not shown are the additional (two times) nine diagrams that are obtained by crossing external momenta.

can considerably simplify the necessary amount of calculations; in the limit of vanishing relative velocity v of the incoming $B^{(1)}$ particles, and after taking into account all symmetries of the process, there remain only a few scalar coefficients to be calculated. Alternatively, one may use the symmetries as a cross-check of the analytical results. This analysis is described in detail in the accompanying paper [IV], so there is no need to repeat it here.

For a subset of contributing diagrams, namely the fermion box diagrams shown in Fig. 5.5, the corresponding cross section is found to be

$$\sigma v = \frac{\alpha_{\text{em}}^2 \alpha_Y^2 g_{\text{eff}}^4}{144\pi m_{B^{(1)}}^2} \left\{ 3|B_1|^2 + 12|B_2|^2 + 4|B_6|^2 - 4\text{Re}[B_1(B_2^* + B_6^*)] \right\}, \quad (5.16)$$

where

$$g_{\text{eff}}^2 \equiv \sum Q^2 Y^2 = \frac{52}{9}, \quad (5.17)$$

and the sum is over all SM fermions with charge Q and hypercharge Y . The three scalar coefficients B_1 , B_2 and B_6 that appear here can be expressed in terms of six known scalar loop integrals, with the corresponding analytical expressions given in the appendix of [IV].

In addition to the relatively small number of fermion box diagrams, there exist numerous diagrams containing scalar particles. The 22 different *types* of diagrams, i.e. those that are not related by any obvious symmetries, are shown in Fig. 5.6. Obviously, it would be a formidable task to calculate all these contributions analytically. Numerically, however, it can be done in a fairly straight-forward way by implementing the necessary Feynman rules of Appendix A in the FormCalc package [74]. The result of this numerical computation is that all the scalar diagrams merely make up a few percent of the total cross section. Note, finally, that the contribution of diagrams containing higher KK excitations is suppressed by the appearance of large

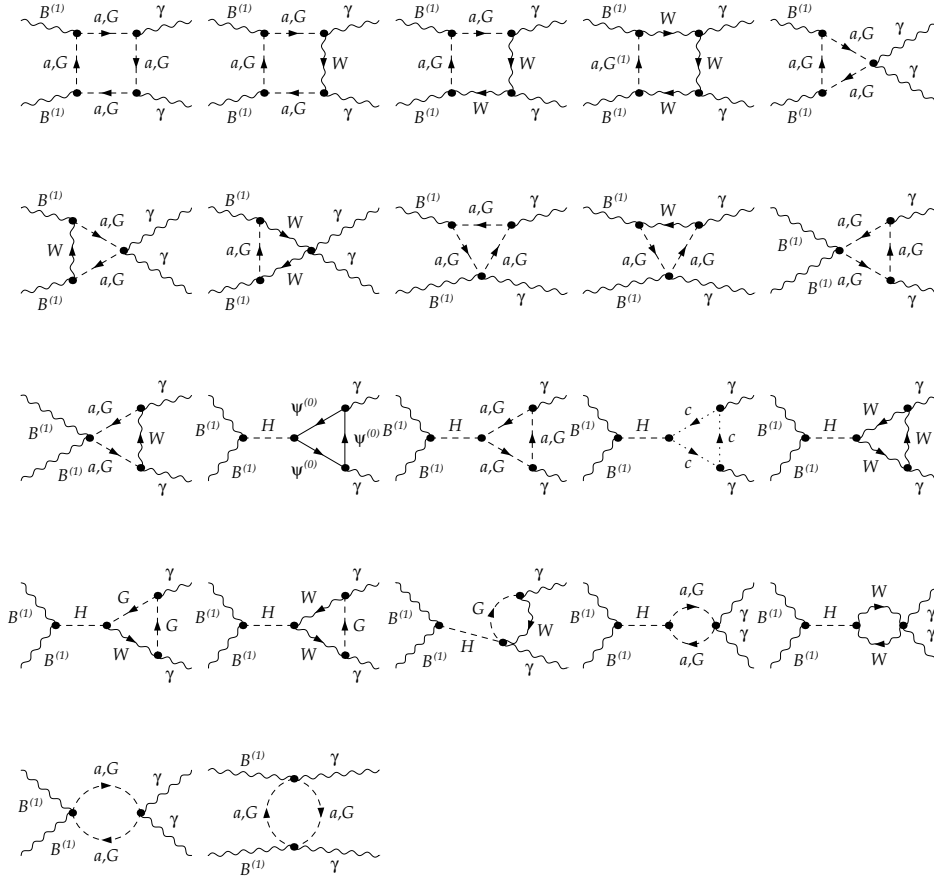


Figure 5.6: The different types of scalar diagrams, up to first KK level, that contribute to $B^{(1)} B^{(1)} \rightarrow \gamma\gamma$.

masses in the propagators; as an illustrative example, this general expectation has been confirmed numerically by including second level KK fermions in the spectrum of states.

In conclusion, the analytical expression (5.16) should give an approximation to the full annihilation rate into two photons that is correct at the percent level. When it comes to observational prospects for such a gamma-ray line from the direction of the galactic center, today's detector resolutions are unfortunately not sufficient to resolve its natural linewidth of about 10^{-3} that results from a Doppler shift due to the galactic velocities of the LKPs. In Fig. 5.7, the expected gamma-ray spectrum around the LKP mass is

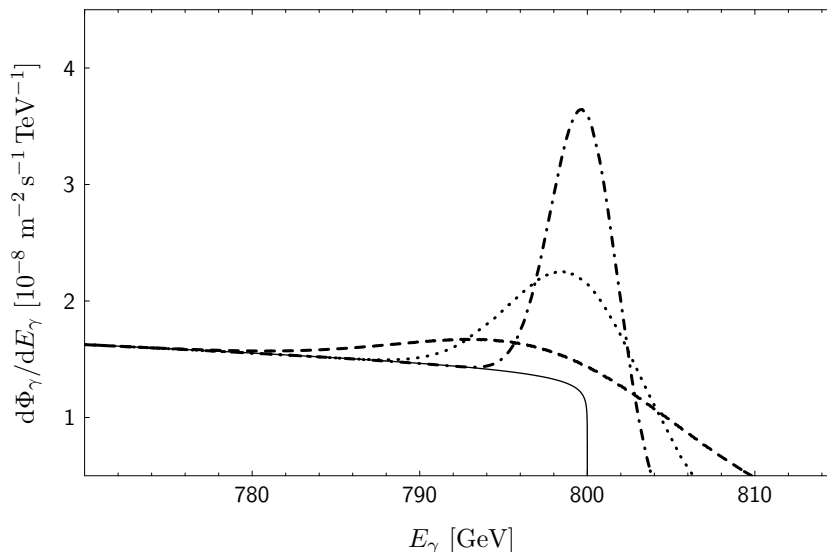


Figure 5.7: The continuous gamma ray flux that is expected from KK dark matter, as described in the previous subsection, is plotted as a solid line. The total flux, including the contribution from direct annihilation and as seen by a detector with a finite Gaussian energy resolution, is shown for $\sigma = 1\%$ (dashed), 0.5% (dotted) and 0.25% (dash-dotted), respectively. The actual linewidth of the signal is about 10^{-3} , with a peak value of $1.5 \cdot 10^{-7} \text{ m}^{-2} \text{ s}^{-1} \text{ TeV}^{-1}$. The example LKP of this figure has a mass $m_{B^{(1)}} = 0.8 \text{ TeV}$ and a mass shift $m_{\xi^{(1)}}/m_{B^{(1)}} = 1.05$; furthermore, a moderate boost factor of $b = 100$ was assumed.

plotted for various detector resolutions; as can be seen, one would need a resolution of at least 1% in order to discriminate the line signal from the continuous signal discussed in the previous section.

To conclude this section, there are two other processes, $B^{(1)}B^{(1)} \rightarrow Z\gamma$ and $B^{(1)}B^{(1)} \rightarrow H\gamma$, that result in a monochromatic gamma-ray line at an energy

$$E_\gamma = m_{B^{(1)}} \left(1 - \frac{m_{Z,H}^2}{4m_{B^{(1)}}^2} \right). \quad (5.18)$$

Due to the high mass of the $B^{(1)}$, these lines cannot be resolved separately, but effectively add to the $\gamma\gamma$ line, thus further enhancing the signal. The diagrams contributing to the $Z\gamma$ line have a very similar structure as for the $\gamma\gamma$ case – except for the fact that Z bosons also have an *axial* vector part in their coupling to fermions. Taking this into account, one can compare the γ and Z coupling strengths to obtain as a quick estimate that the $Z\gamma$ process should enhance the gamma ray signal shown in Fig. 5.7 by about 10% ; this

estimate has been confirmed numerically. The contribution from the $H\gamma$ line, absent in the supersymmetric case, would further enhance the signal. However, since the diagrams that contribute here have a rather different structure, the analysis of this process is much more involved and has not been carried out so far.

5.3.3 Discrimination against other dark matter candidates

As seen in the previous sections for the case of KK dark matter, internal bremsstrahlung from lepton annihilation products gives a very characteristic signature for the gamma-ray spectrum, with a sharp cutoff at the LKP mass. In fact, this is a rather generic effect that should occur in a similar way also for other dark matter candidates, whenever they annihilate into charged particles, thus providing a hitherto undiscussed signature for indirect dark matter detection (see however the very recent [35], where a similar observation was made). Since it is hard to imagine that any astrophysical effect could mimic such a signature, its observation would give a similar strong evidence for the WIMP nature of dark matter as the observation of the line signal from direct annihilation. As an illustration of this idea and for the purpose of a direct comparison with the case of KK dark matter, radiation from charged particle final states will therefore be studied in the following for two different dark matter candidates, the neutralino and a scalar dark matter particle. It will be shown that this type of contribution to the gamma-ray spectrum can have important observational consequences, even in cases where one can not expect as dramatic enhancement factors as $\log m_{B^{(1)}}/m_e$.

Neutralinos

The neutralino is the most well-studied WIMP dark matter candidate and arises as the lightest new particle in supersymmetric extensions of the SM, where all SM fermions (bosons) are equipped with a bosonic (fermionic) supersymmetric partner; for a detailed review on supersymmetric dark matter, see [81, 23, 31]. While the annihilation into (light) leptons is helicity suppressed, a considerable branching ratio can go into charged gauge bosons, depending on the parameters of the model. The focus will therefore in the following be on this particular annihilation channel and the case of heavy neutralinos, since then one can expect large enhancement factors m_χ/m_W , in analogy to what was found in (5.14) for lepton final states.

In general, the neutralino is a linear combination of the superpartners of

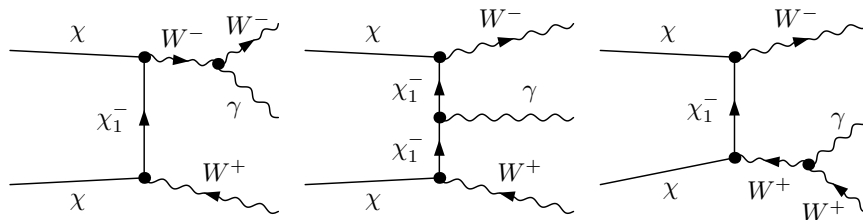


Figure 5.8: Contributions to $\chi\chi \rightarrow W^+W^-\gamma$ for a pure higgsino-like neutralino (crossing fermion lines are not shown).

the gauge and Higgs fields,

$$\chi \equiv N_{11}\tilde{B} + N_{12}\tilde{W}^3 + N_{13}\tilde{H}_1^0 + N_{14}\tilde{H}_1^0. \quad (5.19)$$

However, things simplify considerably if one considers the case of a pure Higgsino, with $N_{13} = \pm N_{14}$ and $N_{11} = N_{12} = 0$, which has to be satisfied approximately for heavy neutralinos if supersymmetry is to provide a unification of coupling constants at the scale of grand unified theories (GUTs). The case of a pure wino gives, up to an overall factor, the same results as for a Higgsino, while a pure bino does not couple to W at lowest order at all. Eventually, one will of course be interested in a full analysis even for the case of mixed states. The main purpose of the present treatment, however, is simply to draw attention to the new kind of signatures one can expect in the case of supersymmetric dark matter.

For a pure Higgsino, the only diagrams with $W^+W^-\gamma$ final states are shown in Fig. 5.8. A peculiarity of supersymmetry is that the neutralino is a Majorana fermion, which means that it is its own antiparticle. In situations like this, one can encounter diagrams with crossing fermion lines. When calculating them, particular care must be taken to treat all spinor indices correctly (see, e.g., [73] for a complete list of Feynman rules); as a cross-check of the results it is therefore of great advantage to have access to an independent method of calculation. This is found by observing that, in the limit of very low relative velocity, the pair of incoming neutralinos must be in an initial state that is an S -wave with pseudoscalar quantum numbers due to the Majorana nature of the neutralino. To project out this state, one inserts the operator

$$P_{1S_0} \equiv -\frac{1}{\sqrt{2}}\gamma^5(m_\chi - \not{p}), \quad (5.20)$$

where p is the momentum of one of the incoming χ , in front of the product of gamma-matrices from the fermion line; instead of summing over all spin

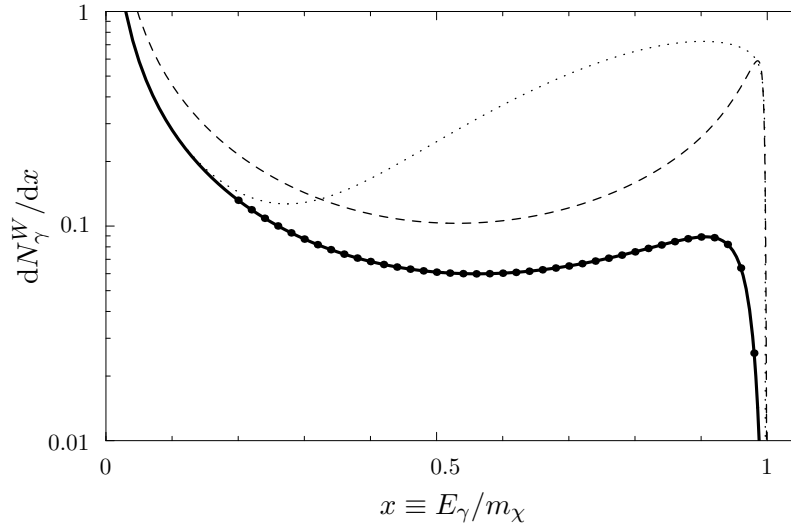


Figure 5.9: The photon multiplicity for the radiative process $\chi\chi \rightarrow W^+W^-\gamma$. As an example, the MSSM model of Table 5.1 below was chosen; the results from a computation with FormCalc [74] for a relative neutralino velocity of 10^{-3} are displayed as dots and the solid line shows the analytical result for the pure higgsino, zero velocity limit. Also shown, as dashed and dotted lines, are two pure higgsino models with a lightest neutralino (chargino) mass of 10 TeV (10 TeV) and 1.5 TeV (2.5 TeV), respectively.

M_2	μ	m_A	$m_{\tilde{f}}$	A_f	$\tan\beta$	m_χ	$m_{\chi_{\pm 1}}$	Z_h	W^\pm	$\Omega_\chi h^2$
3.2	1.5	3.2	3.2	0.0	10.0	1.50	1.51	0.92	0.39	0.12

Table 5.1: MSSM parameters for the model used in Fig. 5.9, and the resulting neutralino mass (m_χ), chargino mass ($m_{\chi_{\pm 1}}$), higgsino fraction (Z_h), branching ratio into W pairs (W^\pm) and neutralino relic density ($\Omega_\chi h^2$), as calculated with DARKSUSY [68] and MICROMEGAS [21]. Masses are given in units of TeV.

states, one then just has to take the trace over the spinor indices. All analytical results of [VI] were obtained by both explicitly calculating the diagrams of Fig. 5.8 and their counterparts with crossed ingoing fermion lines, as well as by applying the projector method (5.20), where one only has to calculate the diagrams that are explicitly given in Fig. 5.8.

The analytical results for the photon multiplicity are shown in Fig. 5.9 and compared with the example of a concrete set of parameters as it might be realized in the minimally supersymmetric standard model (MSSM). To illustrate two different effects that can be singled out in the spectrum, the

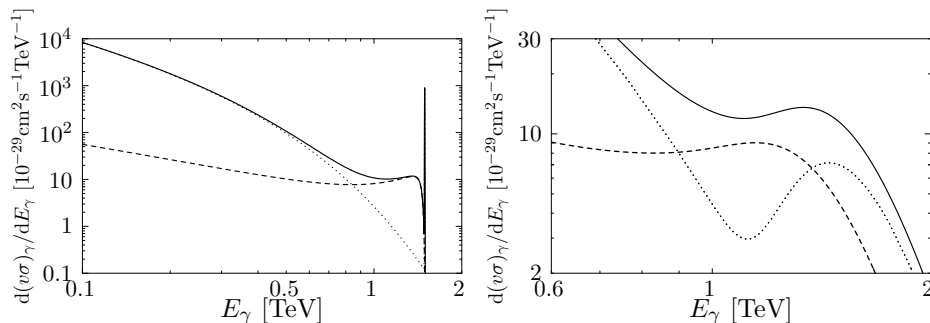


Figure 5.10: The total expected differential photon distribution from $\chi\chi$ annihilations (solid line), using the MSSM model of Table 5.1. The contributions from W fragmentation and $\chi\chi \rightarrow \gamma\gamma$, $Z\gamma$ lines (dotted), as well as from the radiative processes $\chi\chi \rightarrow W^+W^-\gamma$ (dashed), are shown separately. On the left, the actual spectrum is displayed, while the figure on the right shows a zoom-in of what this would look like for a detector with an energy resolution of 15 percent.

hypothetical cases of a very high neutralino mass and a large mass shift between the neutralino and the chargino in the propagator, respectively, are also shown. Both cases lead to a significant enhancement of the photon flux at high energies, albeit for very different reasons. In the limit of high neutralino masses, the outgoing W bosons can be treated as light and are thus expected to show a similar (divergent) infrared behaviour as QED photons; for kinematical reasons, however, a very low-energetic W is automatically accompanied by a high-energetic photon. For large mass-shifts, on the other hand, the effect of longitudinal charged gauge bosons becomes visible. While these polarization states are not possible for a 1S_0 final state with only two vector particles, this channel opens up when an additional photon is added to the final state.

Apart from the processes shown in Fig. 5.8, one expects neutralino induced contributions to the gamma-ray spectrum from W^\pm fragmentation as well as from the $\gamma\gamma$ [27, 29] and $Z\gamma$ [123] lines. The total expected spectrum for the same MSSM model as in Fig. 5.9 is plotted in Fig. 5.10, including what it would look like with a detector resolution of 15%, which is typical for current ACTs. Clearly, the signal from internal bremsstrahlung has two different effects. First, it enhances the peak signal by a factor of 2, even though the peak signal is known to be already very large for high neutralino masses. Secondly, it fills out the 'dip' just below the peak, thereby dramatically increasing the photon flux at somewhat lower energies. In summary, photons radiated from charged gauge boson final states of (heavy) neutralino

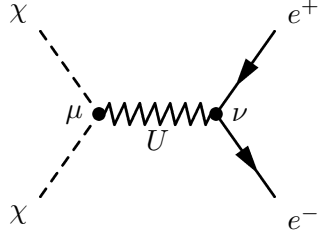


Figure 5.11: The only annihilation channel of the proposed light scalar dark matter candidate that occurs at tree level.

annihilation provide a striking signature and a promising signal to look for. Furthermore, the form of the spectrum should make it rather easy to distinguish between heavy neutralinos and LKPs as dark matter candidates – provided, of course, that the total flux is high enough to be detectable (which depends on the dark matter profile in the halo, as explained in the last sections).

Scalar dark matter

Recently, the proposal of a very light scalar dark matter candidate, with a mass in the range from 1 to 100 MeV, has been discussed in some detail (for a review, see [37]). The underlying particle physics model, however, is not motivated by any fundamental theory but constructed in a phenomenological and rather ad hoc fashion. Still, it is intriguing to see the principal possibility to evade the considerable observational bounds from colliders, i.e. the fact that such a light particle indeed could have escaped detection by for example LEP. A major advantage of this model, and in fact a main reason why it was proposed in the first place, is that it could explain the 511 keV line from e^+e^- annihilation [38] that is observed from the direction of the galactic center and for which so far no astrophysical explanation exists [80].

The idea is that the scalar dark matter particle χ couples to the gauge boson of a new, spontaneously broken $U(1)$ symmetry, called a U boson, whose only coupling to SM particles is to fermions. Pairs of dark matter particles can then annihilate through the s -channel process that is shown in Fig. 5.11. The only other kinematically accessible annihilation channels are into photons and neutrinos, and these are basically postulated not to exist, thereby evading in particular any direct gamma-ray constraints from, e.g., the CMB. Low energetic positrons lose their energy primarily through ionization, so the production of potentially detectable gamma rays from synchrotron radiation or inverse Compton scattering is also avoided in this

model [120].

As it was realized in [20], however, internal bremsstrahlung of the produced e^+e^- pairs is a source of photons that cannot be switched off. To estimate this effect, the authors of [20] used an already available result for the kinematically similar process $e^+e^- \rightarrow \mu^+\mu^-\gamma$; with a corresponding replacement of the appearing masses, this is given by

$$\frac{d\sigma}{dE_\gamma} = \sigma_{\text{tot}} \times \frac{\alpha_{\text{em}}}{\pi} \frac{1}{E_\gamma} \left[\ln \left(\frac{4m_\chi^2}{m_e^2} \left(1 - \frac{E_\gamma}{m_\chi} \right) \right) - 1 \right] \left[1 + \left(1 - \frac{E_\gamma}{m_\chi} \right)^2 \right]. \quad (5.21)$$

Since the lowest order cross section σ_{tot} is determined by the requirement that one can explain the strength of the 511 keV line, the gamma-ray spectrum can be calculated without knowing any details of the couplings of the U boson. A comparison with the EGRET [91] data on the gamma-ray spectrum in that energy range can then be used to constrain the dark matter particle mass to be less than 20 MeV. This means that a large parameter range of the originally proposed model is excluded.

These constraints can be improved by performing the actual calculation for the process that is depicted in Fig. 5.11, with the additional emission of a final state photon. The coupling of the scalar particle to the U boson is given by

$$g(p_1 - p_2)^\mu \quad (5.22)$$

and that of the U boson to electrons by

$$\gamma^\nu (g_R P_R + g_L P_L), \quad (5.23)$$

where p_1, p_2 are the momenta of the incoming particles and g, g_R, g_L are unknown coupling constants. Note that, when compared to the case of KK or neutralino dark matter, the calculation of the radiative correction to the lowest order cross section is considerably complicated by the fact that one may no longer consider the case of vanishing relative velocity between the incoming particles, $v = 0$, since in that limit the coupling between scalar and vector particles vanishes as well. This means that one has more kinematical degrees of freedom and, consequently, the angular integration is no longer trivial to perform.

For the three body final state that is considered here, the cross section is given by [55]

$$d\sigma = \frac{|\mathcal{M}|^2}{64(2\pi)^5 v m_\chi^2} dE_\gamma dE_e d\alpha d\beta d\gamma, \quad (5.24)$$

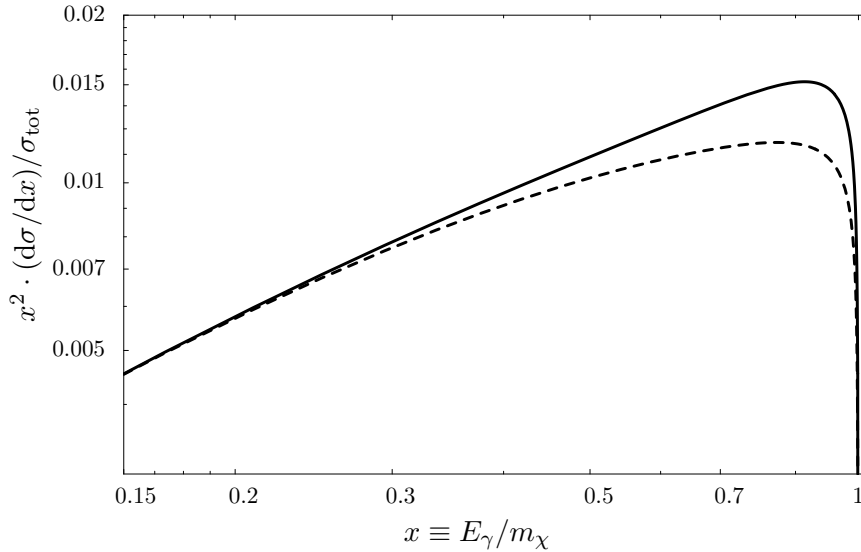


Figure 5.12: The cross-section for scalar dark matter annihilating into e^+e^- pairs plus an additional photon in the final state, for $m_\chi = 20$ MeV and normalized to the lowest order cross section (solid line). The approximation used by [20] is shown as a dashed line.

where E_e is the center-of-mass energy of the electron and α, β, γ are the Euler angles, as defined for example in [112]. Let ϕ_γ, ϕ_+ and ϕ_- be the angles of the γ, e^+ and e^- with \mathbf{p}_1 in the center-of-mass system (CMS), respectively. They can be related to the Euler angles as follows:

$$\cos \phi_\gamma = \cos \alpha \cos \gamma - \sin \alpha \sin \gamma \cos \beta \quad (5.25a)$$

$$\cos \phi_\pm = \cos \alpha \cos(\gamma \pm \varphi_\pm) - \sin \alpha \sin(\gamma \pm \varphi_\pm) \cos \beta. \quad (5.25b)$$

The CMS-angles φ_\pm between the e^\pm and the photon can easily be expressed in terms of E_γ and E_e . Now, it is important to realize that the only way ϕ_γ and ϕ_\pm enter in the Feynman amplitude \mathcal{M} is in the form $v \cos \phi_{\gamma,\pm}$. By expanding $|\mathcal{M}|^2$ in v and retaining merely terms to lowest order, one can therefore greatly simplify the angular integrals in (5.24) so that even the integral $\int dE_e$ becomes analytically performable.

The result is shown in Fig. 5.12, together with the approximate form (5.21) that was used in [20]. Again, the photon spectrum does not depend on the choice of the coupling constants, as everything is related to the zeroth order process of Fig. 5.11. As one can see, the full calculation basically confirms the approximation of [20], especially at lower energies. At high energies, one gets an enhancement of up to 35% as compared to the expression

(5.21). This translates into an improved upper bound of $m_\chi \lesssim 10$ MeV for the allowed scalar dark matter particle's mass, instead of $m_\chi \lesssim 20$ MeV as found in [20].

5.4 High-energetic antiprotons

In contrast to gamma rays, the interaction of antiprotons with the interstellar medium as well as (largely unknown) galactic magnetic fields cannot be neglected. Their propagation should therefore rather be understood as a diffusive process through the galactic halo, and the direction of a detected antiproton at earth reveals only little about its spatial origin. In order to describe the diffusive motion of charged (anti-)particles through the interstellar medium, one usually adopts cylindrical models of the Milky Way, with a thin disk containing all the stars and a much thicker diffusive halo of the same radius R_h ; at the border of this propagation region, the particles are allowed to escape freely. Above a certain threshold, the diffusion coefficient is assumed to scale with the particle rigidity as a power-law, $D(\mathcal{R}) \propto \mathcal{R}^\delta$ ($\delta \sim 0.7$), which means that high-energetic particles tend to lose their energy more quickly. The advantage of such a simple model is that analytical solutions to the diffusion equation are available and that it still gives a rather reasonable account of the basic underlying physics. Analytical solutions are even available when one refines this model considerably, such as allowing for the presence of a galactic wind, blowing the particles away from the disk. One may also take into account the effect of the (time-varying) solar activity on charged particles near earth, as well as reacceleration by stochastic magnetic fields during propagation or shock waves from supernova remnants. In the following, however, the focus will be on the very high-energy regime, where these effects can be neglected compared to the other uncertainties involved (see [24, 53] and references therein). The parameters of the propagation model can be constrained by analyzing the flux of stable nuclei, mainly by fitting the observed boron to carbon ratio B/C [89].

The background flux is dominated by antiprotons from inelastic collisions of cosmic ray protons with hydrogen and helium in the interstellar medium. Since the spectra of both cosmic ray protons and helium nuclei are quite well known, one can again use the B/C ratio to determine the propagation parameters describing the diffusion model and obtain a prediction for the background flux that fits the available antiproton data remarkably well [90]. A clear drawback here is that the highest energy for which such data currently are available is about 40 GeV; this situation will change with

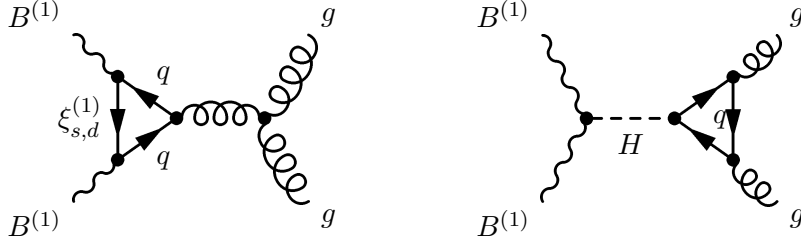


Figure 5.13: Diagrams potentially contributing to $B^{(1)}B^{(1)} \rightarrow gg$, apart from quark boxes as in Fig. 5.5. The first one is exactly cancelled by its antiquark counterpart, while the second is suppressed by $m_q/m_{B^{(1)}}$ due to the Yukawa coupling.

upcoming experiments like PAMELA [40] and AMS-02 [19]. Until then, one has to rely on extrapolations for propagation parameters in the high-energy regime.

Antiprotons from LKP annihilations

Annihilating KK dark matter is an additional source of antiprotons throughout the galactic halo. At tree level, those final states that can hadronize and then fragmentize into antiprotons are top and charm ($\sim 11\%$) as well as bottom quark pairs ($\sim 0.7\%$), charged ($\sim 0.9\%$) and neutral ($\sim 0.5\%$) vector bosons, and Higgs bosons ($\sim 0.6\%$). Another interesting channel is the (loop-suppressed) production of gluon pairs, which has a very similar structure to the process $B^{(1)}B^{(1)} \rightarrow \gamma\gamma$ that was discussed before. Here, however, only the fermion box diagrams displayed in Fig. 5.5 have to be taken into account, with of course no contribution from leptons. In contrast to the two photon case, this is an *exact* statement, valid to zeroth order in the quark masses m_q (which is also the limit in which the two photon analysis has been performed). To see this, note that the only additional diagrams that could potentially contribute are shown in Fig. 5.13. A fermion triangle with only vector couplings, however, is exactly cancelled by its antifermion counterpart; therefore, the first diagram does not contribute at all. The second diagram has a fairly simple Lorentz structure and can be calculated in the same way as described in [IV] for the two photon case. For each quark, one then finds the following contribution to the Feynman amplitude:

$$i\mathcal{M}^{\mu_1\mu_2\mu_3\mu_4} = -i\alpha_s\alpha_Y B_1^{gg,H} \left\{ g^{\mu_1\mu_2} p^{\mu_3} p^{\mu_4} - \frac{1}{2} g^{\mu_1\mu_2} g^{\mu_3\mu_4} \right\}, \quad (5.26)$$

where p is the momentum of the incoming $B^{(1)}$ particles and the scalar coefficient

$$B_1^{gg,H} = \frac{\xi}{4 - m_H^2/m_{\xi^{(1)}}^2} \left(16(1 - \xi)C_0(4, 0, 0; \xi, \xi, \xi) - 8 \right) \quad (5.27)$$

is suppressed by a factor of $\xi \equiv m_q^2/m_{B^{(1)}}^2$ that can be traced back to the Yukawa coupling of the Higgs to the quarks. (The scalar loop integral C_0 is defined in the appendix of [IV]). Even for the top quark, this contributes with less than 2% to the total two gluon cross section. To finally get this total cross section, up to $\mathcal{O}(\xi^0)$, one has thus just to take the expression (5.16), restrict the summation in (5.17) to quarks and substitute the electric charge Q by 1 (this corresponds to setting $g_{\text{eff}}^2 = 11/2$); the color average is then performed by the simple recipe $\alpha_{\text{em}}^2 \rightarrow (2/9)\alpha_s^2$ [26]. As a result, one finds that gluon pairs are as copiously produced as neutral gauge bosons at tree level.

With the exception of the Higgs boson, the fragmentation functions $dN^f/dT(m_{B^{(1)}}, T)$ for any annihilation product f , where T is the \bar{p} kinetic energy, can easily be obtained by Monte Carlo programs such as PYTHIA [116]. From this, the Higgs fragmentation function can be found by letting the Higgs decay in flight and then boosting and adding up the fragmentation functions for all its decay products that fragmentize into antiprotons. To see how this works in detail, boost first with $|\mathbf{v}_H| = \sqrt{1 - m_H^2/m_{B^{(1)}}^2}$ from the CMS into the system where one of the Higgs final states is at rest. In this system, the Higgs decays into some pair of (anti-)particles $X\bar{X}$, each with an energy $m_H/2$ and an angle θ between \mathbf{v}_H and their own direction of motion. Transforming back to the CMS, each of the Higgs decay products has an energy of

$$E_{\text{CMS}}^X = \frac{m_{B^{(1)}}}{2} \left(1 + \sqrt{(1 - m_H^2/m_{B^{(1)}}^2)(1 - 4m_X^2/m_H^2)} \sin \theta \right). \quad (5.28)$$

Since one starts out with a Higgs *pair*, the contribution of this particular annihilation process is given by $2 \cdot dN^X/dT(E_{\text{CMS}}^X, T)$, i.e. twice the amount of antiprotons that a particle with mass E_{CMS}^X decaying into an $X\bar{X}$ pair would give. The total Higgs fragmentation function dN^H/dT is then obtained by summing over all relevant Higgs decay channels and averaging over θ :

$$\frac{dN^H}{dT} = 2 \cdot \frac{1}{4\pi} \int d\Omega \sum_X \frac{dN^X}{dT}(E_{\text{CMS}}^X, T). \quad (5.29)$$

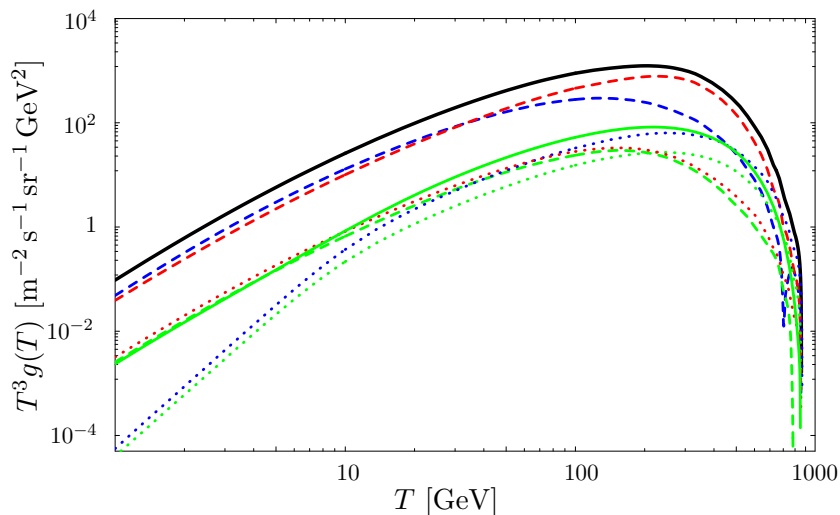


Figure 5.14: The individual contributions to the total antiproton differential spectrum (thick solid line) from quark final states (dashed lines), vector bosons (dotted lines) and the Higgs (light solid line). From top to bottom at the left margin, the corresponding channels are $B^{(1)}$ pair annihilations into $t\bar{t}$, $c\bar{c}$, gg , $b\bar{b}$, HH , W^+W^- and ZZ , respectively. The $B^{(1)}$ mass in this example has been chosen as $m_{B^{(1)}} = 1000$ GeV.

Fig. 5.14 shows the individual contributions to the antiproton differential spectrum from $B^{(1)}$ annihilations,

$$g(T) \equiv \sum_f B^f \frac{dN^f}{dT}, \quad (5.30)$$

where B^f is the branching ratio for the respective annihilation channel and the fragmentation functions have been taken from the DARKSUSY package [68], which uses tabulated results of a large number of events simulated with PYTHIA. For the Higgs, it has been assumed for simplicity that it decays mainly into $b\bar{b}$ and W^+W^- , which is reasonable for a Higgs mass of around 130 GeV [1]. As expected, the contributions from top and charm quarks clearly dominate most of the spectrum. For very high energies, however, charged vector bosons become almost more important. Note also the non-negligible contribution from gluons.

Expected antiproton fluxes

The number of antiprotons per unit time, energy and volume element that are produced by LKP annihilations at some position \mathbf{r} in the galactic halo is described by the source function

$$Q_{\bar{p}}(T, \mathbf{r}) = \frac{1}{2} \langle \sigma_{\text{ann}} v \rangle_{B^{(1)}} \left(\frac{\rho_{B^{(1)}}(\mathbf{r})}{m_{B^{(1)}}} \right)^2 \sum_f B^f \frac{dN^f}{dT}. \quad (5.31)$$

Once one specifies the source function, one can find a solution to the diffusion equation for the setup described at the beginning of this section. Due to the cylindrical symmetry of the problem, it can be written as an expansion in Bessel functions and for the antiproton flux at earth one finds

$$\Phi_{\bar{p}}(R_0, T) = \frac{1}{4\pi} v_{\bar{p}}(T) \sum_{s=1}^{\infty} J_0 \left(\nu_s^0 \frac{R_0}{R_h} \right) M_s^0(0), \quad (5.32)$$

where $v_{\bar{p}}(T)$ is the antiproton's velocity, ν_s^0 the s th zero of J_0 and $M_s^0(0) = M_s^0(0, T)$ is defined in [24]; it involves spatial integrals over the whole propagation region that have to be calculated numerically. A technical problem connected to the computation of the flux (5.32) is that the series only converges rather slowly, taking into account the non-negligible computation time that is required for the numerical integration of $M_s^0(0)$. However, the convergence behaviour can be improved considerably by defining

$$\Phi_i^{(0)} \equiv \frac{1}{4\pi} v_{\bar{p}}(T) \sum_{s=1}^i J_0 \left(\nu_s^0 \frac{R_0}{R_h} \right) M_s^0(0), \quad (5.33a)$$

$$\Phi_i^{(n+1)} \equiv \frac{1}{5} \sum_{j=i}^{i+4} \Phi_j^{(n)}. \quad (5.33b)$$

Fig. 5.15 illustrates the effect of considering $\Phi_i^{(n)}$ instead of the original series $\Phi_i^{(0)}$: Already for low values of n , the convergence is much faster and one can therefore significantly reduce the number of ϕ_s that have to be computed in order to arrive at a given level of accuracy.

The impact of different halo profiles or LKP masses on the expected antiproton flux has been discussed in detail in the accompanying paper [V]. The conclusion is that for smooth halo distributions one cannot expect any distortion of the background spectrum. Allowing for clumpy halo distributions, however, can result in a significant change of the background flux.

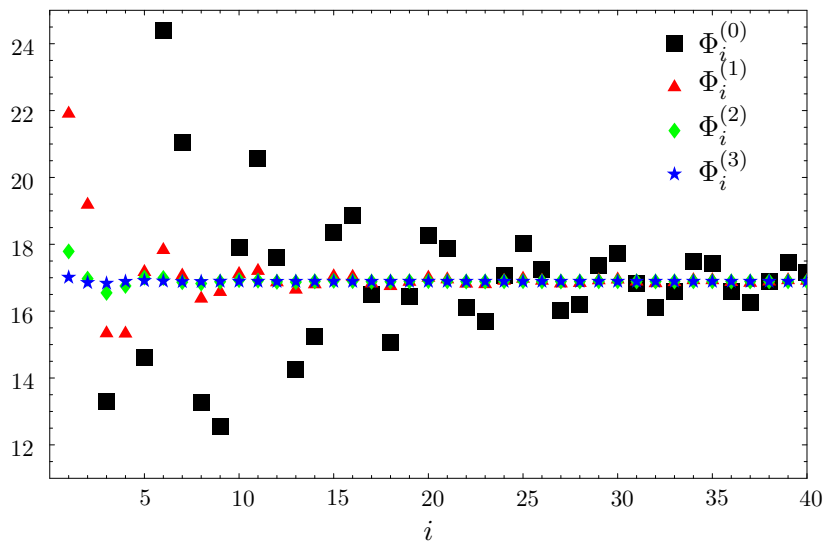


Figure 5.15: The numerical convergence of the flux as calculated at $T = 100$ GeV, in arbitrary units. See text for further details.

This is illustrated in Fig. 5.16 for a boost factor of around 100, which seems quite achievable. In fact, such a distortion in the antiproton spectrum can be considered as a very useful signature for $B^{(1)}$ dark matter when combined with the distinguished peak in the positron spectrum [76]. For the high LKP masses that are cosmologically interesting, this positron peak is usually washed out so that it cannot be distinguished against the background; for boost factors that give a distortion of the antiproton spectrum, however, it has to show up. Such a coincidence of these two signals is absent for example in the case of supersymmetry (where one can get similar distortions of the antiproton spectrum, though sometimes only for even higher boost factors), since there the annihilation of neutralino pairs into light leptons is helicity suppressed. It will therefore be exciting to await upcoming experiments like PAMELA [40] and AMS-02 [19] that will be able to probe the spectrum of both high-energetic antiprotons and positrons.

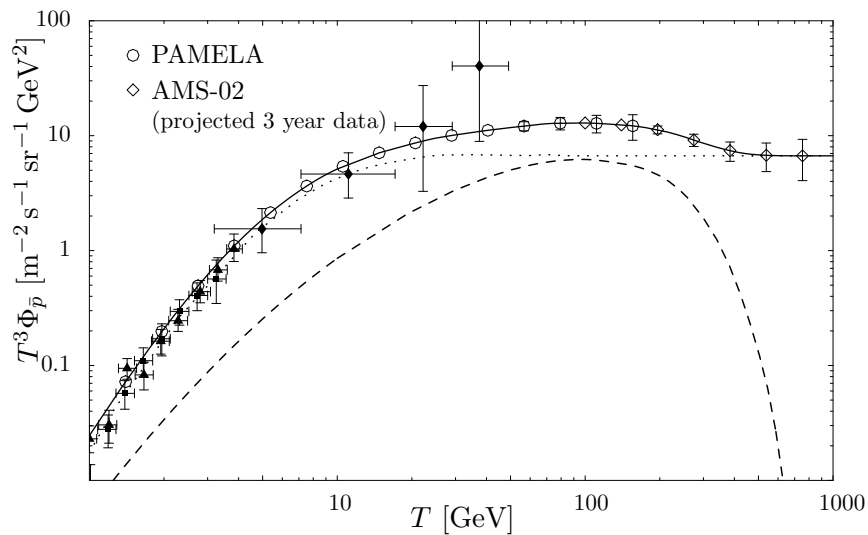


Figure 5.16: (From [V]). The dotted line shows the antiproton background flux as determined in [90], extrapolated for the energy range from 100 GeV to 1 TeV. The expected antiproton contribution from annihilating KK dark matter for the case of a clumpy NFW profile with $f\delta = 200$ (giving a boost factor of about 100) and $m_{B(1)} = 800$ GeV is plotted as a dashed line and the solid line gives the expected total spectrum. The data points are taken from the balloon-borne experiments BESS [99, 88] and CAPRICE [39]. Furthermore, the detectional prospects of PAMELA [40] and AMS-02 [19] are indicated by displaying their projected data after three years of operation.

Chapter 6

Summary and Outlook

The idea that our world consists of more than the observed three spatial dimensions is a fascinating possibility, both conceptually and phenomenologically. In this thesis, a particular extra-dimensional model was scrutinized and its possible implications for cosmology carefully studied. This model of *universal extra dimensions* (UEDs) is basically a higher-dimensional version of the standard model of particle physics, where all particles are allowed to propagate in the higher-dimensional bulk.

It is important to realize that a varying volume of the internal space of any higher-dimensional theory leads to varying coupling constants in the corresponding (effective) four-dimensional theory. Extra dimensions therefore have to be stabilized in order to evade the strong observational bounds on such a variation. In the simplest case of homogeneous extra dimensions, static solutions for their size arise naturally from the higher-dimensional field equations of general relativity during both radiation and vacuum energy dominated eras of the cosmological evolution. During matter domination, however, no static solutions exist. Adding an explicit stabilization mechanism, this situation does not change; it seems, however, that the extra dimensions can be *effectively* stabilized already for very shallow potentials and that any observational bounds therefore can be satisfied rather easily.

The cosmologically most relevant aspect of the UED model is that it naturally gives rise to a dark matter candidate $B^{(1)}$, which is the first Kaluza-Klein excitation of the weak hypercharge gauge boson. In this thesis, prospects for various indirect detection possibilities of Kaluza-Klein dark matter have been studied in some detail and found to be promising. This included, in particular, the contribution of annihilating $B^{(1)}$ particles to the gamma-ray and antiproton spectrum. As a by-product, it was discovered

that charged particle final states from the annihilation of *any* dark matter particle are very interesting in that final-state radiation can contribute significantly to the gamma-ray spectrum. The expected signature, with its sharp cutoff at the dark matter particle's mass, provides a new and promising way for the indirect detection of dark matter. For illustration, this process was therefore studied not only for Kaluza-Klein dark matter, but also for scalar and neutralino dark matter.

An attractive feature of the UED model is that it contains only very few free parameters – in principle only the compactification scale R and the high-energy cutoff Λ – and the whole cosmologically interesting range of these parameters will be scanned throughout by the LHC. This has to be contrasted with the huge parameter space of supersymmetry, where one cannot exclude all neutralino dark matter candidates even if no supersymmetric particles are found at the LHC. There is a second, more phenomenological reason why it is interesting to study the $B^{(1)}$: it can serve as a simple *prototype* for massive vector dark matter particles. So far, there is no direct evidence for the nature of dark matter nor for the existence of supersymmetry. It is therefore important to keep an open mind and seriously consider other dark matter candidates – or, taking into account the plethora of existing proposals, rather *types* of candidates – than only the neutralino, which in this general context may be viewed as the prototype of a Majorana fermion dark matter particle.

For the near future, several obvious roads for a further study of Kaluza-Klein dark matter open up. First, a more detailed investigation of possible astrophysical effects in the context of the indirect detection methods discussed in this thesis should be undertaken. This includes the fate of the produced electrons and positrons as well as a closer look at the propagation model for antiprotons, especially at lower energies, where one in contrast to higher energies already has access to rather accurate data. Secondly, it is certainly worth to reconsider the freeze-out process and to improve the calculation of the $B^{(1)}$ relic density, taking co-annihilations into full account. The cutoff in the power spectrum, finally, that leads to the existence of small dark matter clumps as the first gravitationally bound objects, has so far only been calculated for the neutralino (and for the axion). It would be important to see, whether the scale at which this cutoff appears is a result that is universal for WIMPs or whether the predictions would change in the case of a massive vector dark matter particle like the $B^{(1)}$.

Appendix A

Feynman rules and interaction terms for the UED model

In the following, a complete list of (bulk) interaction terms appearing in the five-dimensional UED model is presented in a way that makes it easy to derive Feynman rules for all particles appearing in the spectrum of the effective 4D theory. In these expressions, 4D Lorentz indices are suppressed whenever there is no risk for confusion. The three-point vertex rules for all states up to the first KK-level are then given explicitly. Here, all momenta are taken to be ingoing.

Since all these interaction terms are located in the bulk, they are KK number conserving. In principle, there also appear counterterms to radiative corrections at the orbifold fixpoints, giving rise to additional interactions that can violate KK number conservation [46]. These terms, however, are suppressed by the cutoff-scale Λ and will therefore not be considered here.

The spectrum of states

As it has been discussed in detail in Section 3.3, the vector part of the spectrum for the 4D theory consists of the SM fields $A^{(0)\mu}$, $Z^{(0)\mu}$ and $W_{\pm}^{(0)\mu}$, as well as their first-level KK excitations; since the Weinberg angle is essentially driven to zero for KK states, $B^{(n)\mu}$, $A^{3(n)\mu}$ and $W_{\pm}^{(n)\mu}$ ($n \geq 1$) are treated as mass eigenstates. For each vector particle, there will be a ghost c that is associated to it. In addition, there appear physical scalar states $H^{(0)}$, $H^{(n)}$, $a_0^{(n)}$, $a_{\pm}^{(n)}$, and Goldstone modes $\chi^{3(0)}$, $\chi^{\pm(0)}$, $G_0^{(n)}$, $G_{\pm}^{(n)}$, $A_5^{(n)}$

in the theory. Finally, for every SM fermion $\psi^{(0)}$, one has two towers of KK fermions $\psi_s^{(n)}$ and $\psi_d^{(n)}$ - except for neutrinos, which only come in a singlet version both at zero and higher KK levels. These physical states are related to those appearing fundamentally in the theory by (3.30), (3.36) and (3.60); in order to derive Feynman rules, it proves very convenient to have also the inverse of these expressions at hand:

$$A_M^3 = s_w A_M + c_w Z_M \quad (\text{A.1a})$$

$$B_M = c_w A_M - s_w Z_M \quad (\text{A.1b})$$

$$Z_5^{(n)} = \frac{m_Z}{M_Z^{(n)}} a_0^{(n)} - \frac{M^{(n)}}{M_Z^{(n)}} G_0^{(n)} \quad (\text{A.2a})$$

$$\chi^{3(n)} = \frac{M^{(n)}}{M_Z^{(n)}} a_0^{(n)} + \frac{m_Z}{M_Z^{(n)}} G_0^{(n)} \quad (\text{A.2b})$$

$$W_5^{\pm(n)} = \frac{m_W}{M_W^{(n)}} a_{\pm}^{(n)} - \frac{M^{(n)}}{M_W^{(n)}} G_{\pm}^{(n)} \quad (\text{A.2c})$$

$$\chi^{\pm(n)} = \frac{M^{(n)}}{M_W^{(n)}} a_{\pm}^{(n)} + \frac{m_W}{M_W^{(n)}} G_{\pm}^{(n)} \quad (\text{A.2d})$$

$$\psi_s^{(n)} = \sin \alpha^{(n)} \xi_d^{(n)} - \cos \alpha^{(n)} \gamma^5 \xi_s^{(n)} \quad (\text{A.3a})$$

$$\psi_d^{(n)} = \cos \alpha^{(n)} \xi_d^{(n)} + \sin \alpha^{(n)} \gamma^5 \xi_s^{(n)} \quad (\text{A.3b})$$

Finally, following the conventions of [103], the propagators for internal particles read

$$\text{for scalars : } \frac{i}{q^2 - m^2 + i\epsilon}, \quad (\text{A.4})$$

$$\text{for fermions : } \frac{i(q + m)}{q^2 - m^2 + i\epsilon}, \quad (\text{A.5})$$

$$\text{for vectors : } \frac{-i}{q^2 - m^2 + i\epsilon} \left(\eta^{\mu\nu} - \frac{q^\mu q^\nu}{q^2 - \xi m^2} (1 - \xi) \right). \quad (\text{A.6})$$

Ghosts and Goldstone bosons have the same propagators as physical scalars, with masses $\sqrt{\xi} m_V$, where m_V is the mass of the associated vector boson.

Three-point vertices

When reducing the five-dimensional Lagrangian $\hat{\mathcal{L}}$ to a 4D Lagrangian \mathcal{L} , one encounters integrals over various combinations of fields that transform even (3.16a) or odd (3.16b) under orbifold transformations. For three even fields X, Y, Z , for example, one has

$$\int_0^{2\pi R} dy XYZ = \frac{1}{\sqrt{2\pi R}} \left\{ X^{(0)} Y^{(0)} Z^{(0)} + X^{(0)} Y^{(1)} Z^{(1)} + X^{(1)} Y^{(0)} Z^{(1)} + X^{(1)} Y^{(1)} Z^{(0)} \right\}, \quad (\text{A.7})$$

while for one even field X and two odd fields U, V , one finds:

$$\int_0^{2\pi R} dy XUV = \frac{1}{\sqrt{2\pi R}} X^{(0)} U^{(1)} V^{(1)}. \quad (\text{A.8})$$

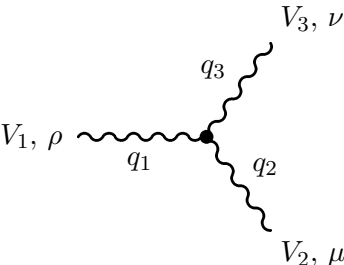
The integration over any other combination of three fields gives zero.

Vector-vector-vector couplings

The interaction terms that are involved here originate from the cubic terms in the 'free' gauge field Lagrangian (3.19),

$$\begin{aligned} \hat{\mathcal{L}}^{(VVV)} = & -i\hat{g} \left[\partial^\nu A^{3\mu} (W_\nu^- W_\mu^+ - W_\nu^+ W_\mu^-) \right. \\ & + A^{3\mu} (\partial_\nu W_\mu^- W^{+\nu} - \partial_\nu W_\mu^+ W^{-\nu} \\ & \left. + \partial_\mu W_\nu^+ W^{-\nu} - \partial_\mu W_\nu^- W^{+\nu}) \right]. \quad (\text{A.9}) \end{aligned}$$

This gives rise to the following 4D Feynman rules:



$$ig_{V_1 V_2 V_3} \left[(q_1 - q_2)^\nu \eta^{\rho\mu} + (q_2 - q_3)^\rho \eta^{\mu\nu} + (q_3 - q_1)^\mu \eta^{\rho\nu} \right]$$

where

$$g_{A^{(0)}W_+^{(0,1)}W_-^{(0,1)}} = -e \quad (\text{A.10})$$

$$g_{Z^{(0)}W_+^{(0,1)}W_-^{(0,1)}} = -c_w g \quad (\text{A.11})$$

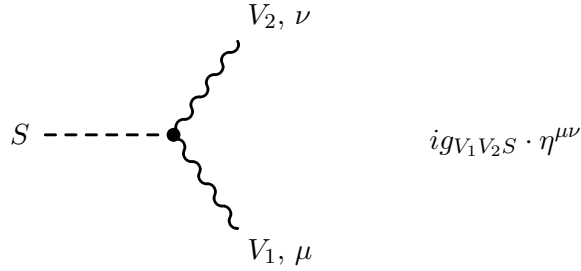
$$g_{A_3^{(1)}W_+^{(0,1)}W_-^{(1,0)}} = -g \quad (\text{A.12})$$

Vector-vector-scalar couplings

The interaction terms that are involved here originate from the cubic parts of the corresponding terms in both the 'free' gauge field Lagrangian (3.19) and the kinetic term of the Higgs Lagrangian (3.25),

$$\begin{aligned} \hat{\mathcal{L}}^{(VV,S)} = & i\hat{g} [W_5^+ (W^- \partial_y A^3) - W_5^+ (A^3 \partial_y W^-) + A_5^3 (W^+ \partial_y W^-) - \text{c.c}] \\ & + \hat{g} \left[\frac{m_Z}{2c_w} H(ZZ) + m_W H(W^+W^-) \right] \\ & - i\hat{g}_Y [m_W \chi^- (BW^+) - \text{c.c}] \end{aligned} \quad (\text{A.13})$$

This gives rise to the following 4D Feynman rules:



where

$$g_{A^{(0)}W_\pm^{(0)}\chi^\mp(0)} = \mp ie m_W \quad (\text{A.14})$$

$$g_{Z^{(0)}W_\pm^{(0)}\chi^\mp(0)} = \pm ig_s^2 m_Z \quad (\text{A.15})$$

$$g_{Z^{(0)}Z^{(0)}H^{(0)}} = \frac{g}{c_w} m_Z \quad (\text{A.16})$$

$$g_{W_+^{(0)}W_-^{(0)}H^{(0)}} = g m_W \quad (\text{A.17})$$

$$g_{A^{(0)}W_\pm^{(1)}G_\mp^{(1)}} = \mp ie M_W^{(1)} \quad (\text{A.18})$$

$$g_{Z^{(0)}W_\pm^{(1)}a_\mp^{(1)}} = \pm ig m_Z \frac{M^{(1)}}{M_W^{(1)}} \quad (\text{A.19})$$

$$g_{Z^{(0)}W_{\pm}^{(1)}G_{\mp}^{(1)}} = \mp igc_w M^{(1)} \frac{M^{(1)}}{M_W^{(1)}} \left(1 + \frac{s_w^2}{c_w^2} \left(\frac{m_W}{M^{(1)}} \right)^2 \right) \quad (\text{A.20})$$

$$g_{Z^{(0)}A^3(1)H^{(1)}} = gm_Z \quad (\text{A.21})$$

$$g_{Z^{(0)}B^{(1)}H^{(1)}} = -g_Y m_Z \quad (\text{A.22})$$

$$g_{W_{\pm}^{(0)}A^3(1)a_{\mp}^{(1)}} = \mp ig m_W \frac{M^{(1)}}{M_W^{(1)}} \quad (\text{A.23})$$

$$g_{W_{\pm}^{(0)}A^3(1)G_{\mp}^{(1)}} = \pm ig M^{(1)} \frac{M^{(1)}}{M_W^{(1)}} \quad (\text{A.24})$$

$$g_{W_{\pm}^{(0)}A^3(1)G_{\mp}^{(1)}} = \pm ig M^{(1)} \frac{M^{(1)}}{M_W^{(1)}} \quad (\text{A.25})$$

$$g_{W_{\pm}^{(0)}B^{(1)}a_{\mp}^{(1)}} = \mp ig_Y m_W \frac{M^{(1)}}{M_W^{(1)}} \quad (\text{A.26})$$

$$g_{W_{\pm}^{(0)}B^{(1)}G_{\mp}^{(1)}} = \mp ig_Y m_W \frac{m_W}{M_W^{(1)}} \quad (\text{A.27})$$

$$g_{W_{\pm}^{(0)}W_{\mp}^{(1)}A_5^{(1)}} = \pm ie M^{(1)} \quad (\text{A.28})$$

$$g_{W_{\pm}^{(0)}W_{\mp}^{(1)}a_0^{(1)}} = \pm ig m_W \frac{M^{(1)}}{M_Z^{(1)}} \quad (\text{A.29})$$

$$g_{W_{\pm}^{(0)}W_{\mp}^{(1)}G_0^{(1)}} = \mp igc_w M^{(1)} \frac{M^{(1)}}{M_Z^{(1)}} \quad (\text{A.30})$$

$$g_{W_{\pm}^{(0)}W_{\mp}^{(1)}H^{(1)}} = gm_W \quad (\text{A.31})$$

$$g_{A^3(1)A^3(1)H^{(0)}} = gm_W \quad (\text{A.32})$$

$$g_{A^3(1)B^{(1)}H^{(0)}} = -g_Y m_W \quad (\text{A.33})$$

$$g_{B^{(1)}B^{(1)}H^{(0)}} = g \frac{s_w^2}{c_w^2} m_W \quad (\text{A.34})$$

$$g_{W_{+}^{(1)}W_{-}^{(1)}H^{(0)}} = gm_W \quad (\text{A.35})$$

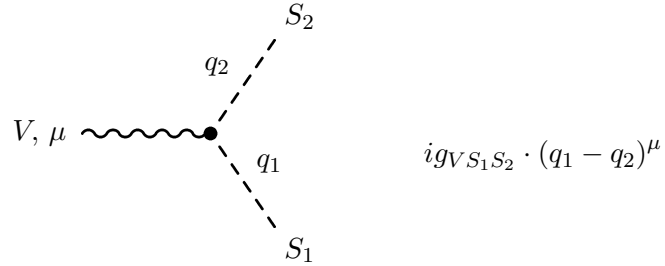
$$g_{W_{\pm}^{(1)}B^{(1)}\chi_{\mp}^{(0)}} = \mp ig_Y m_W \quad (\text{A.36})$$

Vector-scalar-scalar couplings

The interaction terms that are involved here originate from the corresponding cubic parts of both the 'free' gauge field Lagrangian (3.19) and the kinetic term of the Higgs Lagrangian (3.25),

$$\begin{aligned}
\hat{\mathcal{L}}^{(VSS)} = & i\hat{g} [(W^- \partial A_5^3) W_5^+ + (W^+ \partial W_5^-) A_5^3 + (A^3 \partial W_5^+) W_5^- - \text{c.c.}] \\
& + i\hat{e} A [(\partial \chi^+) \chi^- - \text{c.c.}] + \frac{i}{2} (\hat{g} c_w - \hat{g}_Y s_w) Z [(\partial \chi^+) \chi^- - \text{c.c.}] \\
& + \frac{\hat{g}}{2c_w} Z [(\partial H) \chi^3 - H(\partial \chi^3)] + \frac{\hat{g}}{2} [W^+ ((\partial H) \chi^- - H(\partial \chi^-)) + \text{c.c.}] \\
& + i\frac{\hat{g}}{2} [W^+ (\chi^3(\partial \chi^-) - (\partial \chi^3) \chi^-) - \text{c.c.}] \tag{A.37}
\end{aligned}$$

This gives rise to the following 4D Feynman rules:



where

$$g_{A^{(0)}\chi^+^{(0)}\chi^-^{(0)}} = e \tag{A.38}$$

$$g_{Z^{(0)}\chi^+^{(0)}\chi^-^{(0)}} = g \frac{c_w}{2} - g_Y \frac{s_w}{2} \tag{A.39}$$

$$g_{Z^{(0)}\chi^3^{(0)}H^{(0)}} = i \frac{g}{2c_w} \tag{A.40}$$

$$g_{W_\pm^{(0)}\chi^\mp^{(0)}H^{(0)}} = i \frac{g}{2} \tag{A.41}$$

$$g_{W_\pm^{(0)}\chi^\mp^{(0)}\chi^3^{(0)}} = \mp \frac{g}{2} \tag{A.42}$$

$$g_{A^{(0)}a_+^{(1)}a_-^{(1)}} = e \tag{A.43}$$

$$g_{A^{(0)}G_+^{(1)}G_-^{(1)}} = e \tag{A.44}$$

$$g_{Z^{(0)}a_+^{(1)}a_-^{(1)}} = \frac{1}{2} (g c_w - g_Y s_w) \left(\frac{M^{(1)}}{M_W^{(1)}} \right)^2 + g c_w \left(\frac{m_W}{M_W^{(1)}} \right)^2 \tag{A.45}$$

$$g_{Z^{(0)}a_{\pm}^{(1)}G_{\mp}^{(1)}} = \mp \frac{1}{2} (gc_w - g_Y s_w) \frac{m_W}{M_W^{(1)}} \frac{M^{(1)}}{M_W^{(1)}} \quad (\text{A.46})$$

$$g_{Z^{(0)}G_{+}^{(1)}G_{-}^{(1)}} = gc_w \left(\frac{M^{(1)}}{M_W^{(1)}} \right)^2 + \frac{1}{2} (gc_w - g_Y s_w) \left(\frac{m_W}{M_W^{(1)}} \right)^2 \quad (\text{A.47})$$

$$g_{Z^{(0)}H^{(1)}a_0^{(1)}} = -i \frac{g}{2c_w} \frac{M^{(1)}}{M_Z^{(1)}} \quad (\text{A.48})$$

$$g_{Z^{(0)}H^{(1)}G_0^{(1)}} = -i \frac{g}{2c_w} \frac{m_Z}{M_Z^{(1)}} \quad (\text{A.49})$$

$$g_{W_{\pm}^{(0)}a_{\mp}^{(1)}A_5^{(1)}} = \pm g \frac{m_W}{M_W^{(1)}} \quad (\text{A.50})$$

$$g_{W_{\pm}^{(0)}G_{\mp}^{(1)}A_5^{(1)}} = \pm g \frac{M^{(1)}}{M_W^{(1)}} \quad (\text{A.51})$$

$$g_{W_{\pm}^{(0)}a_{\mp}^{(1)}a_0^{(1)}} = \mp \frac{g}{2} \frac{M^{(1)^2}}{M_W^{(1)} M_Z^{(1)}} \left(1 - 2 \frac{m_w^2}{M_W^{(1)^2}} \right) \quad (\text{A.52})$$

$$g_{W_{\pm}^{(0)}G_{\mp}^{(1)}a_0^{(1)}} = \mp \frac{3}{2} g \frac{m_W}{M_W^{(1)}} \frac{M^{(1)}}{M_Z^{(1)}} \quad (\text{A.53})$$

$$g_{W_{\pm}^{(0)}a_{\mp}^{(1)}G_0^{(1)}} = \mp g \left(c_w + \frac{1}{2c_w} \right) \frac{m_W}{M_W^{(1)}} \frac{M^{(1)}}{M_Z^{(1)}} \quad (\text{A.54})$$

$$g_{W_{\pm}^{(0)}G_{\mp}^{(1)}G_0^{(1)}} = \pm gc_w \frac{M^{(1)}}{M_W^{(1)}} \frac{M^{(1)}}{M_Z^{(1)}} \left(1 - \frac{1}{2c_w} \frac{m_W}{M_W^{(1)}} \frac{m_Z}{M_Z^{(1)}} \right) \quad (\text{A.55})$$

$$g_{W_{\pm}^{(0)}a_{\mp}^{(1)}H^{(1)}} = i \frac{g}{2} \frac{M^{(1)}}{M_W^{(1)}} \quad (\text{A.56})$$

$$g_{W_{\pm}^{(0)}G_{\mp}^{(1)}H^{(1)}} = i \frac{g}{2} \frac{m_W}{M_W^{(1)}} \quad (\text{A.57})$$

$$g_{A^{3(1)}\chi_{\pm}^{(0)}a_{\mp}^{(1)}} = \pm \frac{g}{2} \frac{M^{(1)}}{M_W^{(1)}} \quad (\text{A.58})$$

$$g_{A^{3(1)}\chi_{\pm}^{(0)}G_{\mp}^{(1)}} = \pm \frac{g}{2} \frac{m_W}{M_W^{(1)}} \quad (\text{A.59})$$

$$g_{A^{3(1)}\chi^{3(0)}H^{(1)}} = i \frac{g}{2} \quad (\text{A.60})$$

$$g_{A^{3(1)}a_0^{(1)}H^{(0)}} = i \frac{g}{2} \frac{M^{(1)}}{M_Z^{(1)}} \quad (\text{A.61})$$

$$g_{A^3(1)a_0^{(1)}H^{(0)}} = i\frac{g}{2}\frac{m_Z}{M_Z^{(1)}} \quad (\text{A.62})$$

$$g_{B^{(1)}\chi^{\pm(0)}a_{\mp}^{(1)}} = \pm\frac{g_Y}{2}\frac{M^{(1)}}{M_W^{(1)}} \quad (\text{A.63})$$

$$g_{B^{(1)}\chi^{\pm(0)}G_{\mp}^{(1)}} = \pm\frac{g_Y}{2}\frac{m_W}{M_W^{(1)}} \quad (\text{A.64})$$

$$g_{B^{(1)}\chi^3(0)H^{(1)}} = -i\frac{g_Y}{2} \quad (\text{A.65})$$

$$g_{B^{(1)}a_0^{(1)}H^{(0)}} = -i\frac{g_Y}{2}\frac{M^{(1)}}{M_Z^{(1)}} \quad (\text{A.66})$$

$$g_{B^{(1)}G_0^{(1)}H^{(0)}} = -i\frac{g_Y}{2}\frac{m_Z}{M_Z^{(1)}} \quad (\text{A.67})$$

$$g_{W_{\pm}^{(1)}\chi^{\mp(0)}H^{(1)}} = i\frac{g}{2} \quad (\text{A.68})$$

$$g_{W_{\pm}^{(1)}a_{\mp}^{(1)}H^{(0)}} = i\frac{g}{2}\frac{M^{(1)}}{M_W^{(1)}} \quad (\text{A.69})$$

$$g_{W_{\pm}^{(1)}G_{\mp}^{(1)}H^{(0)}} = i\frac{g}{2}\frac{m_W}{M_W^{(1)}} \quad (\text{A.70})$$

$$g_{W_{\pm}^{(1)}a_{\mp}^{(1)}H^{(0)}} = i\frac{g}{2}\frac{M^{(1)}}{M_W^{(1)}} \quad (\text{A.71})$$

$$g_{W_{\pm}^{(1)}\chi^{\mp(0)}a_0^{(1)}} = \mp\frac{g}{2}\frac{M^{(1)}}{M_Z^{(1)}} \quad (\text{A.72})$$

$$g_{W_{\pm}^{(1)}\chi^{\mp(0)}G_0^{(1)}} = \mp\frac{g}{2}\frac{m_Z}{M_Z^{(1)}} \quad (\text{A.73})$$

$$g_{W_{\pm}^{(1)}a_{\mp}^{(1)}\chi^3(0)} = \mp\frac{g}{2}\frac{M^{(1)}}{M_W^{(1)}} \quad (\text{A.74})$$

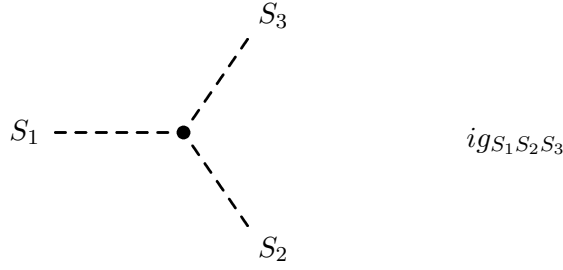
$$g_{W_{\pm}^{(1)}G_{\mp}^{(1)}\chi^3(0)} = \mp\frac{g}{2}\frac{m_W}{M_W^{(1)}} \quad (\text{A.75})$$

Scalar-scalar-scalar couplings

The interactions that are involved here originate from the corresponding cubic parts of both the kinetic and the potential terms of the Higgs Lagrangian (3.25),

$$\begin{aligned}
\hat{\mathcal{L}}^{(SSS)} &= -i\hat{e}A_5 [(\partial_y\chi^+)\chi^- - \text{c.c.}] - \frac{i}{2}(\hat{g}c_w - \hat{g}_Y s_w) Z_5 [(\partial_y\chi^+)\chi^- - \text{c.c.}] \\
&\quad - \frac{g}{2c_w} Z_5 [(\partial_y H)\chi^3 - H(\partial_y\chi^3)] - \frac{g}{2} [W_5^+ ((\partial_y H)\chi^- - H(\partial_y\chi^-)) + \text{c.c.}] \\
&\quad - i\frac{g}{2} [W_5^+ (\chi^3(\partial_y\chi^-) - (\partial_y\chi^3)\chi^-) - \text{c.c.}] - \frac{g}{2c_w} m_Z Z_5 Z_5 H \\
&\quad - gm_W W_5^+ W_5^- H + ig_Y m_W B_5 [W_5^+ \chi^- - \text{c.c.}] \\
&\quad - \frac{\hat{g}}{4} \frac{m_H^2}{m_W} (2H\chi^+\chi^- + HHH + H\chi^3\chi^3)
\end{aligned} \tag{A.76}$$

This gives rise to the following 4D Feynman rules:



where

$$g_{H^{(0)}H^{(0,1)}H^{(0,1)}} = -\frac{3}{2}g \frac{m_H^2}{m_W} \tag{A.77}$$

$$g_{H^{(0)}\chi^+(0)\chi^-(0)} = -\frac{g}{2} \frac{m_H^2}{m_W} \tag{A.78}$$

$$g_{H^{(0)}\chi^3(0)\chi^3(0)} = -\frac{g}{2} \frac{m_H^2}{m_W} \tag{A.79}$$

$$g_{H^{(0)}a_+^{(1)}a_-^{(1)}} = -gm_W \left(1 + \frac{1}{2} \frac{m_H^2}{m_W^2} \left(\frac{M^{(1)}}{M_W^{(1)}} \right)^2 \right) \tag{A.80}$$

$$g_{H^{(0)}a_{\pm}^{(1)}G_{\mp}^{(1)}} = \frac{g}{2} M^{(1)} \left(1 - \frac{m_H^2}{M_W^{(1)2}} \right) \tag{A.81}$$

$$g_{H^{(0)}G_{\pm}^{(1)}G_{\mp}^{(1)}} = -\frac{g}{2} m_W \frac{m_H^2}{M_W^{(1)2}} \quad (\text{A.82})$$

$$g_{H^{(0)}a_0^{(1)}a_0^{(1)}} = -\frac{g}{c_w} m_Z \left(1 + \frac{1}{2} \frac{m_H^2}{m_Z^2} \left(\frac{M^{(1)}}{M_Z^{(1)}} \right)^2 \right) \quad (\text{A.83})$$

$$g_{H^{(0)}a_0^{(1)}G_0^{(1)}} = \frac{g}{2c_w} M^{(1)} \left(1 - \frac{m_H^2}{M_Z^{(1)2}} \right) \quad (\text{A.84})$$

$$g_{H^{(0)}G_0^{(1)}G_0^{(1)}} = -\frac{g}{2c_w} m_Z \frac{m_H^2}{M_Z^{(1)2}} \quad (\text{A.85})$$

$$g_{\chi^3(0)H^{(1)}a_0^{(1)}} = \frac{g}{2c_w} m_Z \frac{M^{(1)}}{M_Z^{(1)}} \left(1 - \frac{m_H^2}{m_Z^2} \right) \quad (\text{A.86})$$

$$g_{\chi^3(0)H^{(1)}G_0^{(1)}} = -\frac{g}{2c_w} M^{(1)} \frac{M^{(1)}}{M_Z^{(1)}} \left(1 + \frac{m_H^2}{M^{(1)2}} \right) \quad (\text{A.87})$$

$$g_{\chi^3(0)a_{\pm}^{(1)}G_{\mp}^{(1)}} = \pm i \frac{g}{2} M^{(1)} \quad (\text{A.88})$$

$$g_{\chi^{\pm}(0)a_{\mp}^{(1)}H^{(1)}} = \frac{g}{2} m_W \frac{M^{(1)}}{M_W^{(1)}} \left(1 - \frac{m_H^2}{m_W^2} \right) \quad (\text{A.89})$$

$$g_{\chi^{\pm}(0)G_{\mp}^{(1)}H^{(1)}} = -\frac{g}{2} M^{(1)} \frac{M^{(1)}}{M_W^{(1)}} \left(1 + \frac{m_H^2}{M^{(1)2}} \right) \quad (\text{A.90})$$

$$g_{\chi^{\pm}(0)a_{\mp}^{(1)}A_5^{(1)}} = \mp i e \quad (\text{A.91})$$

$$g_{\chi^{\pm}(0)a_{\mp}^{(1)}a_0^{(1)}} = \pm i \frac{g_Y}{2} s_w m_Z \frac{M_W^{(1)}}{M_Z^{(1)}} \quad (\text{A.92})$$

$$g_{\chi^{\pm}(0)G_{\mp}^{(1)}a_0^{(1)}} = \mp i \frac{g}{2} M^{(1)} \frac{M_Z^{(1)}}{M_W^{(1)}} \quad (\text{A.93})$$

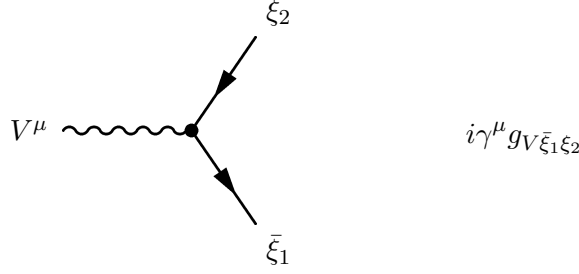
$$g_{\chi^{\pm}(0)a_{\mp}^{(1)}G_0^{(1)}} = \pm \frac{i}{2} (g c_w - g_Y s_w) M^{(1)} \frac{M_W^{(1)}}{M_Z^{(1)}} \quad (\text{A.94})$$

Fermion-fermion-vector couplings

The interaction terms that are involved here originate from the covariant derivative in the kinetic terms of the fermion Lagrangian (3.63). For quarks, they read

$$\begin{aligned}
\hat{\mathcal{L}}^{(QQV)} &= \bar{\psi}_{d,U}^i \gamma^\mu \left(Y_d \hat{g}_Y B_\mu + \frac{\hat{g}}{2} A_\mu^3 \right) \psi_{d,U}^i + \bar{\psi}_{d,D}^i \gamma^\mu \left(Y_d \hat{g}_Y B_\mu - \frac{\hat{g}}{2} A_\mu^3 \right) \psi_{d,D}^i \\
&\quad + Y_{s,U} \hat{g}_Y \bar{\psi}_{s,U}^i \gamma^\mu B_\mu \psi_{s,U}^i + Y_{s,D} \hat{g}_Y \bar{\psi}_{s,D}^i \gamma^\mu B_\mu \psi_{s,D}^i \\
&\quad + \frac{\hat{g}}{\sqrt{2}} V^{ij} \left(\bar{\psi}_{d,U}^i \gamma^\mu W_\mu^+ \psi_{d,D}^j + \bar{\psi}_{d,D}^i \gamma^\mu W_\mu^- \psi_{d,U}^j \right), \tag{A.95}
\end{aligned}$$

where the indices i, j indicate the family. Let $\xi = U, D$ denote the mass eigenstates as given in (3.60) for up ($T^3 = +1/2$) and down ($T^3 = -1/2$) type quarks, respectively. Defining $Q \equiv T_3 + Y = Y_s$ as usual, one can now derive the following Feynman rules:



where¹

$$g_{A^{(0)}\bar{\xi}^{(0)}\xi^{(0)}} = -Qe \tag{A.96}$$

$$g_{A^{(0)}\bar{\xi}_{(s,d)}^{(1)}\xi_{(s,d)}^{(1)}} = -Qe \tag{A.97}$$

$$g_{Z^{(0)}\bar{\xi}^{(0)}\xi^{(0)}} = (T_3 g c_w - Y_d g_Y s_w) P_L - Y_s g_Y s_w P_R \tag{A.98}$$

$$g_{Z^{(0)}\bar{\xi}_d^{(1)}\xi_d^{(1)}} = \frac{g}{c_w} \left(-Y_d s_w^2 + T_3 c_w^2 \cos^2 \alpha^{(1)} - T_3 s_w^2 \sin^2 \alpha^{(1)} \right) \tag{A.99}$$

$$g_{Z^{(0)}\bar{\xi}_s^{(1)}\xi_s^{(1)}} = \frac{g}{c_w} \left(-Y_d s_w^2 + T_3 c_w^2 \sin^2 \alpha^{(1)} - T_3 s_w^2 \cos^2 \alpha^{(1)} \right) \tag{A.100}$$

$$g_{Z^{(0)}\bar{\xi}_s^{(1)}\xi_d^{(1)}} = \frac{g}{c_w} T_3 \sin \alpha^{(1)} \cos \alpha^{(1)} \tag{A.101}$$

¹Observe that one always has $g_{V\bar{\xi}_1\xi_2} = g_{V^\dagger\bar{\xi}_2\xi_1}^*$.

$$g_{A_3^{(1)}\bar{\xi}^{(0)}\xi_d^{(1)}} = T_3 g \cos \alpha^{(1)} P_L \quad (\text{A.102})$$

$$g_{A_3^{(1)}\bar{\xi}^{(0)}\xi_s^{(1)}} = -T_3 g \sin \alpha^{(1)} P_L \quad (\text{A.103})$$

$$g_{B^{(1)}\bar{\xi}^{(0)}\xi_d^{(1)}} = Y_s g_Y \sin \alpha^{(1)} P_R + Y_d g_Y \cos \alpha^{(1)} P_L \quad (\text{A.104})$$

$$g_{B^{(1)}\bar{\xi}^{(0)}\xi_s^{(1)}} = -Y_s g_Y \cos \alpha^{(1)} P_R - Y_d g_Y \sin \alpha^{(1)} P_L \quad (\text{A.105})$$

$$g_{W_+^{(0)}\bar{U}_i^{(0)}D_j^{(0)}} = \frac{g}{\sqrt{2}} V_{ij} P_L \quad (\text{A.106})$$

$$g_{W_+^{(0)}\bar{U}_{d,i}^{(1)}D_{d,j}^{(i)}} = \frac{g}{\sqrt{2}} V_{ij} \cos \alpha_{U_i}^{(1)} \cos \alpha_{D_j}^{(1)} \quad (\text{A.107})$$

$$g_{W_+^{(0)}\bar{U}_{s,i}^{(1)}D_{s,j}^{(i)}} = \frac{g}{\sqrt{2}} V_{ij} \sin \alpha_{U_i}^{(1)} \sin \alpha_{D_j}^{(1)} \quad (\text{A.108})$$

$$g_{W_+^{(0)}\bar{U}_{d,i}^{(1)}D_{s,j}^{(i)}} = \frac{g}{\sqrt{2}} V_{ij} \cos \alpha_{U_i}^{(1)} \sin \alpha_{D_j}^{(1)} \gamma^5 \quad (\text{A.109})$$

$$g_{W_+^{(0)}\bar{U}_{s,i}^{(1)}D_{d,j}^{(i)}} = \frac{g}{\sqrt{2}} V_{ij} \sin \alpha_{U_i}^{(1)} \cos \alpha_{D_j}^{(1)} \gamma^5 \quad (\text{A.110})$$

$$g_{W_+^{(1)}\bar{U}_i^{(0)}D_{d,j}^{(1)}} = \frac{g}{\sqrt{2}} V_{ij} \cos \alpha_{D_j}^{(1)} P_L \quad (\text{A.111})$$

$$g_{W_+^{(1)}\bar{U}_i^{(0)}D_{s,j}^{(1)}} = -\frac{g}{\sqrt{2}} V_{ij} \sin \alpha_{D_j}^{(1)} P_L \quad (\text{A.112})$$

$$g_{W_+^{(1)}\bar{U}_{d,i}^{(1)}D_j^{(0)}} = \frac{g}{\sqrt{2}} V_{ij} \cos \alpha_{U_i}^{(1)} P_L \quad (\text{A.113})$$

$$g_{W_+^{(1)}\bar{U}_{s,i}^{(1)}D_j^{(0)}} = -\frac{g}{\sqrt{2}} V_{ij} \sin \alpha_{U_i}^{(1)} P_L \quad (\text{A.114})$$

(In these expressions, there is of course no summation over i, j .) The above Feynman rules can also be used for leptons by replacing $V^{ij} \rightarrow \delta^{ij}$ and remembering that $Q_U = Y_{s,U} = 0$ (which means that there are no singlet neutrinos).

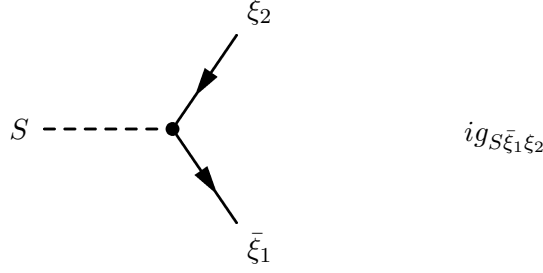
Fermion-fermion-scalar couplings

The interaction terms that are involved here originate from the covariant derivative in the kinetic terms of the fermion Lagrangian (3.63) and the Yukawa coupling (3.65). For quarks, they are given by

$$\begin{aligned} \hat{\mathcal{L}}^{(QQS)} &= i \left(Y_d \hat{g}_Y B_5 + \frac{\hat{g}}{2} A_5^3 \right) \bar{\psi}_{d,U}^i \gamma^5 \psi_{d,U}^i + i \left(Y_d \hat{g}_Y B_5 - \frac{\hat{g}}{2} A_5^3 \right) \bar{\psi}_{d,D}^i \gamma^5 \psi_{d,D}^i \\ &\quad + i Y_{s,U} \hat{g}_Y B_5 \bar{\psi}_{s,U}^i \gamma^5 \psi_{s,U}^i + i Y_{s,D} \hat{g}_Y B_5 \bar{\psi}_{s,D}^i \gamma^5 \psi_{s,D}^i \\ &\quad + i \frac{\hat{g}}{\sqrt{2}} V^{ij} \left(W_5^+ \bar{\psi}_{d,U}^i \gamma^5 \psi_{d,D}^j - \text{h.c.} \right) \end{aligned}$$

$$\begin{aligned}
& -2\sqrt{2}i\hat{g}\left(\frac{m_{D^i}}{m_W}\chi^+\bar{\psi}_{d,U}^i\psi_{s,D}^i+\frac{m_{U^i}}{m_W}\chi^-\bar{\psi}_{d,D}^i\psi_{s,U}^i-\text{h.c.}\right) \\
& -2\hat{g}H\left(\frac{m_{D^i}}{m_W}\bar{\psi}_{d,D}^i\psi_{s,D}^i+\frac{m_{U^i}}{m_W}\bar{\psi}_{d,U}^i\psi_{s,U}^i+\text{h.c.}\right) \\
& +2i\hat{g}\chi^3\left(\frac{m_{D^i}}{m_W}\bar{\psi}_{d,D}^i\psi_{s,D}^i-\frac{m_{U^i}}{m_W}\bar{\psi}_{d,U}^i\psi_{s,U}^i-\text{h.c.}\right), \quad (\text{A.115})
\end{aligned}$$

where the indices i, j indicate the family. To get the corresponding expressions for leptons, one has to set $Y_{s,U} = 0$ and $V^{ij} = \delta^{ij}$. In the following, $\xi = U, D$ will denote up ($T^3 = +1/2$) and down ($T^3 = -1/2$) type mass eigenstates as given in (3.60). When working in unitary gauge ($\xi \rightarrow \infty$), all Goldstone bosons disappear from the theory. Here, the Feynman rules are therefore only given for physical fields:



where²

$$g_{H^{(0)}\bar{\xi}^{(0)}\xi^{(0)}} = -2g\frac{m_\xi}{m_W} \quad (\text{A.116})$$

$$g_{H^{(0)}\bar{\xi}_d^{(1)}\xi_d^{(1)}} = -4g\frac{m_\xi}{m_W}\sin\alpha^{(1)}\cos\alpha^{(1)} \quad (\text{A.117})$$

$$g_{H^{(0)}\bar{\xi}_s^{(1)}\xi_s^{(1)}} = -4g\frac{m_\xi}{m_W}\sin\alpha^{(1)}\cos\alpha^{(1)} \quad (\text{A.118})$$

$$g_{H^{(0)}\bar{\xi}_{(d,s)}^{(1)}\xi_{(s,d)}^{(1)}} = -2g\frac{m_\xi}{m_W}\left(1-2\cos^2\alpha^{(1)}\right)\gamma^5 \quad (\text{A.119})$$

$$g_{H^{(1)}\bar{\xi}^{(0)}\xi_d^{(1)}} = -2g\frac{m_\xi}{m_W}\left(\sin\alpha^{(1)}P_R+\cos\alpha^{(1)}P_L\right) \quad (\text{A.120})$$

$$g_{H^{(1)}\bar{\xi}^{(0)}\xi_s^{(1)}} = 2g\frac{m_\xi}{m_W}\left(\cos\alpha^{(1)}P_R+\sin\alpha^{(1)}P_L\right) \quad (\text{A.121})$$

²Observe that one has $g_{S\bar{\xi}_1\xi_2} = g_{S^\dagger\bar{\xi}_2\xi_1}^*$ for scalar couplings; pseudo-scalar couplings, however, pick up an additional minus sign since $(\psi_1\gamma^5\psi_2)^\dagger = -\bar{\psi}_2\gamma^5\psi_1$.

$$\begin{aligned}
g_{a_0^{(1)}\bar{\xi}^{(0)}\xi_d^{(1)}} &= i\frac{m_Z}{M_Z^{(1)}} \left\{ (T_3 g c_w - Y_d g_Y s_w) \cos \alpha^{(1)} P_R + Y_d g_Y s_w \sin \alpha^{(1)} P_L \right\} \\
&\quad - 4igT_3 \frac{m_\xi}{m_W} \frac{M^{(1)}}{M_Z^{(1)}} \left(\sin \alpha^{(1)} P_R - \cos \alpha^{(1)} P_L \right) \quad (\text{A.122})
\end{aligned}$$

$$\begin{aligned}
g_{a_0^{(1)}\bar{\xi}^{(0)}\xi_s^{(1)}} &= i\frac{m_Z}{M_Z^{(1)}} \left\{ (T_3 g c_w - Y_d g_Y s_w) \sin \alpha^{(1)} P_R + Y_d g_Y s_w \cos \alpha^{(1)} P_L \right\} \\
&\quad + 4igT_3 \frac{m_\xi}{m_W} \frac{M^{(1)}}{M_Z^{(1)}} \left(\cos \alpha^{(1)} P_R - \sin \alpha^{(1)} P_L \right) \quad (\text{A.123})
\end{aligned}$$

$$\begin{aligned}
g_{a_+^{(1)}\bar{U}_i^{(0)}D_{d,j}^{(1)}} &= -4i\frac{g}{\sqrt{2}} \frac{M^{(1)}}{M_W^{(1)}} \delta_{ij} \left(\frac{m_{D_j}}{m_W} \sin \alpha_{D_j}^{(1)} P_R - \frac{m_{U_i}}{m_W} \cos \alpha_{D_j}^{(1)} P_L \right) \\
&\quad + i\frac{g}{\sqrt{2}} \frac{m_W}{m_W^{(1)}} V_{ij} \cos \alpha_{D_j}^{(1)} P_R \quad (\text{A.124})
\end{aligned}$$

$$\begin{aligned}
g_{a_+^{(1)}\bar{U}_i^{(0)}D_{s,j}^{(1)}} &= 4i\frac{g}{\sqrt{2}} \frac{M^{(1)}}{M_W^{(1)}} \delta_{ij} \left(\frac{m_{D_j}}{m_W} \cos \alpha_{D_j}^{(1)} P_R - \frac{m_{U_i}}{m_W} \sin \alpha_{D_j}^{(1)} P_L \right) \\
&\quad + i\frac{g}{\sqrt{2}} \frac{m_W}{m_W^{(1)}} V_{ij} \sin \alpha_{D_j}^{(1)} P_R \quad (\text{A.125})
\end{aligned}$$

$$\begin{aligned}
g_{a_+^{(1)}\bar{U}_{d,i}^{(1)}D_j^{(0)}} &= -4i\frac{g}{\sqrt{2}} \frac{M^{(1)}}{M_W^{(1)}} \delta_{ij} \left(\frac{m_{D_j}}{m_W} \cos \alpha_{U_i}^{(1)} P_R - \frac{m_{U_i}}{m_W} \sin \alpha_{U_i}^{(1)} P_L \right) \\
&\quad - i\frac{g}{\sqrt{2}} \frac{m_W}{m_W^{(1)}} V_{ij} \cos \alpha_{U_i}^{(1)} P_L \quad (\text{A.126})
\end{aligned}$$

$$\begin{aligned}
g_{a_+^{(1)}\bar{U}_{s,i}^{(1)}D_j^{(0)}} &= 4i\frac{g}{\sqrt{2}} \frac{M^{(1)}}{M_W^{(1)}} \delta_{ij} \left(\frac{m_{D_j}}{m_W} \sin \alpha_{U_i}^{(1)} P_R - \frac{m_{U_i}}{m_W} \cos \alpha_{U_i}^{(1)} P_L \right) \\
&\quad - i\frac{g}{\sqrt{2}} \frac{m_W}{m_W^{(1)}} V_{ij} \sin \alpha_{U_i}^{(1)} P_L \quad (\text{A.127})
\end{aligned}$$

(In these expressions, there is of course no summation over i, j .) The corresponding rules for Goldstone bosons can readily be obtained from the full expression (A.115), whenever they should be needed.

Ghost-ghost-vector couplings

The relevant coupling terms follow from the ghost Lagrangian (3.39) as

$$\hat{\mathcal{L}}^{(GGV)} = \hat{g}\epsilon^{ijk}\partial^\mu A_\mu^i \bar{c}^j c^k. \quad (\text{A.128})$$

From this expression, it is straight-forward to derive the corresponding 4D Feynman rules. Since one can always choose to work in unitary gauge ($\xi \rightarrow \infty$), where the ghosts disappear from the theory, this is not done explicitly here.

Ghost-ghost-scalar couplings

These couplings follow from the ghost Lagrangian (3.39) as

$$\hat{\mathcal{L}}^{(GGS)} = \xi \bar{c}^a \left[\hat{g}\epsilon^{ijk}\delta^{ia}\delta^{kb}\partial_y A_5^j - \frac{\hat{g}^a \hat{g}^b \hat{v}}{4} I^{ab} \right] c^b, \quad (\text{A.129})$$

with

$$I = \begin{pmatrix} H & -\chi^3 & \chi^2 & \chi^2 \\ \chi^3 & H & -\chi^1 & -\chi^1 \\ -\chi^2 & \chi^1 & H & -H \\ \chi^2 & -\chi^1 & -H & H \end{pmatrix} \quad (\text{A.130})$$

where $i, j, k \in \{1, 2, 3\}$ and $a, b \in \{1, 2, 3, Y\}$. Again, the corresponding Feynman rules are not given here, but can be derived from the above expression whenever one decides not to work in unitary gauge.

Four-point vertices

Just as for the three-point vertices, one encounters also in this case certain types of integrals over various combinations of odd and even fields. The only integrals that do not vanish, are those over four even fields W, X, Y, Z ,

$$\begin{aligned} \int_0^{2\pi R} dy WXYZ &= \frac{1}{2\pi R} \left\{ W^{(0)} X^{(0)} Y^{(0)} Z^{(0)} + W^{(1)} X^{(1)} Y^{(0)} Z^{(0)} \right. \\ &\quad + W^{(1)} X^{(0)} Y^{(1)} Z^{(0)} + W^{(1)} X^{(0)} Y^{(0)} Z^{(1)} \\ &\quad + W^{(0)} X^{(1)} Y^{(1)} Z^{(0)} + W^{(0)} X^{(1)} Y^{(0)} Z^{(1)} \\ &\quad \left. + W^{(0)} X^{(0)} Y^{(1)} Z^{(1)} + \frac{3}{2} W^{(1)} X^{(1)} Y^{(1)} Z^{(1)} \right\}, \end{aligned} \quad (\text{A.131})$$

over four odd field S, T, U, V ,

$$\int_0^{2\pi R} dy STUV = \frac{3}{4\pi R} S^{(1)} T^{(1)} U^{(1)} V^{(1)}, \quad (\text{A.132})$$

as well as over two odd fields S, T and two even fields X, Y :

$$\int_0^{2\pi R} dy STXY = \frac{1}{2\pi R} \left\{ X^{(0)} Y^{(0)} S^{(1)} S^{(1)} + \frac{1}{2} X^{(1)} Y^{(1)} S^{(1)} S^{(1)} \right\}. \quad (\text{A.133})$$

In the following, all terms in the higher-dimensional Lagrangian that lead to interactions between four fields in the 4D theory will be collected. In contrast to the case of the three-point vertices, however, the corresponding Feynman rules will not be given explicitly; with the help of the above integrals, they can be derived in a rather straight-forward way.

Vector-vector-vector-vector couplings

These couplings derive from the quartic terms in the 'free' gauge field Lagrangian (3.19) and take the form

$$\begin{aligned} \hat{\mathcal{L}}^{(VVVV)} = & -\frac{\hat{g}^2}{2} \left\{ (W^+ W^-) (W^+ W^-) - (W^+ W^+) (W^- W^-) \right. \\ & \left. + 2 (W^+ W^-) (A^3 A^3) - 2 (W^+ A^3) (W^- A^3) \right\}. \end{aligned} \quad (\text{A.134})$$

Vector-vector-scalar-scalar couplings

The interaction terms that are involved here originate from the corresponding quartic terms in both the 'free' gauge field Lagrangian (3.19) and the kinetic term of the Higgs Lagrangian (3.25),

$$\begin{aligned} \hat{\mathcal{L}}^{(VVSS)} = & \hat{g}^2 (W^+ W^-) W_5^+ W_5^- - \frac{\hat{g}^2}{2} \left((W^+ W^+) W_5^- W_5^- + \text{c.c.} \right) \\ & + \hat{g}^2 (A^3 A^3) W_5^+ W_5^- + \hat{g}^2 (W^+ W^-) A_5^3 A_5^3 \\ & - \hat{g}^2 \left((W^+ A^3) W_5^- A_5^3 + \text{c.c.} \right) \left\{ \right. \\ & + \frac{1}{2} \left\{ \frac{1}{2} (2\hat{e}A + \hat{g}/c_w Z)^2 + \hat{g}^2 W^+ W^- \right\} \chi^+ \chi^- \\ & + \frac{1}{4} \left\{ \frac{\hat{g}^2}{2c_w^2} ZZ + g^2 W^+ W^- \right\} [HH + \chi^3 \chi^3] \\ & \left. - \frac{i\hat{g}\hat{g}_Y}{2} B [W^+ (H - i\chi^3) \chi^- - \text{h.c.}] \right\}. \end{aligned} \quad (\text{A.135})$$

Scalar-scalar-scalar-scalar couplings

Couplings between four scalars, finally, derive from the corresponding quartic terms in both the kinetic and the potential parts of the Higgs Lagrangian (3.25),

$$\begin{aligned}
\hat{\mathcal{L}}^{(SSSS)} = & -\frac{1}{2} \left\{ \frac{1}{2} (2\hat{e}A_5 + \hat{g}/c_w Z_5)^2 + \hat{g}^2 W_5^+ W_5^- \right\} \chi^+ \chi^- \\
& -\frac{1}{4} \left\{ \frac{\hat{g}^2}{2c_w} Z_5 Z_5 + \hat{g}^2 W_5^+ W_5^- \right\} [HH + \chi^3 \chi^3] \\
& + \frac{i\hat{g}\hat{g}_Y}{2} (c_w A_5 - s_w Z_5) [W_5^+ (H - i\chi^3) \chi^- - \text{h. c.}] \\
& - \frac{\hat{g}^2}{32} \frac{m_H^2}{m_W^2} (2\chi^+ \chi^- + HH + \chi^3 \chi^3)^2 . \tag{A.136}
\end{aligned}$$

Higher KK levels

From the higher-dimensional interaction terms that were given in this Appendix, one can in principle also derive all necessary Feynman rules for higher KK levels. The only thing that is needed in order to perform these calculations, is a generalization of the integrals over even and odd fields.

When deriving three-point couplings in the 4D theory, for example, one will encounter the following integrals:

$$\begin{aligned}
\int_0^{2\pi R} dy XYZ &= \frac{1}{\sqrt{2\pi R}} \left\{ X^{(0)} Y^{(0)} Z^{(0)} \right. \\
&\quad + \sum_{n=1}^{\infty} [X^{(0)} Y^{(n)} Z^{(n)} + X^{(n)} Y^{(0)} Z^{(n)} + X^{(n)} Y^{(n)} Z^{(0)}] \\
&\quad \left. + \frac{1}{\sqrt{2}} \sum_{n,k,l=1}^{\infty} X^{(n)} Y^{(k)} Z^{(l)} [\delta_{n,k+l} + \delta_{n,l-k} + \delta_{n,k-l}] \right\},
\end{aligned} \tag{A.137}$$

as well as

$$\begin{aligned}
\int_0^{2\pi R} dy XUV &= \frac{1}{\sqrt{2\pi R}} \left\{ \sum_{n=1}^{\infty} X^{(0)} U^{(n)} V^{(n)} \right. \\
&\quad \left. + \frac{1}{\sqrt{2}} \sum_{n,k,l=1}^{\infty} X^{(n)} U^{(k)} V^{(l)} [-\delta_{n,k+l} + \delta_{n,l-k} + \delta_{n,k-l}] \right\}.
\end{aligned} \tag{A.138}$$

As before, the integrals over any other combination of three fields vanish.

Similar expressions can be given as generalizations of (A.131), (A.132) and (A.133); those integrals arise when one derives Feynman rules for the interaction between four fields.

Appendix B

Generalizing to more than one UED

For n UEDs, the simplest compactification choice is $[(\mathbb{S}^1 \times \mathbb{S}^1)/\mathbb{Z}_2]^{n/2}$ if n is even and $[(\mathbb{S}^1 \times \mathbb{S}^1)/\mathbb{Z}_2]^{(n-1)/2} \times (\mathbb{S}^1/\mathbb{Z}_2)$ in case it is odd. The Fourier expansion of fields that are odd and even under orbifold transformations, respectively, then takes the following form:

$$\begin{aligned} \phi_{\text{even}}(x^\nu, y^a) &= \frac{1}{(2\pi R)^{\frac{n}{2}}} \phi_{\text{even}}^{(0)}(x^\nu) + \\ &\frac{\sqrt{2}}{(2\pi R)^{\frac{n}{2}}} \sum_{j_1+\dots+j_n \geq 1} \phi_{\text{even}}^{(j_1 \dots j_n)}(x^\nu) f_{\text{even}}^n(j_i, y^a), \end{aligned} \quad (\text{B.1})$$

$$\phi_{\text{odd}}(x^\nu, y^a) = \frac{\sqrt{2}}{(2\pi R)^{\frac{n}{2}}} \sum_{j_1+\dots+j_n \geq 1} \phi_{\text{odd}}^{(j_1 \dots j_n)}(x^\nu) f_{\text{odd}}^n(j_i, y^a), \quad (\text{B.2})$$

with

$$f_{\text{even}}^n(j_i, y^a) = \prod_{l=0}^{[n/2]-1} \cos\left(\frac{j_{2l+1}y^{2l+1} + j_{2l+2}y^{2l+2}}{R}\right) \cdot \cos\left(\frac{j_n y^n}{R}\right), \quad (\text{B.3})$$

$$f_{\text{odd}}^n(j_i, y^a) = \prod_{l=0}^{[n/2]-1} \sin\left(\frac{j_{2l+1}y^{2l+1} + j_{2l+2}y^{2l+2}}{R}\right) \cdot \sin\left(\frac{j_n y^n}{R}\right), \quad (\text{B.4})$$

where the last factor only appears if n is odd.

The spectrum of states

Let us now discuss how higher-dimensional fields transform under 4D Lorentz transformations – or, more precisely, under

$$SO(3, 1) \times SO(n) \subset SO(d - 1, 1). \quad (\text{B.5})$$

Gauge fields are $SO(d - 1, 1)$ vectors. Under (B.5), they transform as

$$\mathbf{d} \rightarrow (\mathbf{4}, \mathbf{1}) + (\mathbf{1}, \mathbf{n} - \mathbf{4}). \quad (\text{B.6})$$

The first part transforms as a 4D Lorentz vector; it should therefore be even under orbifold transformations so that its zero-mode can be identified with the ordinary 4D gauge fields. The second part describes a set of $(n - 4)$ states that are 4D Lorentz scalars; this part thus has to transform odd under the orbifold projections in order not to get scalar zero modes.

Fermions are $SO(d - 1, 1)$ spinors. As discussed in Section (3.3.4), in the Dirac representation spinors can be written as $\mathbf{s} = (s_0, \dots, s_k)$, where $n = 2k - 2$ for even n and $n = 2k - 1$ for odd n . This is very convenient, since now one can easily relate (parts of) representations of different dimensionalities just by comparing the corresponding eigenvalues s_a . Under (B.5), in particular, spinors decompose as

$$\mathbf{2}^{k+1} \rightarrow (\mathbf{2}^2, \mathbf{2}^{k-1}) = (\mathbf{2}, \mathbf{2}^{k-1}) + (\mathbf{2}', \mathbf{2}^{k-1}). \quad (\text{B.7})$$

This means that one has a set of 2^{k-1} quantities that transform as ordinary 4D spinors under 4D Lorentz transformations, and each of them splits up into two parts of different chirality. All but one of the resulting states have to transform odd under orbifold transformations in order to recover the right spectrum of states for the zero modes.

As a side remark, if n is even, the higher dimensional spinor splits into two chiral parts that transform under 4D Lorentz transformations as

$$\mathbf{2}^k \rightarrow (\mathbf{2}, \mathbf{2}^{k-2}) + (\mathbf{2}', \mathbf{2}^{k-2'}) \quad (\text{B.8})$$

$$\mathbf{2}^{k'} \rightarrow (\mathbf{2}', \mathbf{2}^{k-2}) + (\mathbf{2}, \mathbf{2}^{k-2'}). \quad (\text{B.9})$$

Restricting oneself to states of definite chiralities in the higher-dimensional theory (as one should do when assigning electroweak singlet and doublet states), one can thus reduce the number of chiral states in the 4D theory by a factor of 2.

As apparent from (B.1, B.2), all the states discussed here come equipped with KK towers that are characterized by numbers (j_1, \dots, j_n) .

Collider bounds and cosmological consequences

For $d \geq 6$, the electroweak observables considered in [10] become ever more cutoff-dependent, because the KK spectrum is denser than in the 5D case. For 6D, the inferred lower bound on the compactification scale is $R^{-1} \gtrsim 400\text{-}800$ GeV; however, already beyond a cutoff of $\Lambda \sim 5R^{-1}$, perturbation theory breaks down. In the case of more than two UEDs, the cutoff-dependence is so severe that no reliable estimates for the allowed size of the EDs are available [10].

For two UEDs, one finds two LKPs – $B^{(1,0)}$ and $B^{(0,1)}$ – that are degenerate in mass and do not interact with each other at tree level. The relic density is therefore just twice the value of the 5D case and, accordingly, the preferred mass range in order to account for the required dark matter density lowered by a factor of about $\sqrt{2}$. One might also consider a compactification on $\mathbb{T}^2/\mathbb{Z}_4$ (instead of $\mathbb{T}^2/\mathbb{Z}_2$). In that case one has two stable particles $B^{(0,1)}$ and $B^{(1,1)}$; since the latter is about 40% heavier than the LKP, the relic density calculation is not affected and one therefore arrives at the same LKP mass range as in the 5D case [114]. For more than two UEDs, it is no longer so easy to generalize the results from one UED, since then the number of fermionic degrees of freedom is greatly enhanced (see the discussion above).

References

- [1] E. Accomando *et al.* [ECFA/DESY LC Physics Working Group], “Physics with e+ e- linear colliders”, Phys. Rept. **299** (1998) 1 [arXiv:hep-ph/9705442].
- [2] K. Agashe, N. G. Deshpande and G. H. Wu, “Universal extra dimensions and $b \rightarrow s$ gamma”, Phys. Lett. B **514** (2001) 309 [arXiv:hep-ph/0105084].
- [3] F. Aharonian *et al.* [The HESS Collaboration], “Very high energy gamma rays from the direction of Sagittarius A*”, Astron. Astrophys. **425** (2004) L13, [arXiv:astro-ph/0408145].
- [4] F. Aharonian *et al.* [H.E.S.S. Collaboration], “Serendipitous discovery of the unidentified extended TeV gamma-ray source HESS J1303-631,” arXiv:astro-ph/0505219.
- [5] J. Ahrens *et al.* [AMANDA Collaboration], “Limits to the muon flux from WIMP annihilation in the center of the earth with the AMANDA detector”, Phys. Rev. D **66** (2002) 032006 [arXiv:astro-ph/0202370].
- [6] J. Ahrens *et al.* [The IceCube Collaboration], “IceCube: The next generation neutrino telescope at the South Pole”, Nucl. Phys. Proc. Suppl. **118** (2003) 388 [arXiv:astro-ph/0209556].
- [7] D. S. Akerib *et al.* [CDMS Collaboration], “First results from the cryogenic dark matter search in the Soudan Underground Lab”, Phys. Rev. Lett. **93** (2004) 211301 [arXiv:astro-ph/0405033].
- [8] R. Aloisio, P. Blasi and A. V. Olinto, “Neutralino annihilation at the galactic center revisited”, JCAP **0405** (2004) 007 [arXiv:astro-ph/0402588].
- [9] A. Anderson *et al.*, “Recent developments in solar-system tests of general relativity”, in: H. Sato and T. Nakamura (eds), Proceedings of the Sixth Marcel Grossmann Meeting on General Relativity, World Scientific, Singapore,(1992).
- [10] T. Appelquist, H. C. Cheng and B. A. Dobrescu, “Bounds on universal extra dimensions”, Phys. Rev. D **64** (2001) 035002 [arXiv:hep-ph/0012100].

- [11] T. Appelquist, B. A. Dobrescu, E. Ponton and H. U. Yee, “Proton stability in six dimensions”, *Phys. Rev. Lett.* **87** (2001) 181802 [arXiv:hep-ph/0107056].
- [12] N. Arkani-Hamed, H. C. Cheng, B. A. Dobrescu and L. J. Hall, “Self-breaking of the standard model gauge symmetry”, *Phys. Rev. D* **62** (2000) 096006 [arXiv:hep-ph/0006238].
- [13] N. Arkani-Hamed, S. Dimopoulos and G. R. Dvali, “The hierarchy problem and new dimensions at a millimeter”, *Phys. Lett. B* **429** (1998) 263 [arXiv:hep-ph/9803315].
- [14] C. Armendariz-Picon, V. Mukhanov and P. J. Steinhardt, “A dynamical solution to the problem of a small cosmological constant and late-time cosmic acceleration”, *Phys. Rev. Lett.* **85** (2000) 4438 [arXiv:astro-ph/0004134].
- [15] R. Arnowitt, J. Dent and B. Dutta, “Five dimensional cosmology in Horava-Witten M-theory”, *Phys. Rev. D* **70** (2004) 126001 [arXiv:hep-th/0405050].
- [16] N. A. Bahcall and X. H. Fan, “The Most Massive Distant Clusters: Determining Omega and sigma₈”, *Astrophys. J.* **504** (1998) 1 [arXiv:astro-ph/9803277].
- [17] J. N. Bahcall, C. L. Steinhardt and D. Schlegel, “Does the fine-structure constant vary with cosmological epoch?”, *Astrophys. J.* **600** (2004) 520 [arXiv:astro-ph/0301507].
- [18] D. Bailin and A. Love, “Kaluza-Klein Theories”, *Rept. Prog. Phys.* **50** (1987) 1087.
- [19] F. Barao [AMS-02 Collaboration], “AMS: Alpha Magnetic Spectrometer on the International Space Station”, *Nucl. Instrum. Meth. A* **535** (2004) 134.
- [20] J. F. Beacom, N. F. Bell and G. Bertone, “Gamma-ray constraint on Galactic positron production by MeV dark matter”, *Phys. Rev. Lett.* **94** (2005) 171301 [arXiv:astro-ph/0409403].
- [21] G. Belanger, F. Boudjema, A. Pukhov and A. Semenov, “MicroOMEGAs: Version 1.3”, arXiv:hep-ph/0405253.

- [22] V. S. Berezinsky, A. V. Gurevich and K. P. Zybin, “Distribution of dark matter in the galaxy and the lower limits for the masses of supersymmetric particles”, *Phys. Lett. B* **294** (1992) 221.
- [23] L. Bergström, “Non-baryonic dark matter: Observational evidence and detection methods”, *Rept. Prog. Phys.* **63** (2000) 793 [arXiv:hep-ph/0002126].
- [24] L. Bergström, J. Edsjö and P. Ullio, “Cosmic antiprotons as a probe for supersymmetric dark matter?”, arXiv:astro-ph/9902012.
- [25] L. Bergström, S. Iguri and H. Rubinstein, “Constraints on the variation of the fine structure constant from big bang nucleosynthesis”, *Phys. Rev. D* **60** (1999) 045005 [arXiv:astro-ph/9902157].
- [26] L. Bergström and H. Snellman, “Observable Monochromatic Photons From Cosmic Photino Annihilation”, *Phys. Rev. D* **37** (1988) 3737.
- [27] L. Bergström and P. Ullio, “Full one-loop calculation of neutralino annihilation into two photons”, *Nucl. Phys. B* **504** (1997) 27 [arXiv:hep-ph/9706232].
- [28] L. Bergström, P. Ullio and J. H. Buckley, “Observability of gamma rays from dark matter neutralino annihilations in the Milky Way halo”, *Astropart. Phys.* **9** (1998) 137 [arXiv:astro-ph/9712318].
- [29] Z. Bern, P. Gondolo and M. Perelstein, “Neutralino annihilation into two photons”, *Phys. Lett. B* **411** (1997) 86 [arXiv:hep-ph/9706538].
- [30] R. Bernabei *et al.* [DAMA Collaboration], “Search for WIMP annual modulation signature: Results from DAMA / NaI-3 and DAMA / NaI-4 and the global combined analysis”, *Phys. Lett. B* **480** (2000) 23.
- [31] G. Bertone, D. Hooper and J. Silk, “Particle dark matter: Evidence, candidates and constraints”, *Phys. Rept.* **405** (2005) 279 [arXiv:hep-ph/0404175].
- [32] G. Bertone and D. Merritt, “Dark matter dynamics and indirect detection”, *Mod. Phys. Lett. A* **20** (2005) 1021 [arXiv:astro-ph/0504422].
- [33] G. Bertone, G. Servant and G. Sigl, “Indirect detection of Kaluza-Klein dark matter”, *Phys. Rev. D* **68** (2003) 044008 [arXiv:hep-ph/0211342].

- [34] A. Billyard and A. Coley, “On the correspondence between exact solutions in Kaluza-Klein theory and in scalar-tensor theories”, *Mod. Phys. Lett. A* **12** (1997) 2121.
- [35] A. Birkedal, K. T. Matchev, M. Perelstein and A. Spray, “Robust gamma ray signature of WIMP dark matter”, arXiv:hep-ph/0507194.
- [36] G. R. Blumenthal, S. M. Faber, R. Flores and J. R. Primack, “Contraction Of Dark Matter Galactic Halos Due To Baryonic Infall”, *Astrophys. J.* **301** (1986) 27.
- [37] C. Boehm and P. Fayet, “Scalar dark matter candidates”, *Nucl. Phys. B* **683** (2004) 219 [arXiv:hep-ph/0305261].
- [38] C. Boehm, D. Hooper, J. Silk, M. Casse and J. Paul, “MeV dark matter: Has it been detected?”, *Phys. Rev. Lett.* **92** (2004) 101301 [arXiv:astro-ph/0309686].
- [39] M. Boezio *et al.* [WiZard/CAPRICE Collaboration], “The cosmic-ray anti-proton flux between 3-GeV and 49-GeV”, *Astrophys. J.* **561** (2001) 787 [arXiv:astro-ph/0103513].
- [40] M. Boezio *et al.*, “The space experiment PAMELA”, *Nucl. Phys. Proc. Suppl.* **134** (2004) 39.
- [41] T. Bringmann, M. Eriksson and M. Gustafsson, “Stability of Homogeneous Extra Dimensions”, *AIP Conf. Proc.* **736** (2005) 141 [arXiv:astro-ph/0410613].
- [42] P. Bucci, B. Grzadkowski, Z. Lalak and R. Matyszkiewicz, “Electroweak symmetry breaking and radion stabilization in universal extra dimensions”, *JHEP* **0404** (2004) 067 [arXiv:hep-ph/0403012].
- [43] B. A. Campbell and K. A. Olive, “Nucleosynthesis and the time dependence of fundamental couplings”, *Phys. Lett. B* **345** (1995) 429 [arXiv:hep-ph/9411272].
- [44] A. Cesarini, F. Fucito, A. Lionetto, A. Morselli and P. Ullio, “The galactic center as a dark matter gamma-ray source”, *Astropart. Phys.* **21** (2004) 267 [arXiv:astro-ph/0305075].
- [45] H. C. Cheng, J. L. Feng and K. T. Matchev, “Kaluza-Klein dark matter”, *Phys. Rev. Lett.* **89** (2002) 211301 [arXiv:hep-ph/0207125].

- [46] H. C. Cheng, K. T. Matchev and M. Schmaltz, “Radiative corrections to Kaluza-Klein masses”, *Phys. Rev. D* **66** (2002) 036005 [arXiv:hep-ph/0204342].
- [47] Y. M. Cho, “Reinterpretation of Jordan-Brans-Dicke theory and Kaluza-Klein cosmology”, *Phys. Rev. Lett.* **68** (1992) 3133.
- [48] B. S. De Witt, “Dynamical theory of Groups and Fields”, in: C. De Witt and B. S. De Witt (eds.), *Relativity, Groups, and Topology* [Les Houches 1963], New York: Gordon and Breach (1964).
- [49] J. Diemand, B. Moore and J. Stadel, “Earth-mass dark-matter haloes as the first structures in the early universe”, *Nature* **433** (2005) 389 [arXiv:astro-ph/0501589].
- [50] L. J. Dixon, J. A. Harvey, C. Vafa and E. Witten, “Strings On Orbifolds”, *Nucl. Phys. B* **261** (1985) 678.
- [51] L. J. Dixon, J. A. Harvey, C. Vafa and E. Witten, “Strings On Orbifolds. 2”, *Nucl. Phys. B* **274** (1986) 285.
- [52] B. A. Dobrescu and E. Poppitz, “Number of fermion generations derived from anomaly cancellation”, *Phys. Rev. Lett.* **87** (2001) 031801 [arXiv:hep-ph/0102010].
- [53] F. Donato, N. Fornengo, D. Maurin and P. Salati, “Antiprotons in cosmic rays from neutralino annihilation”, *Phys. Rev. D* **69** (2004) 063501 [arXiv:astro-ph/0306207].
- [54] J. Edsjö, M. Schelke and P. Ullio, “Direct versus indirect detection in mSUGRA with self-consistent halo models,” *JCAP* **0409** (2004) 004 [arXiv:astro-ph/0405414].
- [55] S. Eidelman *et al.* [Particle Data Group], “Review of particle physics”, *Phys. Lett. B* **592** (2004) 1.
- [56] A. Einstein, “The Foundation Of The General Theory Of Relativity”, *Annalen Phys.* **49** (1916) 769 [*Annalen Phys.* **14** (2005) 517].
- [57] V. R. Eke, J. F. Navarro and M. Steinmetz, “The Power Spectrum Dependence of Dark Matter Halo Concentrations”, *Astrophys. J.* **554** (2001) 114 [arXiv:astro-ph/0012337].
- [58] M. Eriksson, *The dark side of the universe*, PhD-thesis, ISBN 91-7155-073-9 (2005).

- [59] V. Faraoni, E. Gunzig and P. Nardone, “Conformal transformations in classical gravitational theories and in cosmology”, *Fund. Cosmic Phys.* **20** (1999) 121.
- [60] E. E. Flanagan, “The conformal frame freedom in theories of gravitation”, *Class. Quant. Grav.* **21** (2004) 3817, [arXiv:gr-qc/0403063].
- [61] V. Fonseca [MAGIC Collaboration], “The MAGIC telescope project,” *Acta Phys. Polon. B* **30** (1999) 2331.
- [62] N. Fornengo, L. Pieri and S. Scopel, “Neutralino annihilation into gamma-rays in the Milky Way and in external galaxies”, *Phys. Rev. D* **70** (2004) 103529 [arXiv:hep-ph/0407342].
- [63] Y. Fujii *et al.*, “The nuclear interaction at Oklo 2 billion years ago”, *Nucl. Phys. B* **573** (2000) 377 [arXiv:hep-ph/9809549].
- [64] E. Garcia-Berro, Y. A. Kuyshin and P. Loren-Aguilar, “Time variation of the gravitational and fine structure constants in models with extra dimensions”, arXiv:gr-qc/0302006.
- [65] N. Gehrels and P. Michelson, “GLAST: The next-generation high energy gamma-ray astronomy mission”, *Astropart. Phys.* **11** (1999) 277.
- [66] H. Georgi, A. K. Grant and G. Hailu, “Brane couplings from bulk loops”, *Phys. Lett. B* **506** (2001) 207 [arXiv:hep-ph/0012379].
- [67] O. Y. Gnedin, A. V. Kravtsov, A. A. Klypin and D. Nagai, “Response of dark matter halos to condensation of baryons: cosmological simulations and improved adiabatic contraction model”, *Astrophys. J.* **616** (2004) 16 [arXiv:astro-ph/0406247].
- [68] P. Gondolo, J. Edsjö, P. Ullio, L. Bergström, M. Schelke and E. A. Baltz, “DarkSUSY: Computing supersymmetric dark matter properties numerically”, *JCAP* **0407** (2004) 008 [arXiv:astro-ph/0406204].
- [69] A. M. Green, S. Hofmann and D. J. Schwarz, “The first WIMPy halos”, arXiv:astro-ph/0503387.
- [70] K. Griest and D. Seckel, “Three Exceptions In The Calculation Of Relic Abundances”, *Phys. Rev. D* **43** (1991) 3191.

- [71] U. Gunther, A. Starobinsky and A. Zhuk, “Multidimensional cosmological models: Cosmological and astrophysical implications”, *Phys. Rev. D* **69** (2004) 044003 [arXiv:hep-ph/0306191].
- [72] A. H. Guth, “The Inflationary Universe: A Possible Solution To The Horizon And Flatness Problems”, *Phys. Rev. D* **23** (1981) 347.
- [73] H. E. Haber and G. L. Kane, “The Search For Supersymmetry: Probing Physics Beyond The Standard Model”, *Phys. Rept.* **117** (1985) 75.
- [74] T. Hahn, “Generating Feynman diagrams and amplitudes with FeynArts 3”, *Comput. Phys. Commun.* **140** (2001) 418 [arXiv:hep-ph/0012260].
- [75] S. Hannestad, “Possible constraints on the time variation of the fine structure constant from cosmic microwave background data”, *Phys. Rev. D* **60** (1999) 023515 [arXiv:astro-ph/9810102].
- [76] D. Hooper and G. D. Kribs, “Probing Kaluza-Klein dark matter with neutrino telescopes”, *Phys. Rev. D* **67** (2003) 055003 [arXiv:hep-ph/0208261].
- [77] D. Hooper and G. D. Kribs, “Kaluza-Klein dark matter and the positron excess”, *Phys. Rev. D* **70** (2004) 115004 [arXiv:hep-ph/0406026].
- [78] D. Hooper and J. Silk, “Searching for dark matter with future cosmic positron experiments”, *Phys. Rev. D* **71** (2005) 083503 [arXiv:hep-ph/0409104].
- [79] C. D. Hoyle, D. J. Kapner, B. R. Heckel, E. G. Adelberger, J. H. Gundlach, U. Schmidt and H. E. Swanson, “Sub-millimeter tests of the gravitational inverse-square law”, *Phys. Rev. D* **70** (2004) 042004 [arXiv:hep-ph/0405262].
- [80] P. Jean *et al.*, “Early SPI/INTEGRAL measurements of galactic 511 keV line emission from positron annihilation”, *Astron. Astrophys.* **407** (2003) L55 [arXiv:astro-ph/0309484].
- [81] G. Jungman, M. Kamionkowski and K. Griest, “Supersymmetric dark matter”, *Phys. Rept.* **267** (1996) 195 [arXiv:hep-ph/9506380].
- [82] T. Kaluza, “On The Problem Of Unity In Physics”, *Sitzungsber. Preuss. Akad. Wiss. Berlin* **K1** (1921) 966.

- [83] A. Kehagias and K. Sfetsos, “Deviations from the $1/r^2$ Newton law due to extra dimensions”, *Phys. Lett. B* **472** (2000) 39 [arXiv:hep-ph/9905417].
- [84] O. Klein, “Quantum Theory And Five-Dimensional Theory Of Relativity”, *Z. Phys.* **37** (1926) 895.
- [85] E. W. Kolb, M. J. Perry and T. P. Walker, “Time Variation Of Fundamental Constants, Primordial Nucleosynthesis And The Size Of Extra Dimensions”, *Phys. Rev. D* **33** (1986) 869.
- [86] K. Kosack *et al.* [The VERITAS Collaboration], “TeV gamma-ray observations of the galactic center”, *Astrophys. J.* **608** (2004) L97 [arXiv:astro-ph/0403422].
- [87] A. D. Linde, “Chaotic Inflation”, *Phys. Lett. B* **129** (1983) 177.
- [88] T. Maeno *et al.* [BESS Collaboration], “Successive measurements of cosmic-ray antiproton spectrum in a positive phase of the solar cycle”, *Astropart. Phys.* **16** (2001) 121 [arXiv:astro-ph/0010381].
- [89] D. Maurin, F. Donato, R. Taillet and P. Salati, “Cosmic Rays below $Z=30$ in a diffusion model: new constraints on propagation parameters”, *Astrophys. J.* **555** (2001) 585 [arXiv:astro-ph/0101231].
- [90] D. Maurin, R. Taillet, F. Donato, P. Salati, A. Barrau and G. Boudoul, “Galactic cosmic ray nuclei as a tool for astroparticle physics”, arXiv:astro-ph/0212111.
- [91] H. A. Mayer-Hasselwander *et al.* [The EGRET Collaboration], “High-energy gamma ray emission from the galactic center”, *Astron. Astrophys.* **335** (1998) 161.
- [92] D. Merritt, J. F. Navarro, A. Ludlow and A. Jenkins, “A Universal Density Profile for Dark and Luminous Matter?”, *Astrophys. J.* **624** (2005) L85 [arXiv:astro-ph/0502515].
- [93] C. W. Misner, K. S. Thorne and J. A. Wheeler, *Gravitation*, New York: Freeman (1995).
- [94] B. Moore, S. Ghigna, F. Governato, G. Lake, T. Quinn, J. Stadel and P. Tozzi, “Dark matter substructure within galactic halos”, *Astrophys. J.* **524** (1999) L19.

- [95] J. F. Navarro, C. S. Frenk and S. D. M. White, “A Universal density profile from hierarchical clustering”, *Astrophys. J.* **490** (1997) 493.
- [96] J. F. Navarro *et al.*, “The Inner Structure of LambdaCDM Halos III: Universality and Asymptotic Slopes”, *Mon. Not. Roy. Astron. Soc.* **349** (2004) 1039 [arXiv:astro-ph/0311231].
- [97] G. Nordström, “On The Possibility Of A Unification Of The Electromagnetic And Gravitation Fields”, *Phys. Z.* **15** (1914) 504.
- [98] K. A. Olive, G. Steigman and T. P. Walker, “Primordial nucleosynthesis: Theory and observations”, *Phys. Rept.* **333** (2000) 389 [arXiv:astro-ph/9905320].
- [99] S. Orito *et al.* [BESS Collaboration], “Precision measurement of cosmic-ray antiproton spectrum”, *Phys. Rev. Lett.* **84** (2000) 1078 [arXiv:astro-ph/9906426];
- [100] W. J. Percival *et al.* [The 2dFGRS Team Collaboration], “Parameter constraints for flat cosmologies from CMB and 2dFGRS power spectra”, *Mon. Not. Roy. Astron. Soc.* **337** (2002) 1068 [arXiv:astro-ph/0206256].
- [101] S. Perlmutter *et al.* [Supernova Cosmology Project Collaboration], “Measurements of Omega and Lambda from 42 High-Redshift Supernovae”, *Astrophys. J.* **517** (1999) 565 [arXiv:astro-ph/9812133].
- [102] M. Persic, P. Salucci and F. Stel, “The Universal rotation curve of spiral galaxies: 1. The Dark matter connection”, *Mon. Not. Roy. Astron. Soc.* **281** (1996) 27 [arXiv:astro-ph/9506004].
- [103] M. E. Peskin and D. V. Schroeder, *An Introduction to Quantum Field Theory*, Westview Press (1995).
- [104] K. Pohlmeyer, “The Nambu-Goto theory of closed bosonic strings moving in 1+3-dimensional Minkowski space: The quantum algebra of observables”, *Annalen Phys.* **8** (1999) 19 [arXiv:hep-th/9805057].
- [105] D. Polarski and A. A. Starobinsky, “Semiclassicality and decoherence of cosmological perturbations”, *Class. Quant. Grav.* **13** (1996) 377 [arXiv:gr-qc/9504030].
- [106] J. Polchinski, “Dirichlet-Branes and Ramond-Ramond Charges”, *Phys. Rev. Lett.* **75** (1995) 4724 [arXiv:hep-th/9510017].

- [107] J. Polchinski, *String Theory. Vol. 2: Superstring theory and beyond*, Cambridge University Press (1998).
- [108] F. Prada, A. Klypin, J. Flix, M. Martinez and E. Simonneau, “Astrophysical inputs on the SUSY dark matter annihilation detectability”, arXiv:astro-ph/0401512.
- [109] L. Randall and R. Sundrum, “A large mass hierarchy from a small extra dimension”, *Phys. Rev. Lett.* **83** (1999) 3370 [arXiv:hep-ph/9905221].
- [110] L. Randall and R. Sundrum, “An alternative to compactification”, *Phys. Rev. Lett.* **83** (1999) 4690 [arXiv:hep-th/9906064].
- [111] A. G. Riess *et al.* [Supernova Search Team Collaboration], “Observational Evidence from Supernovae for an Accelerating Universe and a Cosmological Constant”, *Astron. J.* **116** (1998) 1009 [arXiv:astro-ph/9805201].
- [112] J. J. Sakurai, *Modern Quantum Mechanics*, Addison-Wesley (1985).
- [113] V. Sanglard *et al.* [The EDELWEISS Collaboration], “Final results of the EDELWEISS-I dark matter search with cryogenic heat-and-ionization Ge detectors”, *Phys. Rev. D* **71** (2005) 122002 [arXiv:astro-ph/0503265].
- [114] G. Servant and T. M. P. Tait, “Is the lightest Kaluza-Klein particle a viable dark matter candidate?”, *Nucl. Phys. B* **650** (2003) 391 [arXiv:hep-ph/0206071].
- [115] G. Servant and T. M. P. Tait, “Elastic scattering and direct detection of Kaluza-Klein dark matter”, *New J. Phys.* **4** (2002) 99 [arXiv:hep-ph/0209262].
- [116] T. Sjöstrand, P. Eden, C. Friberg, L. Lönnblad, G. Miu, S. Mrenna and E. Norrbin, “High-energy-physics event generation with PYTHIA 6.1”, *Comput. Phys. Commun.* **135** (2001) 238 [arXiv:hep-ph/0010017].
- [117] L. M. Sokołowski, “Uniqueness Of The Metric Line Element In Dimensionally Reduced Theories”, *Class. Quant. Grav.* **6** (1989) 59.
- [118] D. N. Spergel *et al.* [WMAP Collaboration], “First Year Wilkinson Microwave Anisotropy Probe (WMAP) Observations: Determination of Cosmological Parameters”, *Astrophys. J. Suppl.* **148** (2003) 175 [arXiv:astro-ph/0302209].

- [119] R. Srianand, H. Chand, P. Petitjean and B. Aracil, “Limits on the time variation of the electromagnetic fine-structure constant in the low energy limit from absorption lines in the spectra of distant quasars”, *Phys. Rev. Lett.* **92** (2004) 121302 [arXiv:astro-ph/0402177].
- [120] A. W. Strong and I. V. Moskalenko, “Propagation of cosmic-ray nucleons in the Galaxy”, *Astrophys. J.* **509** (1998) 212 [arXiv:astro-ph/9807150].
- [121] M. Tegmark *et al.* [SDSS Collaboration], “Cosmological parameters from SDSS and WMAP”, *Phys. Rev. D* **69** (2004) 103501 [arXiv:astro-ph/0310723].
- [122] K. Tsuchiya *et al.* [CANGAROO-II Collaboration], “Detection of sub-TeV gamma-rays from the galactic center direction by CANGAROO-II”, *Astrophys. J.* **606** (2004) L115 [arXiv:astro-ph/0403592].
- [123] P. Ullio and L. Bergström, “Neutralino annihilation into a photon and a Z boson”, *Phys. Rev. D* **57** (1998) 1962 [arXiv:hep-ph/9707333].
- [124] J. P. Uzan, “The fundamental constants and their variation: Observational status and theoretical motivations”, *Rev. Mod. Phys.* **75** (2003) 403 [arXiv:hep-ph/0205340].
- [125] J. K. Webb, V. V. Flambaum, C. W. Churchill, M. J. Drinkwater and J. D. Barrow, “Evidence for time variation of the fine structure constant”, *Phys. Rev. Lett.* **82** (1999) 884 [arXiv:astro-ph/9803165].
- [126] J. K. Webb *et al.*, “Further Evidence for Cosmological Evolution of the Fine Structure Constant”, *Phys. Rev. Lett.* **87** (2001) 091301 [arXiv:astro-ph/0012539].
- [127] S. Weinberg, “The Cosmological Constant Problem”, *Rev. Mod. Phys.* **61** (1989) 1.
- [128] C. M. Will, “The confrontation between general relativity and experiment”, *Living Rev. Rel.* **4** (2001) 4 [arXiv:gr-qc/0103036].
- [129] E. Witten, “Dimensional Reduction Of Superstring Models”, *Phys. Lett. B* **155** (1985) 151.
- [130] E. Witten, “String theory dynamics in various dimensions”, *Nucl. Phys. B* **443** (1995) 85 [arXiv:hep-th/9503124].

- [131] I. Zlatev, L. M. Wang and P. J. Steinhardt, “Quintessence, Cosmic Coincidence, and the Cosmological Constant”, *Phys. Rev. Lett.* **82** (1999) 896 [arXiv:astro-ph/9807002].

Accompanying papers

- [I] T. Bringmann, M. Eriksson and M. Gustafsson,
Cosmological evolution of universal extra dimensions,
Phys. Rev. D **68** (2003) 063516 [arXiv:astro-ph/0303497].

- [II] T. Bringmann and M. Eriksson,
Can homogeneous extra dimensions be stabilized during matter domination?,
JCAP **0310** (2003) 006 [arXiv:astro-ph/0308498].

- [III] L. Bergström, T. Bringmann, M. Eriksson and M. Gustafsson,
Gamma rays from Kaluza-Klein dark matter,
Phys. Rev. Lett. **94** (2005) 131301 [arXiv:astro-ph/0410359].

- [IV] L. Bergström, T. Bringmann, M. Eriksson and M. Gustafsson,
Two photon annihilation of Kaluza Klein dark matter,
JCAP **0504** (2005) 004 [arXiv:hep-ph/0412001].

- [V] T. Bringmann,
High-energetic cosmic antiprotons from Kaluza-Klein dark matter,
accepted for publication in JCAP, arXiv:astro-ph/0506219.

- [VI] L. Bergström, T. Bringmann, M. Eriksson and M. Gustafsson,
Gamma rays from heavy neutralino dark matter,
arXiv:hep-ph/0507229.

Reprints were made with permission from the publishers.